Roles of Melanocortin-4 Receptor Signaling Partner Kir7.1 in Energy Homeostasis

BY:

Erica JP Anderson

Dissertation

Submitted to the Faculty of the
Graduate School of Vanderbilt University
in partial fulfillment of the requirements
for the degree of

DOCTOR OF PHILOSOPHY

in

Molecular Physiology and Biophysics

May 10th, 2019

Nashville, Tennessee

Approved:

Danny G. Winder Ph.D.

Roger J. Colbran Ph.D.

Heidi E. Hamm Ph.D

Mark A. Magnuson, M.D.

DEDICATION

To my life partner and husband, William LM Anderson, who challenges, supports, and encourages me to live life well in pursuit of knowledge, to courageously proclaim truth, and to faithfully seek justice and mercy for the greater good.

You keep me laughing and intentional about things that matter eternally.
I have no doubt that our greatest adventures are yet to come.

ACKNOWLEDGEMENTS

This work was made possible by the financial support from NIH grant RO1 DK070332, the Molecular Endocrinology Training Program (METP) training grant NIH T32 DK07563, and collaboration with Pfizer, Inc.

Having glimpsed the finish line of graduate school, I have no doubt that would not have made it this far without my community and mentors tireless guidance and encouragement. It will be a joy to pay forward my debt of gratitude, in my future endeavors

Foremost is the gratitude and credit owed to Dr. Roger Cone. When I joined the Cone Lab I was imparted with four nuggets of sage advise by my new mentor and colleagues: Comparison is the death of joy. Science is a concise and precise exercise. Swim, else' you will sink. And finally, be intentional, be resilient. Be the weed. I now have the scope to understand more fully why I needed these words and all of the other supports, and resources along side me to finish this marathon training. Roger has nurtured my scientific zeal and taught me how to hone the edge of scientific inquiry. By encouraging my development as a civically minded scientist, Roger not only further engrained my scientific identity but allowed me to add depth and breadth to it in order to be more impactful. When I ran into dead ends on my project, and there were quite a few, Roger's guidance gave me confidence and taught me to scope out to the "10,000 foot view" and when I succeeded, Roger celebrated with gusto. It has been an incredible honor to be a graduate student under Roger's tutelage, one that I will forever treasure.

Likewise, I owe sincerest gratitude to the members of my thesis committee: Drs. Danny Winder, Roger Colbran, Heidi Hamm, and Mark Magnuson. Their perceptive acuity and timely wisdom gave me fresh eyes to navigate my project. I may have gone into nearly every meeting with jitters, but I left with renewed vigor to propel me to the next step. My project and interests have presented unusual and difficult hurdles, which they have taken in stride to guide me toward success. My gratitude also goes out to the leadership of MPB, especially Richard O'Brien for his patience in working with me while I have been estranged from my lab in Michigan. I

deeply regard their personal and professional advice and their interest in my development helped me to persevere.

My time in the Cone lab has traversed several eras. I was able to know a couple members of the "Oregon Team" and had the joy of growing as a graduate student under the infamous, Halloween-costume-contest-crushing "Vanderbilt Crew." As a graduate student my formation was molded during conversations and the observed example of other young and experienced scientists around me. Because of the camaraderie and advice I gained while working with: Savannah, Mike, Masoud, Isin, Rachel, Colette, Brandon, Taneisha, Sheridan, Heidi, Julien, Greg, Luis, Max, Chao, Ashley, and a slew of other folks who have passed through the Cone lab, I will have more sure steps as a scientist and friendships I'll continue to cherish.

While I was lucky to find colleagues I enjoyed long work hours with in graduate school, my resolve and sanity may have waivered were it not for the amazing love received, meals shared, hikes to unwind, sincere conversations and constant checking in on how I'm doing and where I'm at on my doctorate. I hope to be a friend with slightly more regular hours for y'all to work with in the near future.

To my parents, grandmother Joan, Pruett and Anderson siblings, all the aunts, uncles, cousins and family I've had since birth, since marriage, or since we decided to claim each other—y'all have contributed much to make this journey feasible and a reality. Dad and Mom, from the day I declared my dream to be a biologist you have believed in me and made sure I had opportunities to do what I love. My family is a truly incredible gift, and I'm so thankful to share this milestone with you. Thank you for teaching me the value of education, trying to understand my mouse woes, and listening to me explain my project countless times.

Through the course of my training I have gained a dynamic bunch of youth from my community "out North" and students from my classrooms who have given me a completely fresh outlook on science communication and education. By knowing them, I began to unravel my understanding of science as a pursuit of knowledge for its own sake or as a means to ameliorate disease alone. Rather I have now grasped the vision of implementing STEM as a lightening rod tool for equitably empowering diverse citizen scientists to dismantle systematic oppression and

injustice in all facets of life that STEM touches (which is basically everything). The hope I carry for these kids has enriched my training and kept me motivated.

Lastly, to my husband Will, who I didn't even know existed when I began graduate school, yet whose incredible love, unwavering support, and constant stream of revitalizing pep talks has been my foundation to finish. You (and Piper) have felt the highs and lows of my training most potently. When I got in antithetical ruts you kept me honest to the source of my identity and value as well as the science undergirding health by making sure I ate meals, slept semi-regular hours, and got outside to exercise at least 25% as often as you do. Your optimism and strength as we pursue both mentally and emotionally difficult professions keeps me ever mindful of the joy in the journey. It's the best to be able to do life with you.

TABLE OF CONTENTS

Page

LIST OF TABLES

Table **Page**

LIST OF FIGURES

Figure **Page**

CHAPTER 1

BACKGROUND AND SIGNIFICANCE

The Human Obesity Epidemic

During the past 40 years the prevalence of obesity spread across US state and international borders making obesity a top ranking national and global health concern. According to the CDC obesity and its comorbid conditions are amongst the leading causes of preventable death, therefore understanding the pathways leading to obesity has potential for tremendous impact on healthcare and health outcomes. In the United States, as of 2012, greater than one-third of adults and 17% of children are obese with a body mass index (BMI) of greater than 30 [1]. The National Heart, Lung, and Blood Institute as well as many other national medical and scientific special interest groups have documented an increased risk for a number of comorbidities linked to obesity including type-2 diabetes, cardiovascular disease, cancer, and stroke. The obesity epidemic incurs staggering work productivity, economic, healthcare, and even national security costs annually. In 2008 $147 billion in direct annual medical costs in the United States were attributed to obesity [2] suggesting that there are vast public health and economic consequences to this epidemic that threatens the nation. These harrowing statistics and quality of life issues emphasize the importance of investigation into the underlying mechanisms that control body weight among individuals in order to understand and eventually treat human obesity with the ultimate goal of reversing the current trends in order to restore a healthy population.

Within the individual, body weight is controlled by a number of complex and interwoven factors. However, in the simplest sense, energy balance and weight maintenance are achieved by adequately balancing energy intake with energy expenditure so that there is no caloric excess or deficit. Energy intake is affected

---

Text and figures have been modified from Anderson et al. (2016).

solely by feeding behaviors and nutrient absorption, in itself highly complex, while energy expenditure is accounted for by physical activity, basal metabolic rate, and diet-induced thermogenesis. Normally, our bodies adequately regulate long-term energy balance via a complex network of homeostatic factors. A variety of genes are known to play roles in regulation of energy balance and serve as useful tools in elucidating the pathophysiologic basis of human obesity. A key player in coordinating energy intake with energy expenditure is the central melanocortin system [3]. Mutations in components of the central melanocortin system are responsible for genetic obesity syndromes. Continuing to elucidate the roles of the melanocortin system in energy homeostasis will provide valuable insight into the treatment of human obesity

The Central Melanocortin System

The melanocortin system was originally understood in terms of the biological actions of α-melanocyte stimulating hormone (α-MSH) on pigmentation by binding the melanocyte stimulating hormone receptor (MSH-R), and adrenocorticotropic hormone (ACTH) on adrenocortical glucocorticoid production by binding the adrenocorticotropin receptor (ACTH-R). With the discovery of other receptor homologues, a family of five melanocortin receptors was defined. MSH-R and ACTH-R were renamed MC1R and MC2R respectively, and the three receptors subsequently cloned were named MC3R, MC4R, and MC5R. The knowledge of POMC mRNA, and melanocortin peptides in the CNS generated enterprising inquiries directed at understanding the direct biological actions of melanocortins in neurobiology. Ultimately, discovery of unique melanocortin receptors expressed in the central nervous system, the melanocortin-3 and melanocortin-4 receptors, resulted in the development of pharmacological tools and genetic models leading to the demonstration that the central melanocortin system plays a critical role in the regulation of energy homeostasis. Herein I will focus on MC4R, a G-protein coupled receptor (GPCR) whose agonist α-MSH, a POMC cleavage product, and inverse agonist AgRP, mediate a variety of physiological processes critical for energy homeostasis, including food intake, energy expenditure through sympathetic and

parasympathetic tone, adaptive thermogenesis, reproductive biology, and glucose homeostasis. By studying MC4R in humans and a variety of analogous model systems, an expanding understanding of MC4R in regulating energy homeostasis has emerged. Indeed, mutations in the MC4R are now known to be the most common cause of early-onset syndromic obesity, accounting for 2-5% of all pediatric obesity cases. While much effort has focused on understanding MC4R neurocircuitry and targeting MC4R agonists for drug discovery as a treatment for common obesity, to date only one α-MSH analogue (Setmelanotide/RM493) has achieved success in the clinic. Even so, setmelanotide is most successful as hormone replacement therapy for patients with POMC null or leptin receptor mutations, thus there is still much to be understood about the physiologic structure and function down to the molecular and cellular level of the melanocortin system.

Types of receptors in the melanocortin family

Understanding of the physiological roles and sites of action of the five melanocortin receptors and their corresponding peptide ligand(s) began to significantly accelerate with their cloning in 1992 [4]. While the first two receptors reported corresponded to the previously characterized melanocyte stimulating hormone receptor (MSHR or MC1R) and adrenocorticotropin hormone receptor (ACTHR or MC2R), ultimately five melanocortin receptors were cloned, and referred to as the MC1R – MC5R due to the absence of any known physiological roles for the MC3R, MC4R, or MC5R at that time. All melanocortin receptors, except MC2R, bind melanocortin peptides containing the conserved heptapeptide core "MEHFRWG," found in α-MSH, while the ACTHR further requires a peptide motif C-terminal to the 13 amino acids found in α-MSH. Each melanocortin receptor mediates diverse physiological responses based on unique affinities to POMC peptide cleavage products α-MSH, β-MSH, γ-MSH, or ACTH in the case of the MC2R.

Anatomical distribution of melanocortins

Interest in the biology of α-MSH prompted identification of its binding sites from a human melanoma sample. The first receptor to be characterized, MSHR renamed

MC1R, was used as the preliminary sequence to clone ACTHR renamed MC2R [4]. MC1R is primarily expressed in melanocytes of the skin and hair and is known for its role in pigmentation, particularly in response to UV exposure. The primary agonist α-MSH binds MC1R to stimulate synthesis of eumelanin (black-brown pigment), whereas the antagonist agouti (agouti signaling protein or ASP) binds MC1R thereby competitively inhibiting the agonist binding and switching the melanocyte to produce pheomelanin (yellow-red pigment). MC2R is expressed solely in the adrenal cortex where its regulation of adrenocortical steroidogenesis helps to maintain cell proliferation and production of glucocortiocoids [5]. MC2R does not bind α-MSH; instead the agonist ACTH, produced and released from the anterior pituitary gland, activates MC2R. Whereas evidence for MC1R or (7366), MC2R in the central nervous system (CNS) was negligible, pioneers of the field suspected additional receptors based on demonstrated effects of melanocortin peptides on learning, behavior, and other central processes. Thus three orphan receptors were identified and cloned.

MC3R and MC4R are both primarily expressed in the CNS. Cloned in 1993 [6] *in situ* hybridization studies delineated the narrow distribution of MC3R within the adult CNS to approximately 30 mapped nuclei. The highest density is found in concentrated sub-regions of the hypothalamus including the arcuate nucleus (ARC), ventromedial nucleus of the hypothalamus (VMH), the limbic system regions of ventral tegmental area (VTA) and nucleus accumbens (NuAcc), central linear raphe, with moderate expression in the anteroventral preoptic nucleus, lateral hypothalamic area (LH), posterior hypothalamic area, medial habenular nucleus, and paraventricular nucleus of the hypothalamus (PVH), and weak signals from a few brainstem nuclei (notably not the nucleus of the solitary tract (NTS)[7-9] [10] [11] [12]. Double labeled *in situ* hybridization validated prior pharmacologic studies by showing that a large component of ARC neurons expressing MC3R are also positive for AgRP or POMC mRNA [13]. MC3R preferentially binds to agonist γ-MSH, another POMC cleavage product, although the receptor potently responds to α-MSH as well. and is antagonized by AgRP (agouti-related peptide). Various MC3R knockout models have demonstrated that disruption of MC3R in mice induces a non-hyperphagic increase in adiposity with reduced lean mass, reduced bone density, and

modest body mass change [14] [15] [16]. Further physiological studies suggest MC3R regulates fast-induced refeeding [17] and entrainment of anticipatory behavior to nutrient intake (54). MC3R in the VTA has a role as a sexually dimorphic node for regulating the mesolimbic dopaminergic system and reward [12]. MC3R peripheral expression is detectable in the stomach, duodenum, kidneys, placenta, heart, monoctyes and macrophages, however the function of the gene at these sites of action has not been well explored [18]. Nonetheless, it is apparent that one of the central MSH peptides likely mediates some effects on feeding and energy homeostasis via the MC3R.

In 1993 two laboratories independently cloned and mapped the human MC4R using polymerase chain reaction with primers having sequence homology to other members of seven transmembrane G-protein coupled receptors and homology screening [19, 20]. This gene, identified on chromosome 18 (q21.3) in human, was comprised of one large exon with an open reading frame of about 1 kbp that encodes a protein of 332 amino acids. Based on sequence alignment analysis, the closest identified GPCR was MC3R, with 58% homology [21, 22]. MC4R is a member of the rhodopsin-like, Class A, G protein-coupled receptor with seven transmembrane domains connected by alternating intracellular and extracellular loops. MC4R has relatively short N and C -termini, and intracellular and extracellular loops, rendering it one of the shortest GPCRs. As a GPCR, MC4R couples to Gαs protein to activate adenylyl cyclase, resulting in production of intracellular cAMP. There is also evidence that this receptor can raise intracellular calcium levels through recruitment of Gαq and IP3 production in heterologous overexpression systems [23-25].

In situ hybridization studies revealed MC4R is widely expressed throughout the central as well as peripheral nervous system, and was later discovered in intestinal colonic L cells—a neuroendocrine cell type (B.L. Panaro et al., 2014). In the hypothalamus MC4R is concentrated in the PVH, LH, and dorsomedial nucleus (DMH). Beyond the hypothalamus, CNS expression of MC4R is found in a variety of nuclei including the dorsal motor nucleus of the vagus (DMX), the intermediolateral (IML) column of the spinal cord, the amgydala, and the bed nucleus of the stria terminalis (BNST). The role of MC4R in neuroendocrine and autonomic control was

alluded to early in its discovery due to expression concentrated in hypothalamic and brainstem nuclei [26].

MC5R was the final melanocortin receptor family member identified and its presence in exocrine cells appears to promote synthesis and secretion of multiple exocrine gland products such as sebaceous lipids in response to the agonist α-MSH [27].

A summary of the types, hallmark sites of expression, function, and ligand interactions of the five melanocortin receptors is provided in Table 1.

Table 1-1. The Melanocortin receptors

Receptor	Sites of expression	Known physiological functions	Agonists	Antagonists
MC1-R	Melanocytes	Pigmentation (regulation of the eumelanin-pheomelanin switch)	α-MSH = β-MSH = ACTH > γ-MSH	Agouti
MC2-R	Adrenal cortex	Adrenocortical steroidogenesis	ACTH	
MC3-R	CNS, GI tract, kidney	Energy homeostasis, natriuresis	γ-MSH = α-MSH = β-MSH = ACTH	AgRP
MC4-R	CNS L-cells	Energy homeostasis, erectile function	α-MSH = β-MSH = ACTH > γ-MSH	AgRP, Agouti
MC5-R	Exocrine cells	Synthesis and secretion of exocrine gland products	α-MSH > β-MSH = ACTH > γ-MSH	

GI, Gastrointestinal.

MC4R and feeding behavior

When the expression of the MC4R gene in the CNS was mapped by in situ hybridization in 1994, the distribution suggested a role in neuroendocrine and autonomic control [19]. Historically, the earliest physiologic evidence of the role of melanocortins in feeding behavior originated before cloning of MC4R, with reports that ICV injection of ACTH (1-24) and α-MSH inhibited the feeding drive induced by IP injection of *kappa*-opiate receptor agonist in in rats. [28, 29]. Stimulation of food intake by α-MSH had also been reported [30], and thus the characterization of receptors for α-MSH in the brain was ultimately needed to clarify these conflicting findings.

The first breakthrough in understanding MC4R physiological function came from discoveries made in MC1R physiology and pharmacology [31]. In 1994, agouti, a 132-amino-acid protein that is produced in the hair follicle, was demonstrated to be a high affinity ligand of the MC1R, competitively blocking α-MSH binding to inhibit α-MSH induced cAMP production [31]. This finding correlated with observations *in vivo* that agouti blocked eumelanin production. Strikingly, agouti was also found to be a high affinity competitive antagonist of α-MSH action at the MC4R, but no other melanocortin receptors [31].

Since agouti gene mutations were found to result from gene rearrangements that produced ectopic expression of agouti [32], it was hypothesized that the inhibition of melanocortin receptor(s) in the brain by agouti may underlie the obesity and metabolic syndrome observed in the yellow (A^y) mouse [31]. The development of the first MC4R antagonist (18), and the creation of two different genetic mouse models would ultimately confirm this hypothesis [33].

In 1997, several studies were published providing direct evidence and establishing a central role of MC4R signaling in regulation of energy homeostasis. ICV injection of MTII, a cyclic analog of α-MSH, was shown to suppress food intake tested in four different mouse models: fasted C57BL/6J, *ob/ob*, and (A^y) mice, and mice injected with neuropeptide Y, and this inhibition was blocked by co-injection of SHU9119, a cyclic peptide antagonist of MC3/4. Furthermore, ICV injection of

SHU9119 alone increased food intake in mice [33, 34]. These findings supported the hypothesis that hypothalamic POMC expressing neurons releasing α-MSH tonically inhibit feeding via activation of MC4R target neurons, and the chronic blockade of this signaling pathway by agouti produces the obesity observed in A^y yellow mice [33]. Together, these findings supported the hypothesis that hypothalamic POMC expressing neurons release α-MSH tonically and inhibit feeding via activation of MC4R target neurons.

Animal models manipulating the melanocortin system by transgene or knockout have been pivotal in advancing our understanding of the role of MC4R in regulation of feeding and energy homeostasis (Table 2). In 1997, the first animal model testing the role of MC4R signaling in the brain was created. MC4R knock-out mice were first derived, by gene targeting via insertion of a neomycin-targeting cassette in embryonic stem cells which were then implanted into pseudo-pregnant dams to make MC4R knockout mice. This model system was used to test the hypothesis that deletion of the MC4R would recapitulate the agouti obesity syndrome [35]. Mice lacking both alleles displayed an early-onset obesity, hyperphagia, increased linear growth, and hyperinsulinemia. Loss of a single allele resulted in intermediate levels of all the phenotypes compared with the wild type and homozygous siblings, indicating involvement of a gene dosage effect, a rare finding in GPCRs [35]. Later, a reversible MC4R knockout model was generated through the insertion of a floxed transcriptional blocking cassette in the 5' region of the gene (MC4R-loxTB) [80] . Along with the $MC4R^{loxP/loxP}$ mouse [155, 278], these tools have enabled site-specific reexpression and deletion of MC4R in mice. These findings further support a model in which the primary mechanism by which agouti induces obesity is chronic antagonism of the MC4R, therefore, establishing MC4R as central regulator of energy balance.

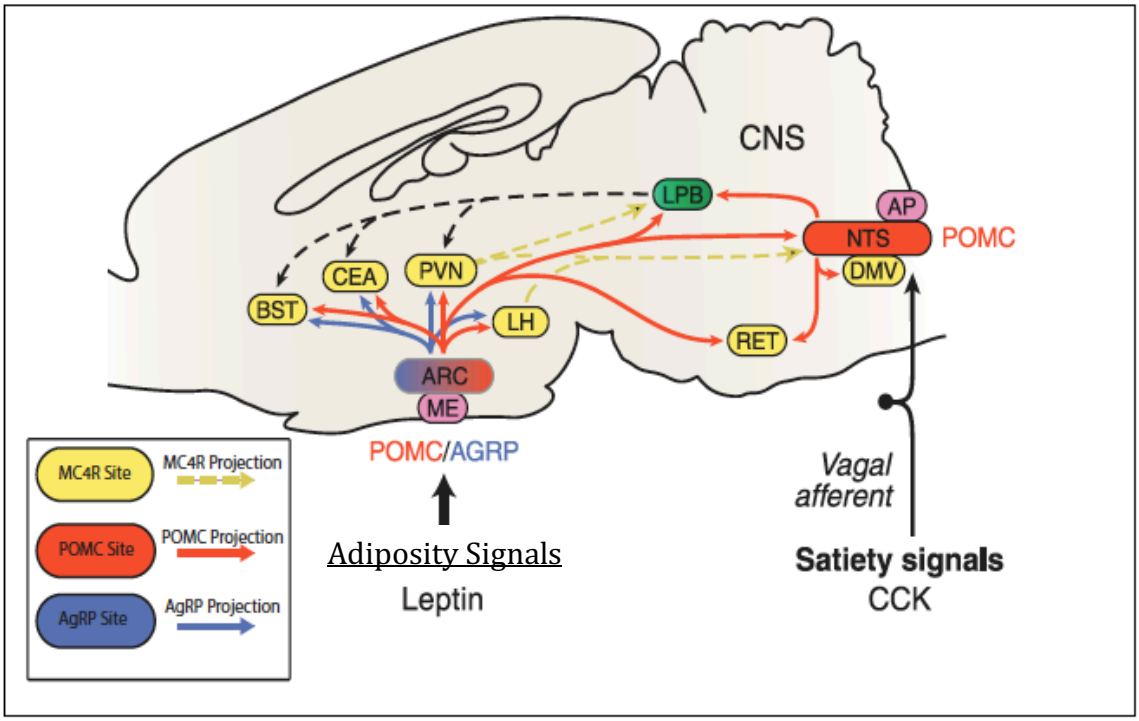

Figure 1-1. A highly simplified schematic of the central melanocortin system Receipt of long-term adipostatic signals and acute satiety signals by neurons in arcuate nucleus and brainstem, respectively. Light blue boxes indicate nuclei containing POMC neurons; yellow boxes indicate nuclei containing MC4R neurons that may serve to integrate adipostatic and satiety signals; and pink boxes show some circumventricular organs involved in energy homeostasis. Red arrows designate projections of POMC neurons; blue arrows show projections of agouti-related protein (AgRP neurons). AP, area postrema; ARC, arcuate nucleus; BST, bed nucleus of the stria terminalis; CCK, cholecystokinin; CEA, central nucleus of the amygdala; DMV, dorsal motor nucleus of the vagus; LH, lateral hypothalamic area; LPB, lateral parabrachial nucleus; ME, median eminence; NTS, nucleus tractus solitarius; PVH, paraventricular nucleus of the hypothalamus; RET, reticular formation. For simplicity, only a fraction of the >100 MC4R target sites are shown, and none of the MC3R target nuclei is indicated. Adapted, with permission, from Fan W, Boston BA, Kesterson RA, Hruby VJ & Cone RD (1997) Role of melanocortin neurons in feeding and the agouti obesity syndrome. Nature 385 165–168.

Table 1-2. Mouse models used to study MC4R and corresponding ligand signaling in obesity

(Anderson, EJP, et al. (2016). Regulation of feeding and energy homeostasis by α-MSH. JME)

Yellow lethal (*Aʸ*) and related alleles (*Aʸ*, *Aᵃʸ*, *Aʷʸ*, *Aⁱᵃᵖʸ*)	Spontaneous mutation resulting in agouti (Asip) ectopic expression, homozygous lethal; unrelated to agouti ectopic expression, moderate hyperphagia, hyperinsulinemia (2–5× normal), late-onset hyperglycemia, lean body mass, ↓ energy expenditure, ↑ sensitivity to stressors, milder obesity syndrome than *ob*/*ob* or *db*/*db*, yellow fur color	Dickie (1962, 1969), Frigeri *et al.* (1983), Bultman *et al.* (1992), Michaud *et al.* (1993, 1994*a*,*b*), Miller *et al.* (1993), Klebig *et al.* (1995)
AgRP transgene	Expression of the AgRP under the control of α-actin promoter, same metabolic phenotype as *Aʸ*, same fur color as wildtype littermates	Graham *et al.* (1997)
AgRP$^{DTR/DTR}$	Cross of mice harboring a loxP flanked diphtheria toxin receptor with animals with Cre recombinase under control of AgRP promoter Ablation of AgRP/NPY neurons of the arcuate nucleus of the hypothalamus, ↓↓ food intake, ↓ body weight, complete ablation results in starvation and death	Gropp *et al.* (2005), Luquet *et al.* (2005), Wu *et al.* (2008*a*,*b*)
POMC$^{-/-}$	Hyperphagic, ↓ energy expenditure, adrenal insufficiency, develop obesity exacerbated with high-fat diet, lighter than littermates-colored dorsal and yellow ventral fur	Yaswen *et al.* (1999), Challis *et al.* (2004)
POMC, AgRP$^{-/-}$	Hyperphagic, ↓ energy expenditure, α-MSH but not AgRP administration rescues wildtype phenotype, lighter than littermates-colored dorsal and yellow ventral fur similar to *POMC*$^{-/-}$	Corander *et al.* (2011)
MC4R$^{-/-}$	Hyperphagic, less obese than *ob*/*ob* or *db*/*db*, early onset obesity (5–7 weeks), ↓ energy expenditure, dosage effect with, +/– animals have intermediate phenotype, increased linear growth, same fur color as wildtype littermates	Huszar *et al.* (1997)
Targeted deletion of MC4R at the PVH	Vglut2-ires-Cre;Mc4r$^{lox/lox}$, targeted deletion of MC4R in glutamatergic neurons: same phenotype as MC4R null mice including ↑ hyperphagia, ↑ body weight, and ↑ linear growth Sim1-Cre;Mc4r$^{lox/lox}$: targeted deletion of MC4R in single-minded 1 positive (SIM1^{+}) neurons: intermediate phenotype between MC4R$^{-/-}$ and Mc4r$^{lox/lox}$ control mice	Balthasar *et al.* (2004), Shah *et al.* (2014)
MC3R$^{-/-}$	Moderate obesity syndrome of late onset (26 weeks), ↑ body weight predominant in females, ↑ adiposity, ↑ energy efficiency, no change in lean mass, no change in linear growth, same fur color as wildtype littermates	Butler *et al.* (2000), Chen *et al.* (2000), Sutton *et al.* (2006)
MC3R, MC4R$^{-/-}$	Augmented obesity syndrome compared with *MC4R*$^{-/-}$ or *MC3R*$^{-/-}$; including ↓ energy expenditure, no change in food ingestion after MTII administration, same fur color as wildtype littermates	Chen *et al.* (2000)
Mahogany (*Atrn*^{mg}) and related alleles (*Atrn*$^{mg\text{-}3J}$, *Atrn*$^{mg\text{-}L}$)	Autosomal recessive mutation reverting the phenotype of *Aʸ* including obesity albeit hyperphagia is present, Atrn encodes for attractin, a melanocortin receptor coreceptor.Atrn^{mg} is a defective splice variant allele that results from a 5 kb retroviral insertion in introns 26 and 27 Fur color reflects eumelanin predominance with diminished pheomelanin, darkened ears, and tail (umbrous coat). Atm$^{mg\text{-}3J}$; a null allele of Atrn, has darker fur	Lane & Green (1960), Dinulescu *et al.* (1998), Gunn *et al.* (1999)
Mahogunin, ring finger 1 (Mgrn1^{md})	Mgrn1 encodes an E3 ubiquitin ligaseThe Mgrn1^{md} allele displays a similar phenotype to Atrn^{mg} and related alleles	Dinulescu *et al.* (1998), Phan *et al.* (2002)
Mrap2$^{-/-}$	Melanocortin receptor accessory protein 2 (MRAP2) knockoutLate-onset ↑ hyperphagia, early onset ↑ body weight, ↑ white fat tissue depots ↓ lean mass, same fur color as wildtype littermates	Asai *et al.* (2013)

AgRP, the endogenous antagonist of MC4R

Another important event in 1997 was the discovery, characterization and mapping of AgRP, an analog of Agouti [36-38]. AgRP mRNA is mainly expressed in the arcuate nucleus of hypothalamus and its levels are increased during fasting, or in *ob/ob* mice, suggesting that AgRP was downstream of leptin action. AgRP binds with high affinity to MC3R and MC4R. Like agouti, it acts as competitive antagonist of α-MSH at these receptors, with only low affinity to MC1R [36]. A single ICV injection of AgRP increases food intake for up to a week, and its co-injection with α-MSH blunts the anorexigenic effects of α-MSH. AgRP also functions as an inverse agonist of MC4R by decreasing cAMP levels produced by the constitutive activity of wild type MC4R [39-41]. This finding promoted the now canonical yin/yang perspective of the regulation of feeding, with POMC neurons and α-MSH inhibiting food intake and energy storage, and AgRP/NPY neurons stimulating food intake and energy storage, in part through AgRP antagonism of MC4R signaling (Figure 2).

In agreement with this model, transgenic mice ubiquitously over expressing human AgRP exhibit obesity but not yellow fur, suggesting that AgRP, unlike agouti protein, is MC3R/MC4R specific, and unable to promote pheomelanin in hair follicle melanocytes [36, 37]. Since MC4R knockout mice exhibit morbid obesity, some expected that AgRP knockout mice might exhibit leanness. However, at first glance, these mice exhibit normal food intake, body composition, growth rates, and normal responses to starvation [42]. Subsequently it was demonstrated that homozygous AgRP knockout mice at 6-months of age do exhibit a very modest reduction in body weight and adiposity with increased metabolic rate, body temperature, and locomotor activity [43]. These mice also exhibit a blunted fast induced refeeding response, a phenotype also found in MC3R knockouts. It is now known that AgRP neurons are GABAergic, and of course express NPY as well, and all three agents regulate downstream MC4R neurons to stimulate feeding [44]. Despite this redundancy, the kinetics of each neurotransmitter is unique. GABA functions in a fast acting manner, regulating bout-to-bout food intake, while NPY and AgRP act

over longer periods and dictate long term energy homeostasis [66]. These findings underscore the importance of the AgRP neuronal system, as well as AgRP action on MC4R in the regulation of energy homeostasis.

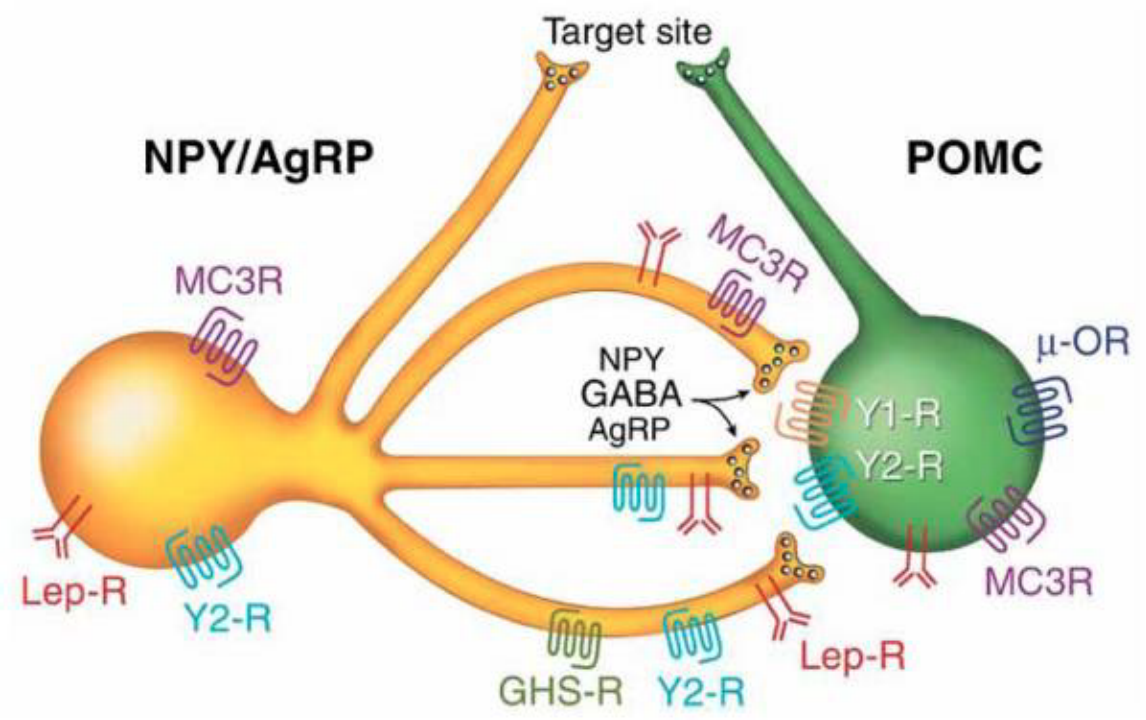

Figure 1-2. Yin-Yang model of control of feeding behavior and energy homeostasis
NPY/AgRP and POMC neurons within the arcuate nucleus form a coordinately regulated network due to dense NPY/ AgRP fibers that project to POMC cell bodies. Some of the receptors for a large number of hormones and neuropeptides known to regulate the network are indicated. These fibers project to many of the same nuclei, where dual release of α-MSH and AgRP were proposed to compete for MC4R binding, to coordinately regulate food intake and energy homeostasis. AgRP, agouti-related peptide; GABA, γ-aminobutyric acid; GHS, growth-hormone secretagogue receptor; Lep, leptin; MC3R, melanocortin 3 receptor; NPY, neuropeptide Y; μ-OR, μ-opiate receptor; R, receptor; GLP-1, glucagon-like peptide 1. Modified, with permission, from Cowley MA, Smart JL, Rubinstein M, Cerdan MG, Diano S, Horvath TL, Cone RD & Low MJ (2001) Leptin activates anorexigenic POMC neurons through a neural network in the arcuate nucleus.

POMC and AgRP Neurons: Expression of endogenous agonist, inverse agonist, and biased agonist of MC4R

To truly understand MC4R action in the CNS, it is critical to understand the neuroanatomical substrate underlying the central melanocortin system (Figure 1-1). Neurons expressing MC3R, MC4R, POMC neurons and AgRP neurons collectively constitute the primary neural components of this system. POMC-derived peptide hormones α-, ß-, and γ-MSH act as melanocortin receptor agonists (Figure 1-3), albeit at different affinities, on MC3R and MC4R in the central nervous system (CNS). AgRP is a competitive antagonist of MSH binding to MC4R, but is also a biased agonist of MC4R signaling, as discussed in more detail below [45].

AgRP was identified by its homology to Agouti and its expression is restricted to ARC and adrenal gland with very low expression in lung, kidney, testis and ovaries [36, 46]. Within the CNS, AgRP neurons are restricted to arcuate nucleus of the hypothalamus (ARC^{AgRP}). Most AgRP neurons (~90%) express another potently orexigenic peptide hormone, neuropeptide Y (NPY). Unlike AgRP, NPY is one of the most abundant and widely expressed neuropeptides in the mammalian brain. Likewise, POMC neurons within the ARC (ARC^{POMC}) express another gene coding for an anorectic peptide called cocaine- and amphetamine-regulated transcript (CART). $ARC^{AgRP/NPY}$ and $ARC^{POMC/CART}$ neurons, henceforth referred to as ARC^{AgRP} and ARC^{POMC}, are chemically and anatomically distinct, however approximately 25% of the ARC^{AgRP} neurons are derived from the same lineage as ARC^{POMC} neurons during development [47]. In the rodent ARC^{AgRP} neurons are expressed homogenously throughout the rostrocaudal axis of the ARC. Reciprocally, most ARC^{POMC} neurons are located in the anterior and medial sector of the ARC. In the rat ARC^{POMC} neurons are more laterally distributed compared to the mouse [48]. Earlier studies quantifying ARC^{POMC} neurons by ß-Endorphin immunohistochemistry [49] or using mice expressing GFP under POMC promoter [48] have reported around 3000-3500 POMC neurons in the rodent ARC. However a recent report quantifying the POMC neurons by immunohistochemistry using an antibody specific to POMC precursor estimated around 9000 POMC immunoreactive cells [50]. The number of ARC^{AgRP} neurons,

analyzed using mice expressing GFP in an AgRP-dependent manner. was estimated to be between 8000-10,000 [50, 51],

Expression of POMC follows a dynamic pattern throughout gestation, and POMC positive brain regions in the adult mice reveal that POMC expression in many regions in the developing embryo is transient. In adult rodents, POMC mRNA was detected by northern blot in hypothalamus, amygdala and the cerebral cortex but was not detectable in midbrain or cerebellar RNA preparations [52]. A 5` truncated version of POMC mRNA lacking the signal sequence was also detected in amygdala, midbrain and cortex as well as in several peripheral tissues. The role of this truncated version is unclear as it cannot produce active POMC derived peptides [53]. POMC was detected in the nucleus tractus solitaries (NTS) and lateral reticular formation of the rat brainstem initially by immunohistochemistry against ACTH [54, 55] and later by *in situ* hybridization [56]. Most neurons identified as POMC positive by labeling strategies involving POMC-Cre mediated recombination, which account for transient POMC expression that does not persist into the adulthood, do not express POMC in the adult brain. In this context, mice expressing GFP under POMC promoter yielded more satisfactory anatomical data of adult ARC^{POMC} neurons as there is almost 100% overlap of GFP and POMC expressions in the ARC, but not in other brain regions [57]. More recent and comprehensive studies comparing POMC-Cre, POMC-GFP and sensitive in situ hybridization techniques have concluded that POMC expression in the adult mouse brain is restricted to ARC and NTS (Figure 1-1) [58].

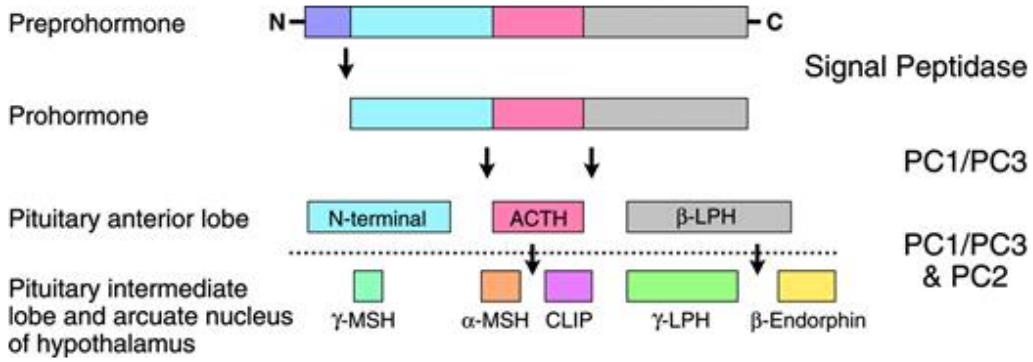

Figure 1-3. Structure and processing of the POMC hormone precursor. Graphic shows the processing of the POMC preprohormone into mature melanocortin and β-endorphin peptides in the pituitary and hypothalamus by prohormone convertases 1-3. (Graphic from Endocrine Review 2006) https://doi.org/10.1210/er.2006-0034

ARC^{AgRP} and ARC^{POMC} receive inputs from other hypothalamic nuclei including the PVH, DMH, VMH, and LH. Extra-hypothalamic nuclei such as the lateral septum and BNST also innervate these neurons [59]. Neurons with cell bodies in the hippocampus, medial mammillary nucleus and VTA appear to selectively innervate ARC^{POMC} neurons, but not ARC^{AgRP} neurons [59]. NTS^{POMC} neurons receive inputs primarily from other neurons mostly within the brainstem [59]. However neurons originating from PVH and amygdala also innervate NTS^{POMC} neurons [59]

ARC^{AgRP} and ARC^{POMC} neurons project to a large number of intra- and extra-hypothalamic brain regions, and many reciprocal connections have been found. Within the hypothalamus, ARC^{AgRP} and ARC^{POMC} neurons send overlapping projections to many hypothalamic nuclei including PVH, LH, ventromedial nucleus of the hypothalamus (VMH), posterior hypothalamus (PH), DMH, and medial preoptic nucleus/area (mPOA) [13]. ARC^{AgRP} neurons innervate extra-hypothalamic sites such as the BNST, the lateral parabrachial nucleus (LPB), central nucleus of the amygdala, and periaqueductal gray (PAG) [51, 59]. ARC^{POMC} neurons innervate many extra-hypothalamic regions including BNST, lateral septum, nucleus accumbens, LPB, the periaqueductal gray, and the DMX. NTS^{POMC} neurons send projections out to innervate other neuron types within the brainstem [59]. The extensive overlap between regions

innervated by both AgRP and POMC neurons also supports the dual regulation of central melanocortin signaling by α-MSH and AgRP (Figure 1-2). Collectively, POMC neurons appear to innervate multiple regions not receiving AgRP innervation, such as the DMX.

Besides neuronal inputs, ARC^{AgRP} and ARC^{POMC} neurons are under direct regulation of hormonal and nutrient-related signals. Both neurons express leptin receptors, while only ARC^{AgRP} neurons express ghrelin receptors. A recent report suggested that the AgRP neurons that project within the hypothalamus did not express LepRb, which was not true for ARC^{POMC} neurons [51]. Around 30-40% of AgRP neurons exhibit leptin-induced STAT3 phosphorylation [60]. Virtually no ARC^{POMC} neurons in the NTS exhibit leptin-induced STAT3 phosphorylation or c-Fos induction [49]. Nonetheless, about 60% of ARC^{POMC} neurons are leptin-responsive. In addition, fasting decreases POMC expression in both ARC and NTS, but only ARC POMC expression can be rescued by leptin [49, 61]. Deletion of LepRb from ARC^{AgRP} and ARC^{POMC} neurons results in obesity and hyperleptinemia [60, 62] in both genders of mice. Deletion of LepRb from both neuronal populations is additive [60]. While these results should be evaluated taking into account the problems inherent with the developmental problems associated with the Cre lines used, these studies suggest that POMC and AgRP neurons mediate only part of leptin's effects on energy homeostasis [58].

Initial studies with optogenetics found that 1 hour hCh2R stimulation of ARC^{AgRP} neurons induced 0.85g of food intake in satiated mice [63] [64]. The frequency of stimulation was proportional to the magnitude of food ingested indicating that this effect was presumably due to increased action potential frequency [63]. Interestingly, the acute phase of ARC^{AgRP} stimulated food intake was maintained on the A^y background and therefore independent of MC4R inhibition [63]. Similar experiments using designer receptors exclusively activated by designer drugs (DREADDS) also found that hM3Gq activation of ARC^{AgRP} neurons resulted in increased food intake and reduced oxygen consumption. hM4Gi mediated inhibition reduced food intake indicating that ARC^{AgRP} regulated feeding is bidirectional [65]. Furthermore, chronic hM3Gq activation of ARC^{AgRP} neurons was found to cause an obesity phenotype that could be reversed following cessation of CNO administration

[65]. By combining ARC^{AgRP} DREADDs with existing KO mouse models, follow up studies revealed that NPY or GABA was necessary for the acute effects ARC^{AgRP} activation while AgRP was sufficient for the long-term effects of ARC^{AgRP} activation [66]. More recent experiments have used hCh2R and DREADDs to further define how ARC^{AgRP} neurons encode a negative valance signal for energy depletion [67] and how they evoke typified energy seeking behaviors even in the absence of food [68]. Together, these studies establish a critical role of AgRP neurons in the regulation of feeding behavior and serve as a model by which to study the role of other genetically defined populations.

Optogenetics and DREADDs have also been used to study the role of POMC neurons in feeding behavior. Chronic but not acute optogenetic stimulation of ARC^{POMC} neurons was found to reduce food intake and cause weight loss [69, 70]. Importantly, unlike ARC^{AgRP} dependent feeding, the satiating effect of ARC^{POMC} stimulation was lost on the A^{y} background and therefore dependent on MC4R signaling [63]. This finding has been repeated with hM3Dq activation of ARC^{POMC} neurons whereby animals displayed a 50% reduction of food intake and a 6% drop in their total body mass [70]. Furthermore, chronic but not acute hM4Di mediated inhibition of ARC^{POMC} neurons was found to cause hyperphagia, but only after 24 hours. Although this finding points toward a role for α-MSH signaling in regulating long term energy balance, these studies are at odds with pharmacological data that have shown robust acute anorexic effects of MC4R agonists [71]. While it is possible that supraphysiological α-MSH dosing paradigms used during pharmacological studies might be responsible for some of this effect, NTS^{POMC} neurons have also been implicated in acute feeding behavior. Indeed, acute hM3Dq stimulation of NTS^{POMC} neurons has been found to cause acute anorexia while chronic activation of this population does not seem to effect food intake [70]. The mechanism that underlies the discordance between anatomical subsets of POMC neurons remains unknown, however, it is likely a result of their distinct projection fields [59]. Alternatively, acute stimulation of ARC^{POMC} has been shown to promote endocannabinoid evoked feeding which may be responsible for the delayed response of ARC^{POMC} neurons but not NTS^{POMC} neurons [72].

MC4R Neurons

MC4R expressing neurons serve to integrate energy status signals from ARC^{AgRP} and ARC^{POMC} neurons and relay the assimilated status throughout the CNS (Figure 1-4). The MC4R is more broadly distributed than other melanocortin receptor family members. MC4R exhibits expression in many CNS nuclei with a striking presence in the hypothalamus, NuAcc, and DMX. Mapping via *in situ* hybridization localized MC4R to over 100 distinct nuclei [26]. Hypothalamic nuclei of highest concentration include—the suprachiasmatic preoptic nucleus, anteroventral periventricular nucleus supraoptic nucleus, PVH, VMH, DMH, tuberomammillary nucleus, and the lateral hypothalamic area. Notable brainstem labeling is found in the superior colliculus, DMX, substantia nigra, raphe, and reticular formation. Following these high expression zones, several regions of the amygdala and isocortex have moderate expression. MC4R may play a role in olfactory response due to its location in discrete cortical rejoins. MC4R has also been identified in CA1 and CA2 regions of the hippocampus, throughout the bed nuclei of the stria terminalis (BNST) and striatum, and with minimal expression in the thalamus [7, 9, 26, 73] [74-77] [78]. Outside of the CNS, MC4R mRNA expression has been detected in astrocytes, spinal cord, heart, lung, kidney, and testis [18]. Localization and distribution of MC4R has been further confirmed by studies using a mouse model expressing GFP under control the MC4R promoter [79].

Additional genetic and pharmacologic modeling systems inducing or repressing MC4R gene function in specific neuronal populations have mapped some neuroanatomical functions of these cells bodies and begun to reveal how the MC4R serves to regulate energy homeostasis. For example MC4R in the PVH is essential for regulating appetite, while MC4Rs expressed in cholinergic preganglionic parasympathetic neurons are necessary for regulating energy expenditure [80, 81]. One peripheral MC4R-mediated pathway was described after detection of high levels of MC4R expression in enteroendocrine L cells [82]. Data shows the receptor mediates release of L cell products PYY and GLP-1 in both mouse and human [82], in response to exogenous administration of α-MSH and its analogues, and of course

these peptides have known secondary effects on feeding. The physiological role of MC4R at this site, and the origin of the ligand, likely an α-MSH peptide, remains unknown.

Optogenetics and DREADDs have also been used to characterize the MC4R target sites that are necessary and sufficient and for evoked feeding behaviors. Despite evidence of a functional inhibitory ARC^{AgRP} -> ARC^{POMC} projection, co-activation of these two populations did not blunt light evoked ARC^{AgRP} feeding [64] [51]. However, site-specific photostimulation of GABAergic ARC^{AgRP} terminals within the PVH was found to be sufficient for acute feeding behavior [64] [83]. This effect was replicated with hM4Gi mediated silencing of PVHSIM1 neurons indicating that inhibition of this population is sufficient for feeding behavior. Furthermore, co-activation of PVHSIM1 cell bodies and ARC^{AgRP} efferents did not cause food intake. Initially, PVHOXT neurons (a subpopulation of PVHSIM1 neurons) were thought to be the mediators of ARC^{AgRP} -> PVH induced food intake [64]. However, both *ex vivo* and *in vivo* experiments have challenged this finding [83] Sutton et al., 2014; Z. Wu et al., 2012). Using channelrhodopsin (ChR1)-assisted circuit mapping (CRACM), ARC^{AgRP} fibers were found to evoke time locked IPSCs within 83% of PVH MC4R cells and 0% of PVHOXT expressing cells [83]. MC4R neurons were also found to be distinct from OXT neurons as evidenced by immunohistochemistry. Co stimulation of inhibitory ARC^{AgRP} fibers and PVH^{MC4R} were also found to block evoked feeding behavior while PVHOXT did not. PVH^{MC4R} neurons also displayed projections to and elicited activation of the LPBN, thereby provoking a satiety response [83]. In addition to the PVH, ARC^{AgRP} neurons are known to project to numerous other brain regions. Using a similar efferent projection stimulation strategy, ARC^{AgRP} fiber activation in the BNST, LH and PVT was sufficient for evoked feeding behavior [51]. This contrasts with ARC^{AgRP} fibers that project to ARC^{POMC} neurons, PBN, CEA, and PAG which do not evoke feeding. Interestingly, while the BNST and the LH both express MC4R, inhibition of MC4R neurons within these sites does not appear to be responsible for the increased food intake seen with ARC AgRP afferent stimulation, suggesting a primary role for GABA [83]. These studies indicate the complexity of MC4R pathway neuron nodes of signaling, kinetics, as well as receptor coexpression

that merits further study. .

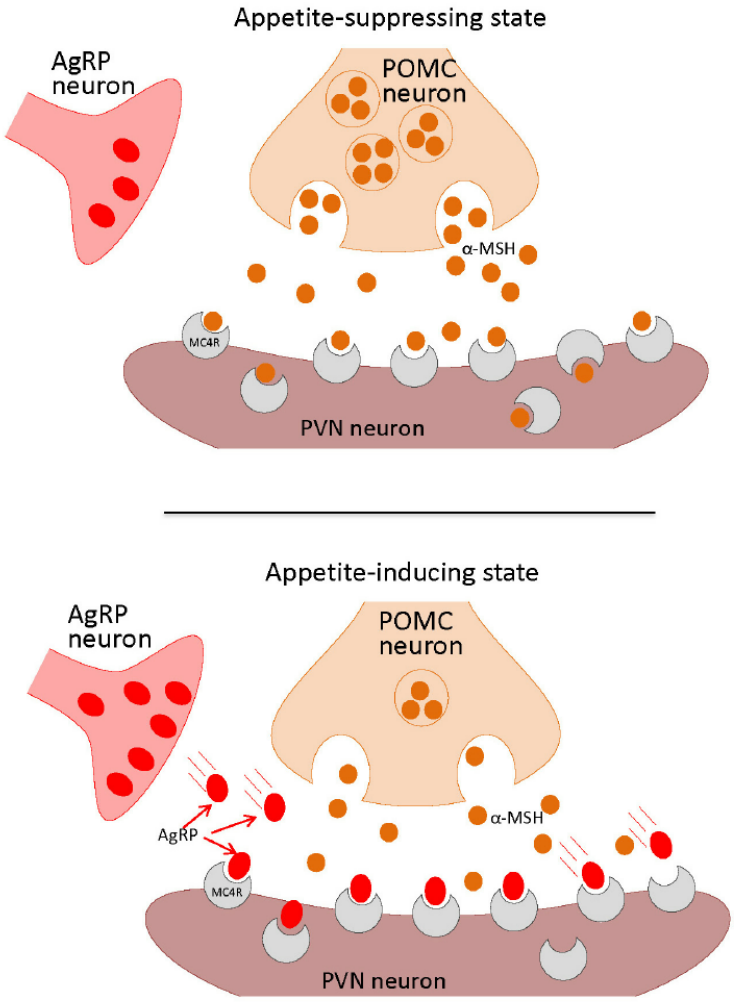

Figure 1-4. Interactions between AgRP and α-MSH at distal MC4R sites in the PVN

POMC neurons produce α -MSH that acts on MC4Rs in the PVN to suppress food intake. Increased activity of AgRP neurons causes the release of AgRP peptide from nerve terminals in the PVN. AgRP binds to the MC4R and antagonizes the effect of α -MSH at the MC4R. By preventing the actions of α -MSH in the PVN, AgRP helps to increase food intake. AgRP neurons also produce NPY, however NPY acts on NPY Y1 and Y5 receptors in the PVN independently from the MC4R. Reichenbach, Alex & Stark, Romana & Andrews, Zane. (2012). Hypothalamic control of food intake and energy metabolism. The Human Hypothalamus: Anatomy, Functions and Disease.

MC4R signal transduction

Melanocortin receptors (MCR) are members of the rhodopsin-like, Class A branch of the seven transmembrane-spanning domain G protein coupled receptor (GPCR) superfamily. An extended set of co-receptors, signaling partners, and alternate endogenous ligands enrich the tapestry of responses that result from α-MSH or other POMC cleavage product stimulation at each receptor (Figure 1-3). This functional diversity played an important role in the discovery of many of the components of this system [5].

α-MSH binding to MC4R leads to dissociation of the coupled heterotrimeric G-protein complex by stabilizing an active form of the receptor [84] [85]. This process leads to a conformational change in the complex that facilitates the exchange of GDP for GTP on the Gαs [86]. Upon dissociation, Gαs associates with and activates adenylyl cyclase through a direct protein-protein interaction [87]. This process continues until GTP is converted to GDP by the GTPase activity of Gαs. During the time it is activated by Gαs, adenylyl cyclase catalyzes conversion of ATP to cAMP [88] cAMP goes on to function as a diffusible second messenger until it is cleaved into AMP by phosphodiesterases [89]. cAMP is able to bind to the PKA regulatory subunits causing a conformational change in the protein structure [90]. This enables the catalytic subunits of PKA to phosphorylate target proteins including channels that regulate neuronal excitability [91] [92]. In addition to PKA, cAMP can activate PKA independent pathways including the EPAC pathways [93]. This pathway appears to be essential for MC4R mediated changes in gene transcription in cell lines and also appears to be essential for MC4R action *in vivo*, at least in the sense that deletion of Gαs in MC4R neurons recapitulates the obesity syndrome seen with MC4R deletion [94]. There is also evidence that MC4R can increase intracellular calcium levels through recruitment of Gαq and IP3 production in heterologous overexpression systems [25] [95] [23].

Furthermore, studies on AgRP signaling have found that AgRP leads to MC4R activation of the pertussis toxin sensitive Gi/o inhibitory protein in the hypothalamic GT1-7 cell line [96]. The ability to signal through Gi/o led to the hypothesis that MC4R could potentially couple to G-protein inwardly rectifying potassium channels

(GIRKs); known to be activated by Gβγ binding following release from Gi heterotrimers [97]. These results highlight the possibility that MC4R can signal through different G-proteins with opposing actions depending on the ligand, the classical Gαs stimulatory protein activated by α-MSH binding, versus Gi/o inhibitory protein activated by AgRP binding. The ability to signal through Gi/o led to the hypothesis that MC4R could potentially couple to GIRKs that are activated by Gβγ binding following release from the Gi complex [98]. However, this finding has not been seen in *ex vivo* brain slices.

Data on the mechanism of α-MSH and AgRP signaling through MC4R also relies on the use of electrophysiological slice preparations from mice in which MC4R neurons have been transgenically labeled with GFP [99] [100] [79]. In this preparation, α-MSH depolarizes and AgRP hyperpolarizes MC4R neurons when added to the bath [278]. PKA mediated MC4R signaling has been shown to cause neuronal hyperpolarization within the DMX through activation of a K_{ATP} channel, thereby showing PKA regulates aspects of MC4R signaling in many nuclei. In this study, the adenylyl cyclase activator forskolin as well as the PKA activator 8-BrcAMP were able to mimic the effect of the MC4R agonist MTII. Inhibition of PKA with H89 or KT-5720 was further shown to abolish the MTII mediated hyperpolarization. Within the IML of the spinal cord, PKA was found to be essential for MC4R mediated depolarization. In this cell population, MC4R-PKA signaling was dependent on the activation of a non-specific cation channel. Within the hippocampus, MC4R induces synaptic strengthening in a PKA dependent manner [91]. This results in an increase in synaptic spine number and AMPA surface expression via PKA phosphorylation of GluA1. Furthermore, deletion of the inhibitory domain of PKA (RIIβ) is able to reverse the obesity syndrome in A^y mice [101]. Together these studies demonstrate a critical role of PKA in α-MSH induced activation and inhibition of MC4R within the IML, DMX, and hippocampus – regions that lack AgRP innervation. Additional studies have found a distinct MC4R signaling modality within the PVN – a region with high amounts of AgRP innervation [102].

Using a *ex vivo* slice preparation and high throughput flux assay a novel MC4R signaling pathway through the inward rectifying potassium channel Kir7.1 was discovered in 2015 ([103] [104] . The details and impact of this discovery on our evolving understanding of MC4R signaling are discussed further in the following section, "Discovery of a Role for Kir7.1 in the Melanocortin System," and depicted in Figure 1-5.

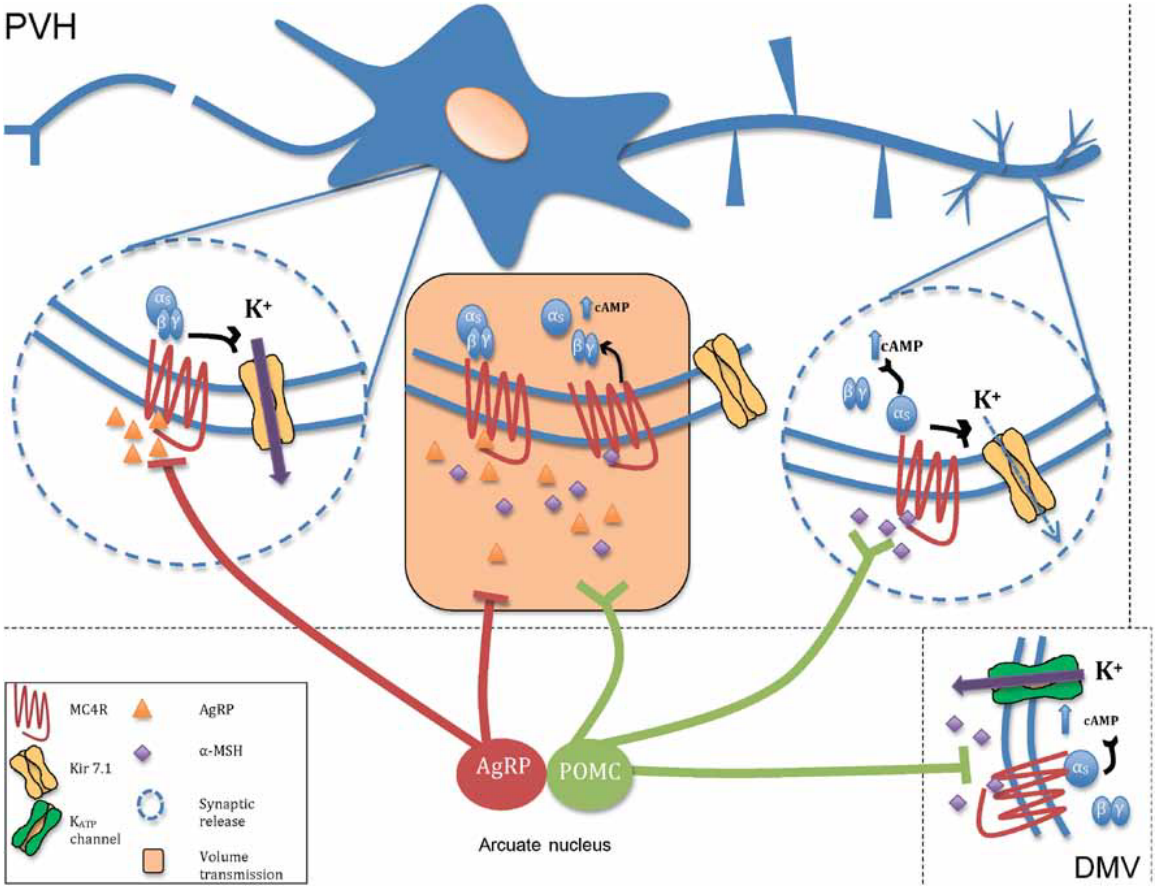

Figure 1-5. A new model of MC4R microcircuitry
The Yin–Yang model of α-MSH and AgRP action (Fig. 1) suggested competitive binding of these peptides to individual MC4R sites (orange box), and anatomical data suggest in regions where these peptides undergo volume release, that competition for binding to the MC4R may occur. New subcellular anatomical data suggest that in the PVH, AgRP synaptic contacts predominate at cell bodies, while POMC synaptic contacts predominate at distal dendrites. Along with the fact that AgRP immunoreactive fibers are only observed in a subset of MC4R expressing nuclei containing POMC-immunoreactive fibers, α-MSH may this often act independently of AgRP (right circle). At these sites, α-MSH may be expected to signal through both cAMP, and Kir7.1. The ability of AgRP to act independently of α-MSH as a potent hyperpolarizing agonist, via regulation of Kir7.1, suggests the likely existence of independent AgRP sites of action (left circle). Another MC4R signaling pathway, involving cAMP/PKAdependent activation of KATP channels and **α**-MSH-induced hyperpolarization, has been demonstrated in MC4R neurons in the dorsal motor nucleus of the vagus in the brainstem (bottom right). Thus, **α**-MSH and AgRP utilize a diversity of signaling modalities to regulate feeding and energy homeostasis through the MC4R. Modified, with permission, from Ghamari-Langroudi M, et al. (2015).

Phenotype of MC4R mutations in humans and mice

The primary function of MC4R is to regulate food intake and energy expenditure, and this role for the receptor has been shown to be evolutionarily conserved in vertebrates from fish to human. MC4R knockout mice as well as human mutants present with an early-onset severe obesity associated with increased fat mass, and lean mass [35, 105]. Additionally, MC4R regulates insulin secretion, lipid metabolism, bone mineral density, and body length. The MC4R-induced phenotypes also exhibit a gene-dosage effect, unusual for GPCR genes. Herein we describe the methods for understanding the phenotype and types of genetic alleles leading to MC4R mutations.

In 1998 the Froguel and O'Rahilly research groups conducted two independent analyses of the MC4R gene in individuals with childhood obesity and in a non-obese control population. Through these studies they identified the first frameshift mutations in the MC4R gene in children with severe early onset obesity [105, 106]. The vast majority of MC4R deficient obese individuals have deleterious heterozygous mutations of the receptor, which underscores the notion of a MC4R gene dosage effect. This finding demonstrated the evolutionarily conserved role of MC4R in energy balance in humans, and generated great interest in α-MSH signaling in the CNS in general, and the MC4R in particular in regard to development of new obesity therapeutics.

Initial studies estimated a mutation prevalence of 6% in cohorts of pediatric obesity (Farooqi et al., 2003). More recent estimates place the incidence at closer to 2% in this population, although the numbers refer exclusively to coding mutations [107]. In the general population, the rate of MC4R mutations is 0.05% with a substantial enrichment in the obese population to about 0.5-1% . 166 unique MC4R mutations have been identified by receptor coding analysis from patient cohorts representing an array of ethnic origins (Figure 1-6) [108] [109] [110] [111] [112] [113] [114] [115] [116] [117] [118] [119] [120] [121] [122] [123] [124] [125] [126]. Ethnic origin may also contribute to prevalence of MC4R mutations, severity of obesity, and age of obesity onset. Amongst these mutations at least 122 are

missense, 7 nonsense, two in-frame deletion, and dozens of frame shift mutations have been documented throughout the MC4R structure. No mutations have been identified in the MC4R promoter and although some polymorphisms and SNPs near MC4R exist, defective MC4R transcription does not appear to be a major contributor to severe disease pathology [127].

The clinical spectrum of MC4R associated obesity closely aligns with the syndrome in the mouse. Both organisms display severe hyperphagic obesity, increased linear growth, severe hyperinsulinemia, incomplete growth hormone suppression, reduced rates of obesity associated hypertension, reduced urine norepinephrine levels, increased lean mass and increased bone mineral density [120] [112] [128]. Furthermore, loss of the MC4R enhances a preference for fat over sucrose in both mice [129] [130] and humans [131].

The discovery of MC4R mutations in human cohorts has also furthered the understanding of MC4R receptor pharmacology. MC4R mutations have been grouped into 5 distinct classes (Figure 1-6). Class I mutations include nonsense, frameshift, and missense mutations that cause an absence or reduction of protein synthesis, or are hypomorphic alleles. These mutations include the nonsense mutations Y16Stop, Y35Stop, C277Stop and Y287Stop and missense mutations R7C, I69M, M79I, S94N, D146N, & I301T. Class II mutations cause reduced surface expression largely due to defects in receptor folding and/or trafficking. Many of mutations in this class, including S58C, E61K, N62S, I69T, G98R, T162I, R165W, W174C, C271Y, and P272L, P299H, [132] remain trapped intracellularly, get polyubiquitinated and are degraded by the proteasome [133]. This process appears reversible as MC4R selective receptor chaperones can act to promote receptor trafficking, indicating the necessity for potential therapies to be used in a mutation specific manner [134]. Class III mutations exhibit normal expression levels, but result in reduced ligand binding and include P48S, V50M, F51L, I102S, D126Y, R165Q, A175T, A219, G238D, L250Q, S295P, and D298A. Class IV mutations have normal receptor expression and ligand binding but have reduced ligand stimulated signaling or reduced basal activity in cAMP activation assays. These include the obesity associated N terminal region mutations R7H, T11S/A, R18C/H/L, S30F, and D37V which have been shown to

reduce basal receptor activity without altering ligand mediated signaling [85], as well as a number of mutations that reduce E_{max} for cAMP activation. Indeed, SNPs in the MC4R non-coding sequence are a major GWAS signal contributing to BMI. Class V mutations are mutations with an obesity association without differences in protein expression, ligand binding or signaling. In addition to discovering obesity associated MC4R mutations, a V103I allele (2-9% of the general population) [135] and I251L allele (0.41-1.21% of the general population) [136] have increased ligand mediated receptor activity and basal receptor activity, respectively. Not surprisingly, these receptors are associated with both leanness and reduced serum triglyceride levels [137]. The sum effect of the majority of melanocortin defects is early onset obesity in both mice and humans. The broadening catalog of melanocortin receptor mutations and their associated diversity of defects indicates a possibility for a multiplicity of class specific pharmacologic targets. These designer drugs could thus target both syndromic, nonsyndromic, and common obesity. Concurrently the catalog of melanocortin receptors represents multiple points of accessing studies to understand the melanocortin rheostat of energy homeostasis.

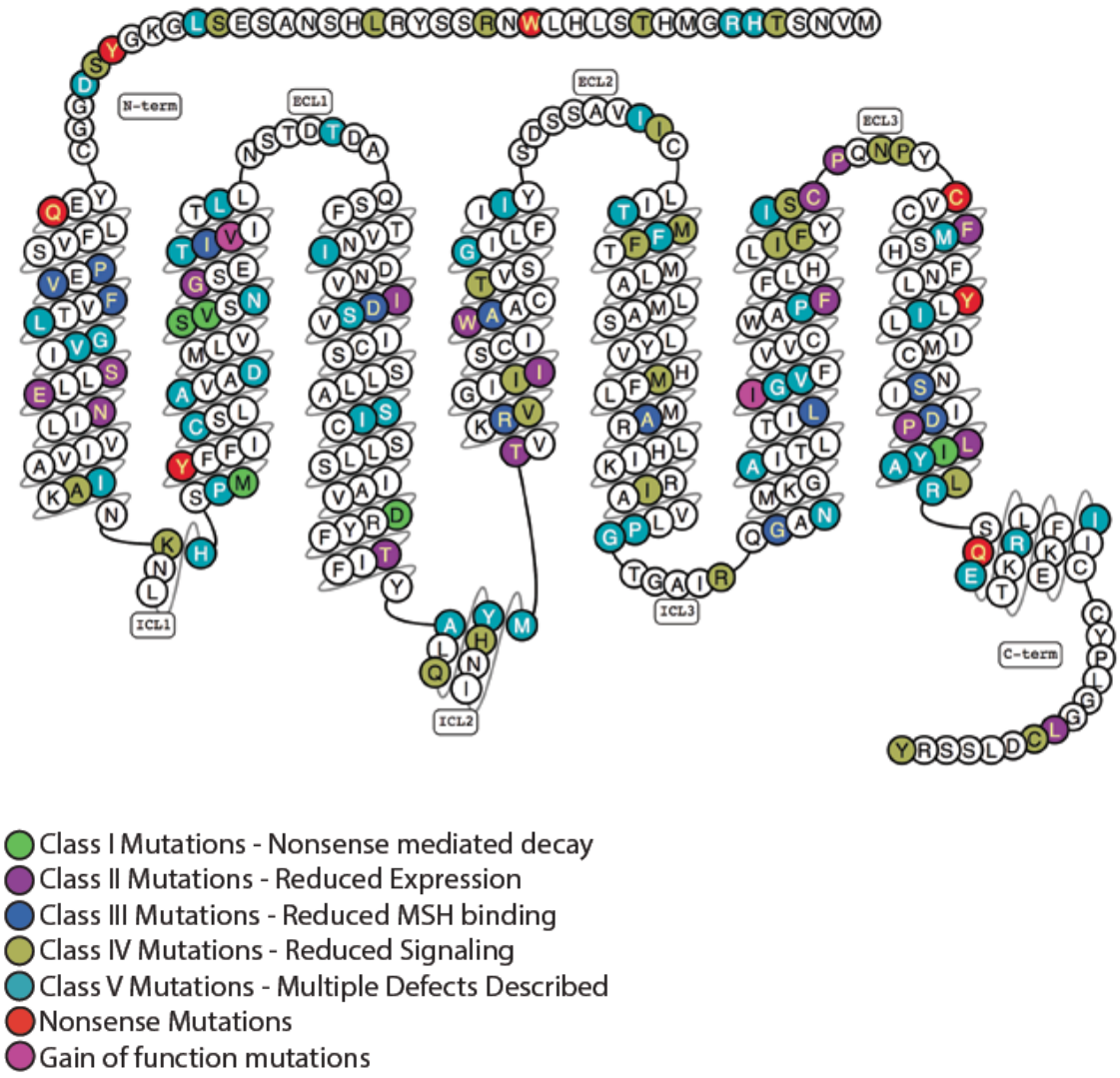

Figure1-6. Human mutations of the MC4R
MC4R mutations have been found throughout the receptor and cause obesity. Catalogued mutated residues account for 32% of the MC4R. Mutations affect a variety of functions including those that reduce protein levels, lead to hypomorphic proteins, and reduce basal activity. Certain mutations can also increase receptor activity and are associated with a lean phenotype. Modified from [77].

MC4R and energy expenditure

Early studies elucidated the role of MC4R in regulating food intake. Additionally, MC4R has been implicated in the regulation of energy expenditure. This hypothesis has been examined across multiple modalities including basal energy expenditure, adaptive thermogenesis, and sympathetic tone. An initial study using indirect calorimetry found a reduction of body weight normalized VO2 in 8-9 week old male Mc4r-/- mice [138]. However, this time point is after a detectable increase in adiposity [139]. This fact is critical for the proper interpretation of the experiment as the authors correct VO2 by dividing by the larger MC4R body weight. Furthermore, this correction assumes a linear relationship between body weight and energy expenditure that does not intersect at Y=0 implying that an organism with a mass of 0g could somehow expend energy. The authors do find that pair feeding was unable to normalize body weight in Mc4r-/- females. However, this was not present in males suggesting a sexual dimorphic component to MC4R regulated energy expenditure. When food intake and energy expenditure measurements were analyzed from day 21-35 of MC4R-/- Weide et al. (2003) conclude that excessive fat deposition is driven by hyperphagia rather than hypometabolism, supported by disregulation of NPY and POMC expression [140]. Butler et al. (2001) reported no difference in basal VO2 when dividing by body weight raised to the 0.75 power to correct for allometric scaling [141]. Rather than dividing by body weight, the body weight-VO2 interaction should be compared by ANCOVA as is now standard in the field [142]. A more recent study compared the basal VO2 and energy expenditure in Mc4r-/- rats using the ANCOVA methodology found no difference in co-variation between body weight and energy expenditure [143]. Despite no difference in basal VO2, most studies on Mc4r-/- mice have found a significant increase in the respiratory exchange ratio suggesting increased glucose utilization in these animals [143] [144].

The absence of MC4R is further exacerbated in conditions of caloric excess such as high fat diet induced obesity. Typically, mice exposed to high fat diet respond by rapidly increasing diet-induced thermogenesis and increasing physical

activity. Studies by Butler et al. and collaborators found that MC4R-/- mice have an impaired response to an increase in fat content, resulting in decreased insulin sensitivity in addition to impaired energy expenditure and hyperphagia [144] [145]. Restoration of MC4R expression solely in the PVN and amygdala showed that MC4R in these nuclei is responsible for food intake, whereas MC4R in other neurons regulate energy expenditure [80]. Indeed this study concludes that change in food intake accounts for 60% of the effect of MC4R loss of function on energy balance, while the remaining 40% is due to changes in energy expenditure.

Pharmacological studies have also been used to examine the role of MC4R tone in basal whole animal energy expenditure. Studies have found that administration of an MC4R agonist leads to an increase in basal energy expenditure in mice [146], rats [147] [148] and humans [149]. In mice, IP administration of MTII causes a biphasic modification of energy expenditure [146]. Within ten minutes of compound administration, total animal energy expenditure is suppressed while RER is increased for approximately one hour. This effect appears to be non-specific as it occurs in MC4R knockout animals. Following the initial suppression, there is then a dose dependent two-hour increase in energy expenditure and decrease in RER. This effect is mirrored by an increase in body temperature and that is due to brown fat thermogenesis. In rats, MTII administration displayed a dose dependent increase in 3 hour VO2 in both lean and diet induced obese and lean Zucker rats [147]. Furthermore, the respiratory quotient is reduced in animals injected with α-MSH indicating an increase in fat utilization. MC4R agonists have also been administered to humans, in attempt to test efficacy for MC4R drug therapies for metabolic syndrome. Subcutaneous administration of RM-493 – an MC4R agonist that lacks a pressor effect in primates [150]– was able to raise resting energy expenditure by 6.4% (95%CI: 0.68-13.2) as well as lower the respiratory quotient (from 0.848 ± 0.022 to 0.833 ± 0.021) [149]. MC4R modification of whole organism VO2 has also been shown to be bi-directional. Both acute [151] and chronic [152] ICV administration of AgRP leads to a suppression of oxygen consumption in rats [152]. Whether this effect is due to a reduction in basal MC4R signaling is unclear. In some reports, the neutral antagonist HS014 is unable to suppress VO2 [148] while in

others, HS014 lead to a reduction in energy expenditure and VO2 [153]. Thus, while the loss of MC4R plays an unclear role in basal energy expenditure, a change in MC4R signaling tone is able to modulate energy expenditure.

The underlying mechanism behind how MC4R changes energy expenditure has been examined. The degree of MC4R tone has been shown to correlate with the metabolism of several peripheral organs. Brown adipose tissue (BAT) was the first peripheral organ that MC4R was found to regulate. MTII injection dose-dependently increased sympathetic nerve traffic to thermogenic BAT, and this effect was blocked by SHU9119 [154]. RFP labeled pseudorabies virus injection into the interscapular brown fat pad of MC4R-GFP mice leads to co-localization in nuclei that regulate sympathetic tone [155]. Furthermore, when Mc4r-/- mice were placed on high fat diet, there was no induction of the mitochondrial uncoupling protein - UCP1 – within the BAT. An independent study confirmed this finding pharmacologically and further described how MC4R regulates peripheral lipid metabolism [156]. ICV injection of SHU9119 led to an increase in lipid uptake and triglyceride storage in white adipose tissue (WAT). Mc4r-/- mice were also found to have increased insulin sensitivity of WAT while pharmacological inhibition of MC4R decreased sympathetic nerve activity and muscle/BAT glucose utilization. While the precise mechanism for this effect remains undetermined, it is presumed to due to MC4R regulation of sympathetic tone.

MC4R cardiovascular pressor effect and therapeutic implications

While MC4R modulation of BAT, WAT and skeletal muscle metabolism is a useful therapeutic tool, a barrier to successful drug design has been that MC4R also regulates cardiovascular function. ICV, but not intravenous, injection of α-MSH has been found to increase heart rate and blood pressure. This effect is lost in Mc4r-/- animals, who concordantly exhibit hypotension, relative to BMI matched controls, and can be blocked through administration of an MC4R antagonist [157] [158]. However, chronic administration of α-MSH eventually leads to a reduction in mean arterial pressure [159] and physical activity. The acute effects of α-MSH injection on the cardiovascular system are nucleus dependent. Injection of a MC4R agonist into

the PVN causes a subsequent increase in blood pressure and renal sympathetic nerve activity [160]. Likewise, injection of a MC4R agonist directly into the C1-T3 region of the IML was found to increase heart rate without changing blood pressure [161] and overexpression of α-MSH in the NTS also increases heart rate [162]. An increase in blood pressure and heart rate can be blunted by the addition of a combined α/β blocker thus demonstrating the role of sympathetic nervous system in this process [163 2003]. This increase in sympathetic output contrasts with what happens when α-MSH is injected into the DMX [160] [164]. Injection of MTII into this region results in a rapid reduction of blood pressure and heart rate. This effect is MC4R specific as it can be blocked by SHU9119 or HS014 in a dose dependent manner. Similar to the set of energy expenditure experiments discussed above, the ability of MC4R to regulate blood pressure is bi-directional. Inhibition of the MC4R with SHU9119 or AgRP leads to hypotension and bradycardia [165] [166 & Hall, 2004] [167]. This effect is centrally mediated, as IV injection does not replicate this effect. MC4R compounds lacking a cardiopressor activity have been synthesized and tested in humans [149] [168 Wulff, & Hansen, 2014], validating the use of MC4R agonists in the treatment of common obesity.

Beyond acute regulation of blood pressure, MC4R signaling is further implicated in autonomic control of heart function as a critical mediator of obesity-associated hypertension. Blood pressure recordings of Mc4r-/- mice showed that they were normotensive despite being profoundly obese, hyperinsulinemic and hyperleptinemic [169]. Furthermore, the Mc4r-/- mice did not become hypertensive on a high salt diet [170]. This effect can be replicated pharmacologically. MC4R inhibition with SHU9119 to obese Zucker rats resulted in a greater reduction of blood pressure than lean controls [171]. Since both insulin [172] and leptin [173] have been shown to cause hypertension through increases in sympathetic tone, this finding has implicated MC4R as a common mediator of leptin and insulin's effects. Studies in humans have replicated this finding as patients with heterozygous loss of the MC4R are protected from the hypertensive effects of obesity and have reduced 24 hour urinary catecholamine levels [128]. Selective knockout studies have been informative with respect to the nucleus that regulates obesity associated increases

in blood pressure. The prevention of leptin-induced hypertension in $POMC_{LepR}$ knockout mice has implicated the hypothalamus and brainstem in this process [174]. An initial attempt was made to see if this effect was specific to the hypothalamus or autonomic neurons by re-expressing MC4R in the loxTB MC4R mouse with SIM-1- Cre as a paraventricular neuron marker [80] or ChAT as a general autonomic neuron marker [175]. While both SIM1-Cre; MC4R lox-$TB_{+/+}$ and ChAT-Cre; MC4R lox-$TB_{+/+}$ became similarly obese, only the ChAT-Cre; MC4R lox-$TB_{+/+}$ animals became hypertensive in response to obesity [176]. Based on these studies, it appears that the hindbrain Leptin-> NTS_{POMC} -> IML_{MC4R} pathway is essential in this process but the role of presynaptic parasympathetic MC4R neurons within DMX remains to be determined. Recently, Litt et al. identified a novel mechanism for cardiomyopathy in patients with MC4R loss of function. MC4R null mice develop dilated cardiomyopathy due to underlying mitochondrial defects promoting reactive oxygen species production which mediates cardiomyocyte tissue damage [177]. Thus even though defective MC4R results in bradycardia and reduced obesity-associated hypertension, MC4R regulation of autonomic tone implies other complications may arise leading to heart failure in individuals with mutated MC4R.

MC4R therapeutic design

A variety of drug design strategies can and have been implemented to address defects in naturally occurring MC4R mutations. For example synthetic ligands could be derived to correct class III and class IV mutants in order to provide customized exogenous ligand in the absence of receptor response to endogenous ligand. Small molecule pharmacological chaperones may increase surface expression of class II intracellularly retained MC4R mutants by assisting their trafficking. Upon agonist stimulation MC4R undergoes receptor desensitization by PKA and GPCR kinase receptor phosphorylation and arrestin-conveyed receptor internalization [92], however, recently a novel twist to positive allosteric modulator drug design called biased unmatched bivalent ligand (BUmBL) has been

implemented to design heterobivalent MC4R ligands. These ligands link agonist to antagonist small peptide moieties to enhance Gαs while minimally activating β -arrestin recruitment [178] (Figure 1-7). This is an intriguing approach that may offer promising therapies in the future. Furthermore some MC4R peptide agonists have been shown to more efficiently recruit receptor internalization [179]. This presents an attractive target for some MC4R mutants, but may not be as effective for common obesity.

Designer agonists of MC4R have long been sought as a therapeutic target for treating common obesity. Yet despite rigorous efforts, multiple proposed selective compounds, and tremendous need, successful human clinical trials of compounds designed to target MC4R have largely been hampered by adverse cardiovascular affects and treatment of sexual dysfunction. [168] [180]. Some preliminary success in compound discovery has been made using high throughput screening methods to delineate MC4R-active organic compounds or analogue structures that can serve as motifs of natural peptides [181]. Synthetic chemistry has generated cyclic modifications to non-selective agonist, lactam-cycles MTII and antagonist, SHU9119, commonly used [182] [183]. MTII has also been modified to generate bremelanotide, which has been used in clinical trials to treat erectile dysfunction and female hypoactive sexual desire disorder (HSDD) [184] [185]. Much like other melanocortin agonists, the positive clinical outcomes of bremelanotide did not outweigh efficacy concerns regarding the cardiovascular effects and clinical trials for application other than female HSDD have been halted.

Few anti-obesity drugs have passed and been approved by the FDA draft guidance [186]. The clinical parameters for successful drug induced weight loss are >5% of initial body weight sustained for at least 12 months. Because obesity is the manifestation of a multilayered physiologic syndrome, with complex etiology, and intertwines many organ systems and pathologies, few drugs have met the bar in regard to safety [186] In 2016 the FDA did award orphan drug status to the first α-MSH based therapeutic for obesity, RM-493, or setmelanotide. This α-MSH analogue was awarded orphan drug status for POMC deficiency and Prader-Willi-Syndrome [187]. Setmelanotide, an analogue significantly more potent than α-MSH, induces

weight loss in wild-type rodents, is less sensitive in MC4R heterozygous mice, and is inactive in MC4R null mice, therefore although setmelanotide leads to weight loss in patients with MC4R deficiency, meaningful weight loss in some MC4R patients may not be achievable. Short-term weight loss appears to be achieved by an increase in REE and a shift in substrate oxidation to fat, with no adverse effect on heart rate or blood pressure [149]. Improvements in energy homeostasis have been effectively observed in patients with mutations in the POMC mechanism pathway including *POMC* and *LEPR* deficient patients [188] [189]. Remarkably, the weight loss in these patients was between 10-30% rather than the clinically accepted 5%. This weight loss has been maintained for at least a year, far longer than drugs for common obesity on the market and seemingly avoiding tachyphylaxis. Despite potential pitfalls the emergence of an approved MC4R agonist therapy affirms the necessity for further research into MC4R pharmacology and signaling as a latent potential target for treatment of obesity.

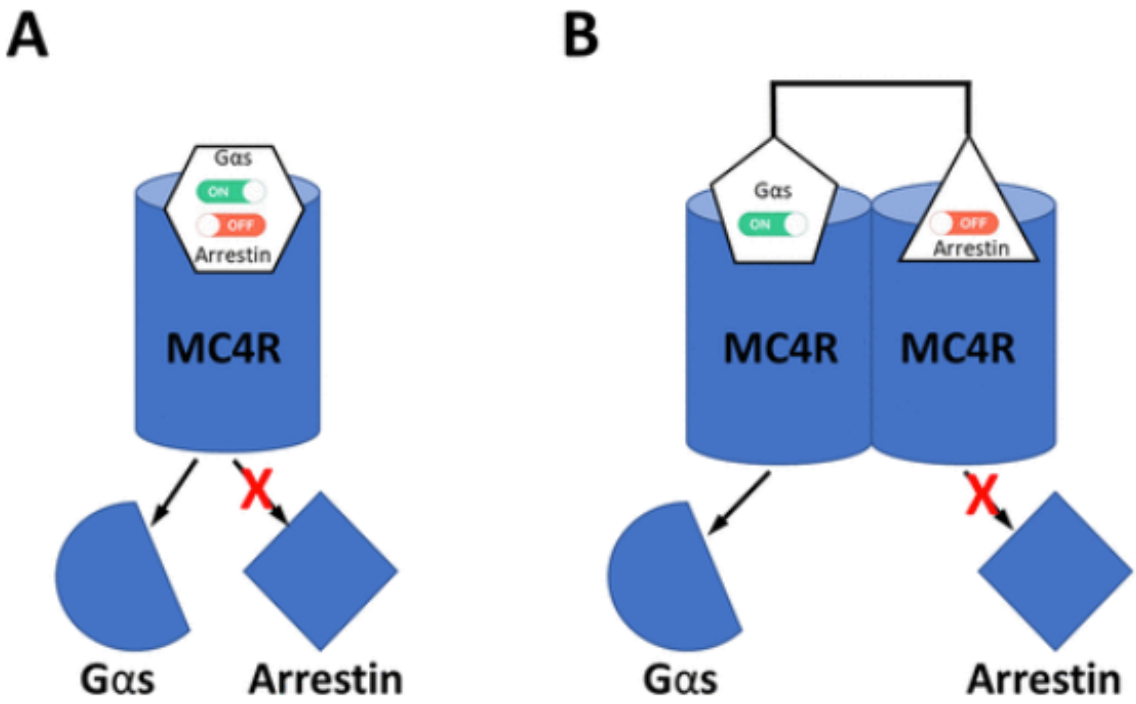

Figure 1-7. Schematic comparison of models for biased agonism.
A) Common model for biased ligand action wherein a ligand binds to a monomeric unit of a GPCR such as MC4R and thereby induces the conformational changes in the GPCR to signal increased interaction with one effector (Gαs) and diminished interaction with another effector (arrestin). B) Proposed model for biased ligand action wherein each of the two pharmacophores of a heterobivalent ligand interacts with its respective GPCR homodimer such that the interaction of each pharmacophore with its respective GPCR monomer and/or the interactions between the GPCR monomers induce the conformational changes in the GPCR dimers to signal increased interactions with one effector (Gαs) and diminished interactions with another effector (arrestin). Modified from (Topiol, S, 2018).

Discovery of a Role for Kir7.1 in the Melanocortin System

As a GPCR the canonical pathway for MC4R signaling has long been established as a mechanism whereby agonist binding promotes conformational change, generating intracellular signaling via coupling with heterotrimeric G-proteins. Conventionally, Gαs-coupled mediated activation of MC4R is the most vigorously and broadly investigated signaling pathway. This pathway has many physiologic implications critical for the MC4R loss of function phenotype, including anorexigenic signaling in the hypothalamus resulting in negative energy balance. Paradoxically, MC4R mutation analysis from obese individuals has shown that some mutations increase receptor basal activity, cAMP production, and respond to antagonists, yet obesity prevails [190] [191, 192] [193]. Several mechanisms may contribute to this phenotype. MC4R is known to undergo constitutive endocytosis in Neuro2A cells [194], however *in vivo* studies of other constitutively active GPCRs show the increase in cAMP is degraded by desensitization and/or induction of phosphodiesterase [195] [196]. A particularly interesting hypothesis for this phenotype is that Gαs signaling through MC4R may operate in parallel with another G-protein independent pathway to regulate energy homeostasis. Ghamari-Langroudi et al. investigated this hypothesis by pharmacologically blocking consecutive components affiliated with G-protein signaling in an *ex-vivo* slice preparation to identify an apparent G-protein independent pathway downstream of MC4R [104]. These studies leading to the discovery of Kir7.1 mediated depolarization of MC4R PVN neurons are further described herein.

Ex-vivo slice

Using an *ex-vivo* slice preparation of the PVN, α-MSH was found to depolarize MC4R neurons identified via GFP fluorescence, while AgRP infusion led to hyperpolarization thereby inhibiting MC4R neuron firing ability. To examine the Gαs–adenylyl cyclase-cAMP-PKA pathway specifically, cells were exposed to a series of specific inhibitors. Unlike previous studies, the α-MSH induced depolarization result remained in the presence of the G-protein inhibitors GDPβS

and gallein, a Gβγ blocker, and U0126, a MAPK inhibitor, narrowing out the role of GIRKs in α-MSH induced depolarization. Remarkably, Gαs, adenylyl cyclase, and cAMP signaling were also ruled out because α-MSH induced depolarization was also retained in the presence of the adenylyl cyclase inhibitor SQ22536, the cAMP inhibitor Rp-cAMPs and the PKA inhibitor H-89 [45].

Subsequently, current-voltage ramp analysis indicated that α-MSH generates an inward current closure of a steady-state-K^+-mediated inward rectifier (Kir) current, thus a Kir channel was responsible for the effect. In this experiment α-MSH was shown to reduce the inward rectification current of the cell while AgRP was able to increase it. From there, a specific Kir subunit, Kir7.1, was proposed to be a component of the channel responsible for this result using a panel of specific Kir channel blockers developed by Swale et al. [197]. Studies described below in HEK293 cells reinforced the finding that α-MSH and AgRP regulate Kir7.1 conductance. Furthermore, other inward rectifiers such as Kir2.3 and Kir4.1 channels did not couple to MC4R in cultured cells. However, the molecular mechanism by which AgRP mediates this effect currently remains unknown and will require further studies to be definitively clarified. As Kir channels form homo and hetero-tetramers, it remains to be determined whether MC4R modulates homo-tetramers of Kir7.1 or hetero-tetramers with other Kir channel subunits.

The discovery of G protein independent coupling of MC4R to Kir7.1 has suggested that AgRP is both a competitive antagonist of α-MSH action at the MC4R as well as a biased agonist that can act independently through MC4R binding to open Kir7.1 and hyperpolarize neurons (Figure 1-5). New neuroanatomical data supports both the original yin-yang model of α-MSH and AgRP competing for MC4R binding in areas of volume release from POMC and AgRP/NPY neurons (Figure 1-2), as well independent α-MSH and AgRP actions in different brain regions and on different subcellular domains of the target MC4R neurons. Briefly, both confocal microscopy [198] and electronmicroscopy [199] of PVH neurons suggests that while there are areas of likely volume release of both peptides, PVH cell bodies receive mostly AgRP synaptic contacts, while small distal dendrites receive mostly POMC synaptic

contacts. Thus, the microcircuitry is far more complex than originally suggested, in turn having profound impact on models of α-MSH and AgRP action *in vivo* (compare Figure 1-1 and 1-5).

Thallium assay in HEK293 cells

In addition to using conventional patch clamp techniques, Ghamari-Langroudi, Digby [200] employed a high throughput thallium (Tl^+) flux assay to further investigate the kinetics of MC4R-Kir7.1 signaling *in vitro*. This assay was originally designed to quickly and quantifiably detect potassium channel opening in order to characterize small molecule modulators of Kir channels [201]. It was adapted to characterize MC4R mediated regulation of Kir7.1 signaling and its modulators by Litt et al. [202]. To study the molecular mechanism of this interaction, HEK293 cells stably expressing MC4R and Kir7.1-M125R, improving the assay signal by increasing channel conductance, were exposed to α-MSH to induce channel closure. Tl^+ and K^+ are equally permeant ions through K^+ channel, thus detection of an intracellular Tl^+ -sensitive dye can be used to determine channel conformation and activity. Similar to whole cell recordings, a competitive inhibitor of cAMP-dependent protein kinases, Rp-cAMP was unable to block to α-MSH induced, MC4R mediated Kir7.1 flux. Co-expression of a dominant negative Gαs-construct that blocks the canonical Gαs-AC-cAMP signaling pathway also did not affect the EC_{50} of the α-MSH dose-response curve. In this system α-MSH mediates closure of Kir7.1 channels with an IC_{50} of $10^{-7.5}$ M, while AgRP mediates an increase in Tl^+ flux through Kir7.1 with an EC_{50} of $10^{-8.6M}$ [104]. Furthermore AgRP did not appear to couple to cAMP inhibitory protein Gαi, or to recruit arrestin. This response is specific to an interaction between MC4R and Kir7.1 as determined by expression of other melanocortin family members and inward rectifying potassium channels within this system. Ghamari-Langroudi et al. reported changes in potency for well characterized tool compounds of MC4R, where MSH analogue MC4-NN2-0453, with an EC_{50} of $4.9x10^{-9}$ M in intracellular cAMP accumulation assays, was found to have an increased potency of $4.9x10^{-10}$ M in a thallium flux assay, used to measure Kir7.1 coupling. This suggests a synergistic effect of α-MSH and cAMP on

Kir7.1 closure. Taken together, these findings reveal a novel MC4R signaling pathway, and some interesting pharmacological paradigms for the receptor, whereby some ligands have been found to favor the typical Gαs pathway versus Kir7.1. This opens an avenue for potential creation of biased ligands that favor the ion channel direct interaction/activation paradigm over classical G-protein signaling [203] [201] [204].

Kir7.1 and the Inward Rectifier Channels

Since the experiments in this thesis are focused on Kir7.1, a brief introduction of the inward rectifier potassium channels is in order. Inward rectifying K_+ currents (Kir) were first identified more than a half a century ago [205]. Since their discovery Kir channels have been characterized and classified into seven subfamilies (Kir1.x-Kir7.x) (Figure 1-8.B) [206]. These subfamilies are described by functional groups: 1) classical Kir channels (Kir2.x), 2) G protein-gated Kir channels (Kir3.x), 3) ATP-sensitive K^+ channels (Kir6.x), and 4) K^+- transport channels (Kir1.x, Kir4.x, Kir5.x, and Kir7.x). Kir channels regulate critical cellular parameters including resting membrane potential, action potential duration and hormone release via alleviating movement of K^+ into rather than out of the cell. Due to their role in regulating these processes, Kir channels are critical for the proper function of cardiac myocytes, neurons, pancreatic β-cells, renal epithelial cells, glia and epithelial cells. Thus, a better understanding of how Kir channels are regulated holds potential for future drug discovery.

Invariably, Kir channels are regulated by the signaling lipid PIP_2, which enables channel opening through direct binding with elements of the Kir channel [207] [208]. Besides PIP_2, factors that gate Kir channel conductance are unique to each sub-family and may include ions, polyamines, nucleotides, lipids, phosphorylation, and a variety of intracellular proteins. For instance, the G protein-coupled inward-rectifying channels (GIRK, Kir3.x) are opened by the βγ subunits of heterotrimeric G proteins [209], while Kir6.2 (K_{ATP}) is sensitive to intracellular ATP levels and regulated by the accessory sulfonylurea receptor [210]. Because Kir channels are insensitive to membrane voltage, when mechanisms like the

aforementioned are absent, the channel is active at all E_m. Despite extensive understanding of some Kir channels, the regulatory mechanisms of other Kir channels, including Kir7.1 remain largely uncharacterized.

Structure and expression

Like all ion channels, the Kir family channels serve as a protein pore for a specific ion, K^+, to pass through the cell membrane in order to passively maintain resting membrane potential and/or to actively facilitate electrical properties such as neuronal firing of cells. The first two Kir channels, Kir2.1 and Kir1.1, were isolated by expression cloning techniques in 1993 [211]. The primary structure derived from these channels is the same motif as Kir7.1, two membrane-spanning domains (TM1 and TM2), linked by an extracellular pore-forming region (H5) otherwise known as the "ion selectivity filter", and cytoplasmic amino (NH_2)- and carboxy (COOH)-terminal domains (Figure 1-8.A). The sequence of Kir7.1 is unique from other channel subtypes as it only shares ~38% homology with its closest family member, Kir4.2. Studies from Tateno et al. indicated that the C-terminus of Kir7.1 is a critical determinant for the plasma membrane localization of Kir7.1 protein [212]. Indeed the amino acid 1-54 N-terminus resides had no effect on plasma membrane transport, but by cleaving the original length of the C-terminus 204 amino acid residues down to 166 amino acid residues, Kir7.1 failed to traffic to the plasma membrane. An intracellular blocker, often Mg^{2+} or polyamines block outward K^+ flux.

A functional Kir channel is comprised of four transmembrane couplet strands forming a tetrameric complex [213] [214]. Due to the homology of the basic Kir subunit, both homotetramers and heterotetramers have been observed, although heteromerization is most commonly found between members of the same subfamily [215]. One isoform of Kir7.1 has been sequenced; and while Kir7.1 may form heterotetramers, no such assembly has been identified so far. In addition to sequencing domain analysis, x-ray crystallography has provided details of the three-dimensional structure of Kir channels Kir1.1, Kir2.1, Kir3.1, and Kir3.2 subunits down to the atomic level [216] [217] [218] [219] [220]. Notably, both NH_2 and

COOH terminals extend into the cytoplasm and may interact with each other to form a cytoplasmic gating regulator domain that is linked to, but distinct from the transmembrane domain.

Broadly, Kir channels are expressed in a vast array of cell types including: cardiac myoctyes, neurons, blood cells, osteoclasts, endothelial cells, epithelial cells, glial cells, and oocytes [206]. Kir7.1 has notable expression density in a diverse set of tissues, including kidney, uterine muscle, retinal pigment epithelium, intestine, lung, melanophores, and brain, where its localization is known to be polarized in membrane "macrodomains." The first noted expression of Kir7.1 in the CNS was found by *in situ* hybridization in the choroid plexus [221]. Later, immunolocalization improved this resolution by showing Kir7.1 at the apical membrane of the rat choroid plexus epithelium [222]. Recently a knock-in mouse expressing a Kir7.1 haemagglutinin (HA)-tagged protein was created to further improve characterization of tissue distribution and as a modeling tool for localization studies [223]. This mouse, Kir7.1-HA, was made using a CRISPR/Cas9 knock-in strategy, and the HA-epitope had no adverse effect on channel function as detected by whole-cell current and native cell patch-clamp. The distribution of Kir7.1 as determined by Western blot and HA-fluorescent immunoreactivity confirmed and added granularity to prior localization knowledge of Kir7.1. Kir7.1-HA was detected in the choroid plexus, rentinal pigment epithelium, ileum of small intestine, inner medulla of kidney, basolateral expression in the respiratory tract epithelium from trachea to bronchiole, and the epithelium of the nasal cavity and nasopharnyx of newborn animals. This presence no doubt contributes to the embryonic lethality phenotype seen in prior attempted knockout studies[224]. The Kir7.1-HA is a convenient and reliable animal model that will be useful to further parse Kir7.1 function.

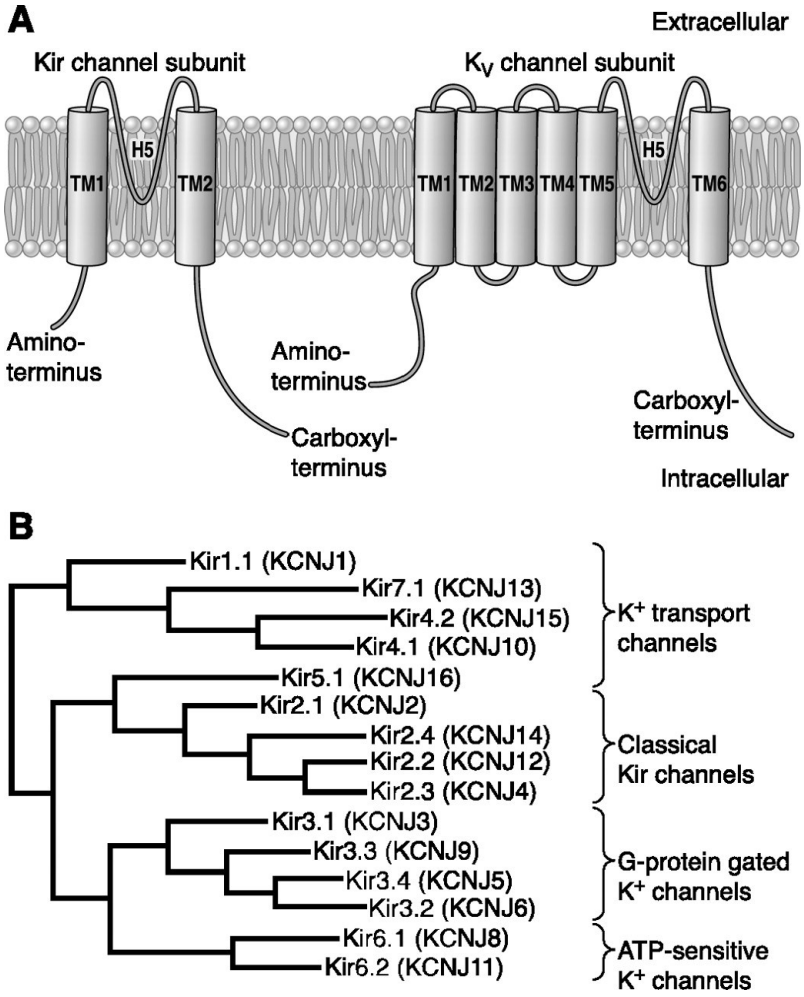

Figure 1-8. Basic structure and Kir channel phylogenetic tree.
A) Primary structure of the Kir channel subunit (*left*). Each Kir subunit contains two transmembrane (TM1 and TM2) regions, a pore-forming (H5) loop, and cytosolic NH_2 and COOH termini. As a comparison, the structure of voltage-gated K^+ (K_v) channel subunit, which possesses six transmembrane (TM1-TM6) regions, is shown on the *right.* B) Amino acid sequence alignment and phylogenetic analysis of the 15 known subunits of human Kir channels. These subunits can be classified into four functional groups. Modified from (Hibino et al., 2010).

Functional studies in electrophysiology and uterine smooth muscle

The physiological activity and function of Kir channels is dependent upon regulation of pore opening, ion flux, and channel localization within the cell. There is still much to understand regarding channel subtype regulation although some functional studies have been conducted. Changes in Kir channel conformation can modulate ion flux and channel pore opening kinetics. Furthermore, localization of Kir channels, whether on epithelial cell apical or basolateral membrane or pre-or post-synaptic sites in neurons, greatly impacts the functional role and consequence of Kir channel activity. Kir channel subfamily members have varying degrees of inward rectification from weak to strong where Kir1 << Kir3 <Kir2. Kir7.1 is distinct from other Kir channels due to its exceptionally small, single channel conductance (~50fS) [225], low sensitivity to external barium cationic blockade, and inward rectification independent of external K^+ concentration [226]. Since its discovery 20 years ago by three independent groups, knowledge of the physiological roles of Kir7.1 has been sparse, but the studies available have yielded important perspectives on the consequences of receptor mutations and downstream systemic effects of normally functioning Kir7.1 [221] [227] [228].

Kir7.1 appears to play a role in cerebrospinal fluid (CSF) secretion as well as cell volume regulation due to its presence in the lateral and fourth ventricle choroid plexus on the apical membrane of epithelial cells. From this location electrophysiological analysis suggests Kir7.1 may contribute to the resting potential of the cell as well as serving as an apical leak pathway for ~90% of the K^+ ions pumped into the cell by the Na^+/K^+-ATPase [229].

Recent studies have found upregulated Kir7.1 expression in uterine myocytes hyperpolarizes the uterus, promoting quiescence during gestation [230]. Kir7.1 as a target for uterine dysfunction therapy was initially defined by GWAS enrichment in myometrial smooth muscle [231]. Kir7.1 is important in this tissue for regulating uterine excitability during pregnancy. During the majority of pregnancy, labor may be in part inhibited by high expression of Kir7.1 promoting quiescence during gestation. Subsequently during labor the decline of Kir7.1 expression, as mimicked

by lentiviral miRNA knockdown in mice, promotes contractile force and duration by depolarizing the plasma membrane and promoting voltage-gated calcium entry. The Kir7.1 specific inhibitor, VU590, was tested in mice in the absence or presence of oxytocin to induce and support long contractions in uterine tissue. Thus, this single channel, Kir7.1, has direct and profound functional implications for uterine contractility [231]. Additionally, the effects of blocker VU590 on spontaneous and agonist-induced contractions of human pregnant myometrium were tested *in vitro* [232]. While VU590 modifies contractility, confirming the role of Kir7.1, it does not produce the types of contractions that would be necessary for use as a clinical therapeutic. Nevertheless these studies have exciting implications for magnitude of physiologic effects Kir7.1 can induce.

Known mutants –jaguar and autosomal dominant vitreo-retinopathies

Several naturally occurring Kir7.1 mutations with functionally deleterious properties have been catalogued in zebrafish and humans. These mutations result in a variety of channel defects including depolarization of the resting membrane potential, disruption of Kir7.1 currents, premature truncation and degradation, and altered protein localization. Similar to the functional effect, the types of mutated alleles also manifest from a variety of sequenced point mutations (Table 1-3).

Table 1-3. Known point mutations in Kir7.1 human and fish mutants

Allele inheritance	cDNA sequence	Protein sequence	Functional effect	Disease association	Reference
Homozygous, missense	359T>C	Ile120Thr	Cone-rod dysfunction, clumped pigmentation	LCA? early onset cataract	Khan, 2014
Homozygous nonsense	496C>T	Arg166X	Cone-rod dysfunction, clumped pigmentation	LCA	Sergouniotis, 2011
Homozygous missense	722T>C	Leu241Pro	Cone-rod dysfunction, clumped pigmentation	LCA	Sergouniotis, 2011
Dominant-negative	484C>T	Arg162Trp	Depolarized and fragile cells	SVD	Hejmancik, 2008
Compound heterozygote	314G>T & 655C>T	Ser105Ile & Gln219*	Cone-rod dysfunction, clumped pigmentation	*LCA*	Perez-Roustit, 2017
Haploinsufficient?	Obe^{tc271d}	Thr128Met	Abnormal pigment pattern formation	*Jaguar/obelix*	Iwashita, 2006
Haploinsufficient?	Obe^{td15}	Leu130Phe	Abnormal pigment pattern formation	*Jaguar/obelix*	Iwashita, 2006
Haploinsufficient?	Jag^{b230}	Phe168Leu	Abnormal pigment pattern formation	*Jaguar/obelix*	Iwashita, 2006

Prior studies have identified that a mutation disrupting $Kir_{7.1}$ conductance is responsible in a dose dependent manner for disorganizing the stripe pattern in *obelix* (aka *jaguar)* zebrafish [233]. The appearance of a homozygous *jaguar* mutant is spots rather than broader dark stripes due to defective xanothophores (yellow pigment) appearance adaption in response to melanophores (black pigment), which express MC1R, depolarization and dispersion signal [234]. In fish, *Kcnj13*/Kir7.1 is required for melanophore function [235]. When Kir7.1 is disrupted, mutant melanophores cannot respond correctly to the melanosome dispersion signal derived from the sympathetic neuron and the melanosome aggregation is constitutively activated. Interestingly, the defect in *jaguar/obelix* melanophores may segregate to neuronal signaling as the melanorphores were still responsive to hormone epinephrine. Because pigment pattern appeared to have near complete penetrance, the dominant phenotype of *jaguar* mutations may be caused by haploinsufficiency for the gene [236]. From sequencing analysis thus far, *jaguar* is a mutation that appears to occur in the pore region (T128M and L130F) or in the TM2 helix (F168L), resulting in suppression of Kir7.1 currents.

Two diseases have been associated with mutations in human *KCNJ13*. Both are vitreoretinopathies, progressive congenital eye disorder often ultimately resulting in blindness—snowflake vitreoretinal degeneration [237] (SVD) and Leber's congenital amaurosis [238] (LCA). Both disease mechanisms have families whose sequence results have traced mutated genes of interest back to a large array of culprits, including, but not exclusive to Kir7.1 dysfunction [239] [240].

SVD is an autosomal dominant pathology characterized as a developmentally progressive eye disease affecting the retina and vitreous with an end stage of retinal detachment [241]. A low prevalence the disorder has been described in multiple families. Genomic analysis of SVD patients has revealed a heterozygous mutation (484C>T, R162W) in the Kir7.1 gene (Table 1-3) (Figure 1-9). This mutation was mapped to the short polypeptide chain between the TM2 α-helix and the COOH terminus, which may play a role in channel activation by prematurely depolarizing

RPE cells resulting in Ca2+ overload and cell death [242] [237]. As an example of one channelopathy mutant, the R162W Kir7.1 channel carries a nonselective cation current that disrupts the channel-closed state in a CHO-K1 cell overexpression system, depolarizing the cells and increasing their fragility. Additionally, this mutation resulted in a non-functional channel in heterologous expression studies that rendered wildtype channel nonfunctional too through a dominant negative mechanism. Although Kir7.1 is not a structural component of the vitreous, the degeneration of cell types like the RPE where Kir7.1 is expressed, may cause the abnormalities in the retina of SVD patients as well.

LCA is a particularly rare, severe and early-onset form of retinal degeneration. At least 25 genes have been implicated in 70% of LCA cases, one of which is *KCNJ13* [243]. Using genome-wide scans, sequencing, and immunoreacivity assays *Kcnj13* was identified as a critical gene responsible for inward rectification of retinal pigment epithelial (RPE) cells [244] [238] [245] (Table 1-3) (Figure 1-9). Multiple studies have been conducted to determine how point mutations in Kir7.1, mainly expressed on the RPE apical membrane, induce such detrimental effects on neighboring cell types. Recently, Shahi et al conducted an in depth analysis of electroretinograms (ERG) after Kir7.1 suppression by shRNA or blocker VU590. These ERGs, which reflect photoreceptor hyperpolarization in response to light, suggest that a decrease in RPE Kir7.1 channel activity contributes directly to the abnormal ERG associated with blindness via alterations in sub-retinal space K+ homeostasis in the vicinity of the photoreceptor outer segment [240]. Kir7.1 mRNA and protein expression is much higher in RPE cells than retinal cells, thus *Kcnj13*-related-blindness originates at the RPE cells and is not due to defective retina. Additionally, York et al recently described the interaction of GPCR–Kir7.1 in RPE cells *in vitro* where a oxytocin (OXT)-stimulated inhibition of Kir7.1 activity is through a PIP2-dependent Ca^{2+} response of the oxytocin receptor [246]. This discovery of Kir7.1 interacting indirectly with another GPCR in a different tissue type further validates the necessity to study G-protein independent regulation mechanisms by ion-channels.

The Cone lab's discovery of MC4R's unique signaling pathway through Kir7.1 in a brain slice preparation and in transfected cells suggests that this channel may also play a crucial role in MC4R function *in vivo*. Indeed an *in vivo* role for an AgRP $Kir_{7.1}$ signaling pathway is supported by evidence from an AgRP analogue, mini-AgRP, which has normal affinity for MC4R yet weaker induction of food intake in rats, and reduced ability to couple MC4R to Kir7.1 [247, 248]. Additionally, zebrafish with Kir7.1 morpholino knockdown exhibit reduced linear growth, a phenotype identical to a response induced by MC4R activation (Figure 1-10) [45]. Data presented in this thesis sought to test the hypothesis that Kir7.1 is required for normal function of the MC4R *in vivo.*

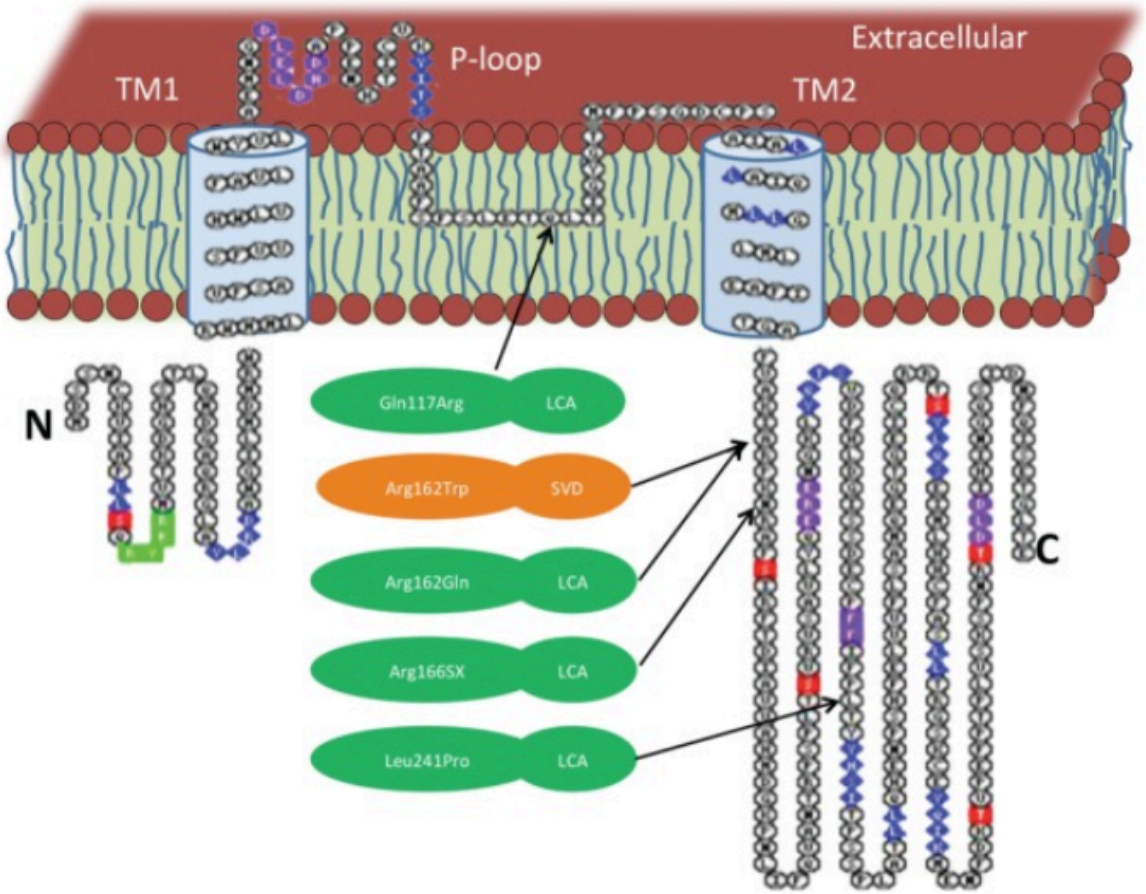

Figure 1-9. Kir7.1 membrane topology and mutations causing LCA and SVD. Localization of consensus sites for phosphorylation by Casein Kinase II (^{T}321 and ^{T}337), PKA (^{S}287) and PKC (^{S}14, ^{S}169 and ^{S}201) shown in red filled squares, as well as various protein trafficking signals (green boxes: ER retention signal; purple diamonds: diacidic motif; blue diamonds: dileucine motif). LCA and SVD mutation locations are also shown as filled circles indicated by arrows. Localization of mutations on the topological image is based on the TOPO2 program. TM – transmembrane. (Modified from Kumar, et al. 2014).[249]

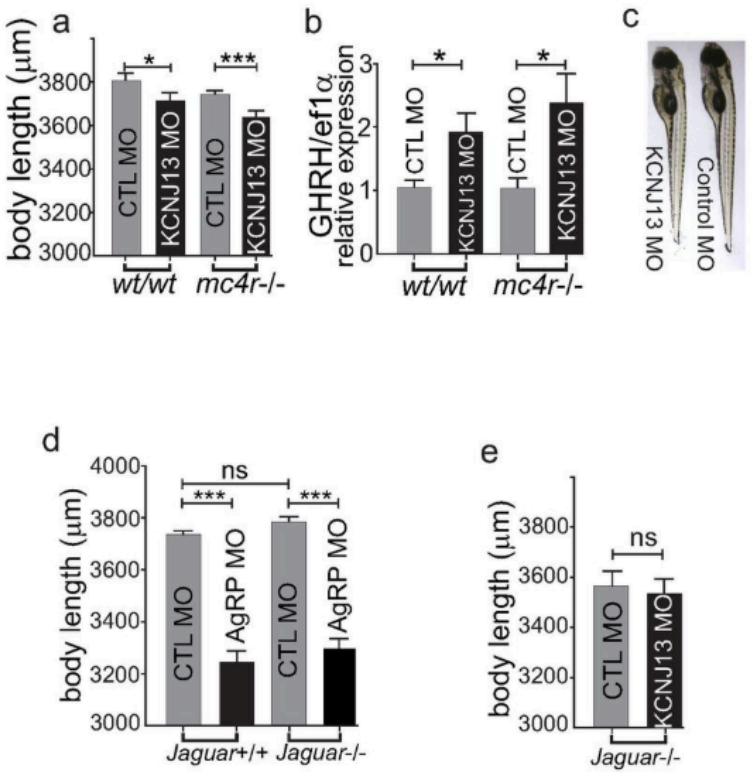

Figure 1-10. Effects of Kir7.1 and MC4R signaling in larval zebrafish.
A-C) Knock-down of the *Kcnj13* gene by *kcnj13* morpholino oligonucleotide (MO) suppresses the axial growth of larvae in wild-type and *mc4r* null zebrafish. Sibling wild-type or *mc4r*-null zygotes were bred and injected with antisense *kcnj13* morpholino oligonucleotide at day 0. **A)** The axial body length was measured at 5 dpf. Each group of 30 fish was harvested for RNA extraction and cDNA synthesis. **B)** Relative expression of *ghrh* mRNA was measured and normalized to the house keeping gene *ef1a* with qRT–PCR. The wild type fish that were injected with MO against *kcnj13* expressed significantly higher copies of *ghrh* mRNA than those that were injected with control MO. (control MO, $n = 9$, 1.056 ± 0.116 vs *kcnj13* MO, $n = 9$, 1.935 ± 0.294, unpaired t-test, $P < 0.05$). MC4R-null fish that were injected with *kcnj13* MO have significantly higher GHRH expression than MC4R-null fish that were injected with control MO (control MO, $n = 9$, 1.040 ± 0.164 vs *KCNJ* MO, $n = 8$, 2.395 ± 0.461, one-way ANOVA, $P < 0.05$). **c**, Representative WT fish injected with *kcnj13* MO vs control MO. D-E) *jaguar* wild-type and null mutant siblings were bred and injected with 7.5 ng non-targeting standard control or 7.5 ng antisense morpholino oligonucleotide targeting *agrp* or *kcnj13*. **D)** Knockdown of AgRP with *agrp* MO in the absence of Kir7.1 also reduces larval growth (mean ± s.e.m., $n = 43$, $P < 0.001$, unpaired t-test). **e**, The deletion of Kir7.1 in *jaguar* null blocks effects of *Kcnj13* MO on MC4R-mediated inhibition of growth (mean ± s.e.m., $n = 58$, unpaired t-test). Data are representative of three independent experiments. (From Ghamari-Langroudi, et al., 2015)

Knockout attempts

In 2015 two attempts were made to generate a *Kcnj13* knockout mouse model using 1) the CRISPR-Cas9 zygote injection system [250] and using 2) the Velocigene method for targeted deletion of the full coding sequence in mice [224] in order to verify and further study the pathogenic role of human *Kcnj13* mutations, such as LCA and SVD. Both strategies achieved germline transmission, however all homozygous null *Kcnj13-/-* mutant mice died within a couple hours after birth on postnatal day zero (P0). This is an interesting discovery as ablation of *KCNJ13* in humans by point mutation as seen in LCA does not appear to have adverse off target effects outside of the eye, and zebrafish with homozygous *Kcnj13* mutations have only a pigmentation phenotype. This may be a consequence of tetramer formation, tissue specific localization, or cell specific regulation. Herein phenotypic characteristics of both mouse models will be described.

Because complete ablation of *Kcnj13* resulted in postnatal lethality, Zhong et al. worked upstream of founder line breeder crosses, using another strategy within the CRISPR-Cas9 by using F0-generation mice which showed 80% mosaicism in the RPE [250]. Indeed mosaic expression correlated with decreased response to light and photoreceptor degeneration, mimicking the human LCA RPE phenotype. By using mosaic animals, regions with healthy wt RPE cells and *Kcnj13* mutant cells were compared within the same eye. Whereas RPE cells with defective Kir7.1 survived, adjacent photoreceptors showed signs of cell degeneration. Interestingly, the functionality of wildtype RPE cells was sufficient to rescue tangential photoreceptors affected by mutant RPE cells. Thus it appears Kir7.1 acts in a non-cell autonomous manner and is necessary in RPE cells to indirectly regulate and maintain photoreceptor survival (as detected by TUNEL staining).

Later in 2015 Villanueva et al. delineated prominent mechanisms underlying early postnatal lethality in mice lacking Kir7.1 in a transgenic model where ablation of *Kcnj13* is concordant with expression of inserted lacZ-reporter to drive β-galactosidase expression under transcriptional control from the *Kcnj13* promoter as an internal reporter of channel tissue distribution [224]. Heterozygous *Kcnj13* $^{+/-}$

female x *Kcnj13* $^{+/-}$ breeding pairs produced fetal offspring with expected Mendelian distribution of 25% *Kcnj13* $^{+/+}$, 25% *Kcnj13* $^{-/-}$ and 50% *Kcnj13* $^{+/-}$ and typical *in utero* development from 11.5-18.5 days post coitum (dpc). Thus postnatal embryonic lethality was not due to extreme defective embryonic development, and lethal abnormalities must accumulate during the final days of development and at P0. It is well established that Kir7. 1 is present in epithelial tissues where it colocalizes with the Na^+/K^+pump, likely serving to recycle K^+ in order to maintain a negative membrane potential compatible for the pump. By examining sections from several tissues and organ systems with established *Kcnj13* expression for changes in histology and presence of pathological morphology indicators by β-galactosidase in *Kcnj13* $^{-/-}$ the likely cause of postnatal lethality was determined. Lung morphometry, showed that *Kcnj13* $^{-/-}$ P0 lungs did not appear to be fully distended, however, this was not the likely cause of lethality as retardation was only moderate. Strikingly, Kir7.1 is expressed extensively in epithelial cells along the respiratory tree from the trachea to the bronchioles and alveoli, where it may have a role in gas exchange, mucocilliary clearance, and/or adsorption or secretory functions of fluid along the airway. Another potential cause of postnatal lethality is craneo-facial malformation in *Kcnj13* $^{-/-}$ mice. Indeed, these mice had complete secondary cleft palate and the expression of *Kcnj13* in epithelium covering the palatal processes coincides with the point palate sealing should take place (14.5-16.5 dpc). Kcnj13 also appears to regulate tracheal smooth muscle cell organization, polarity and cartilage formation during development (Yin, et al. 2018). Without functional Kcnj13, mutant postnatal mice died due to defects in tracheal tubulogenesis and respiratory air sacs. Thus *Kcnj13* $^{-/-}$ PO pups failed to thrive in part due to lack of nutritional uptake. It has been hypothesized that channel activity, controlling membrane potential mediating fluxes in K+ may invoke cell migration, proliferation, or differentiation critical for palatal sealing and these mechanisms all merit further investigation as means by which Kir7.1 may regulates cellular functions.

Prior studies of characterizing Kir7.1 were limited to *in vitro* systems, acute slice, or global knockout. Because it appears that MC4R has two distinct modes of signaling, through Gαs and Kir7.1, that have yet to be interrogated with regard to

their control of either the diverse physiological functions of the MC4R, or the kinetics of the responses of the MC4R to its endogenous ligands. I originally proposed to evaluate the physiological roles, and kinetics, of variant MC4R signaling modalities through tissue specific and systemic knockout mouse models, and through pharmacological assessment. I hypothesize that MC4R functions as a rheostat of energy homeostasis by utilizing both tissue specific Gαs and Kir7.1 signaling modalities as well as unique kinetic aspects of these modalities.

CHAPTER 2

LOSS OF Gαs FUNCTION IN MC4R

Introduction

Heterotrimeric G-proteins are a group of membrane associated complexes that are critical for signaling at the plasma membrane and convey the signal to other intracellular sites through signaling partners. Each G-protein is comprised of an α-subunit which binds guanine nucleotide and mediates signals from GPCRs to downstream effectors as well as a βγ dimer, all of which are encoded on distinct genes. When G-protein Gαs couples to cell surfaces receptors it stimulates adenylyl cyclase and downstream production of cAMP. Because Gαs is ubiquitously expressed and interacts with many GPCRs, changes in Gαs expression, be it gain of constitutive signaling function or loss of function deleterious mutation often have notable physiologic consequences [251]. Notably, compensatory changes in G-protein subunit subtype accumulation have been observed *in vitro* after silencing of individual subunit genes [252] [253]. Thus because this is a developmental model a compensatory mechanism may occur in our proposed model. Nevertheless, we thought this unlikely with heterozygous expression of Gαs specifically in MC4R cells, making the Gαs flox; MC4R-Cre mouse model a useful tool to understand G-protein dependent signaling through MC4R.

CNS expression of Gαs, encoded by the *Gnas* gene, is maternally imprinted except for in the NTS, thus the paternal copy of *Gnas* is epigenetically silenced hypothalamic nuclei [254] [255]. This leads to a parent-of-origin-specific metabolic phenotype, which manifests in conditions with Gαs loss of function mutations like Albright hereditary osteodystrophy [256]. The Weinstein laboratory has progressively used Gαs parent-of-origin-specific, Gαs tissue specific, and most recently Gαs cell type specific deletion models to elucidate the role of Gαs and other G-protein subunit signaling pathways in metabolic syndrome [257] [94] [258] [259] [260]. While it is apparent that functional maternal allele Gαs is necessary for

energy homeostasis, it remained unclear which G-protein subunits are necessary, for features of MC4R regulated response, and in what nuclei.

When Gαs expression was deficient in PVH and amygdala, via SIM1-Cre targeted deletion, animals had a small reduction in energy expenditure, no change in linear growth, a gender specific gain in lean and fat mass, no change in thermogenesis, reduced food intake response to MTII, reduced baseline systolic blood pressure (BP), lack of BP induction to MTII, and gender specific change in glucose metabolism [260] [259]. Gαs deficiency in the DMH results in obesity with reduced energy expenditure, reduced heart rate, reduced UCP1 BAT activation with no metabolic response to cold, yet no change in food intake [258]. Mice with $G_{q/11}\alpha$ specific loss in the PVH, which stimulates phospholipase C, developed severe hyperphagic obesity, increased linear growth, impaired glucose metabolism only in older, male mice, with no effect on energy expenditure [259]. Thus $G_{q/11}\alpha$ may selectively target appetite regulation. However these studies targeted whole hypothalamic nuclei, and thus did not directly address MC4R - Gαs coupling.

A more recent study in mice where Gαs is excised by Cre-lox recombinase specifically in MC4R cells recapitulated the MC4R deletion syndrome with morbid, early onset obesity, increased food intake, decreased energy expenditure, impaired insulin sensitivity, increased linear growth, and reduced cold-induced thermogenesis [94]. Curiously, these animals have reduced heart rate, but unlike prior deletion model no impairment of blood pressure. Likewise animals lack a response to exogenous agonist MTII in stimulating L-cell PYY release, yet PYY, a post-prandial hormone whose secretion is stimulated by MC4R- α–MSH-induced-cAMP pathway, is elevated at baseline. These discrepancies indicate potential dysfunction in MC4R cells due to off-target effects of Cre recombinase or aberrant expression defects, as Gαs and MC4R are widely present in many cell types early in the developing embryonic brain [261]. Thus, MC4R-specific deletion of Gαs largely recapitulates the metabolic syndrome observed with MC4R deficiency. However, no controls were included that could address a potential developmental effect of Gαs deletion on the development of MC4R neurons.

At the beginning of our studies of Kir7.1, we exchanged mouse model lines with the Weinstein lab (MC4R-t2A-Cre in exchange for Gαs $^{fl/fl}$) in order to study, compare, and cross-validate the loss of Gαs in MC4R cells to the loss of *Kcnj13* in MC4 cells under the same conditions and with the same experimenter. Unfortunately, my work to characterize the phenotype of Gαs $^{fl/fl}$;MC4R-Cre Tg was stalled by inability to surmount postnatal P0 lethality of mice with this genotype in our facilities, despite mimicking Weinstein lab breeding pair conditions and paradigm precisely. Indeed the Weinstein lab along with many other groups has reported lethality of *Gnas* germline knockout models as early as 10.5 days post coitum (dpc). [254] [251]. This is to be expected for total deficiency of a key cellular signaling molecule that is ubiquitously expressed. In many inbred genetic background strains heterozygous deletion of *Gnas* was also lethal. Even in the CD-1 outbred strain, only 20% of heterozygous pups survived to weaning though they were born at expected Mendelian ratios. Thus there appears to be a flaw with the Gαs $^{fl/fl}$;MC4R-Cre Tg model system. In our subsequent studies we characterize the phenotypic response of Gαs $^{fl/+}$;MC4R-Cre Tg on a Black Swiss mixed C57BL/6 mixed background with the Gαs flox allele inherited from the maternal allele (breeding pairs = Gαs$^{fl/fl}$ dam on 100% Black Swiss background x MC4R-t2A- Cre Tg sire) in order to achieve full PVN penetrance of Gαs flox under various parameters of known MC4R action.

Results

Chow diet response in Gαs heterozygote

To determine the effect of heterozygous deletion of Gαs $^{fl/+}$;MC4R-Cre Tg we studied male and female mouse weight gain from four weeks to 22 weeks of age compared to control Gαs $^{fl/+}$;MC4R-Cre wt littermate control animals (Fig 2-1). Contrary to the Weinstein results, during this time no significant difference was detected at any week or overall by multiple t-test and one-way ANOVA respectively. Body composition was also unchanged (not shown).

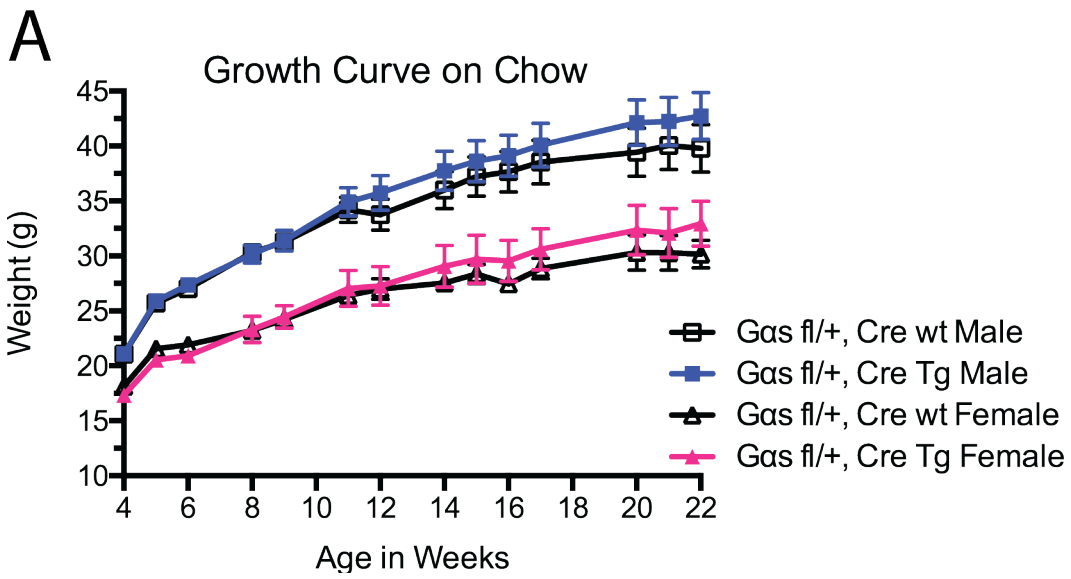

Figure 2-1. No obesigenic effect from heterozygous loss of Gαs in male and female mice on chow diet.
Growth curves on chow of $G\alpha s^{fl/+}$; MC4R-Cre Tg and $G\alpha s^{fl/+}$; MC4R-Cre wt males and females. Flox allele inherited from $G\alpha s^{fl/fl}$ dam on 100% Black Swiss background . One way ANOVA with multiple comparisons. (n = 6-9/group, *P<0.05, **P<0.005, ***P<0.0005, ****P< 0.0001)

Diet-induced obesity and glucose tolerance response in Gαs heterozygote

The loss of MC4R in neurocircuitry pathways regulating energy homeostasis impacts response to chow and high fat diet [130]. In order to test effective response to a metabolic stressor, mice were fed high fat diet (Research Diets D12492, 60% kcal fat by volume) to induce obesity. Effective utilization of caloric excess is an indicator of normally functioning MC4R signaling. Dually housed male and female mice of the same genotype were switched from chow to HFD at 7-8 weeks of age and maintained on *ab libitum* HFD until groups were 19-20 weeks of age. Growth and food intake were monitored weekly for 11 weeks. Heterozygous loss of maternal G-protein subunit Gαs resulted in significant weight gain compared to control growth curves (Fig 2-2.A) starting at 5 weeks and continuing through 11 weeks. The overall weight gain growth profile of female $G\alpha s^{fl/+}$;MC4R-Cre Tg was significantly greater than $G\alpha s^{fl/+}$;MC4R-Cre wt mice as measured by one way ANOVA with multiple comparisons. No obesigenic effect was observed in males over this time course.

HFD energy intake as measured by the sum of kcal consumed per mouse from 1 to 14 days was assessed to determine if hyperphagia occurred in mice on HFD. Female Gαs $^{fl/+}$;MC4R-Cre Tg mice trended toward hyperphagic from 1-7 days, however normal intake compared to control animals had resolved by 14 days and there was no significant difference overall as measured by multiple t-tests with Holm's Sidak correction. There was no significant difference in male HFD consumption. Feed efficiency calculation (Fig 2-2.C) showed that female Gαs $^{fl/+}$;MC4R-Cre Tg mice weight gain on HFD (energy density 5.21 kcal/g) was due to a significant change in feeding efficiency from 1-14 days on HFD as determined by two-way ANOVA with multiple comparisons (95% CI of diff 15.3 to 44.2, P****) and this efficiency appears to continue through the duration of HFD exposure. Measurements of body composition by NMR scan showed that after consuming HFD for 20 weeks, heterozygous loss of Gαs caused a significant elevation in both female %fat mass (Fig 2-2.D), *P = 0.0013, and %lean mass (Fig 2-2.E), *P = 0.0011, while we did not measure an effect in males as measured by multiple t-tests with Holm's Sidak correction.

Another means of challenging energy homeostasis is via HFD and chow diet cycling. In order to test animals weight and feeding response and utilization of fluctuating energy source, *ab libitum* chow and HFD were intermittently switched every seven days. No significant effect was observed in growth curves of male (Fig 2-3.A) or female (Fig 2-3.C) or corresponding energy intake measured by kcal consumed in male (Fig 2-3.B) or female (Fig 2-3.D) mice.

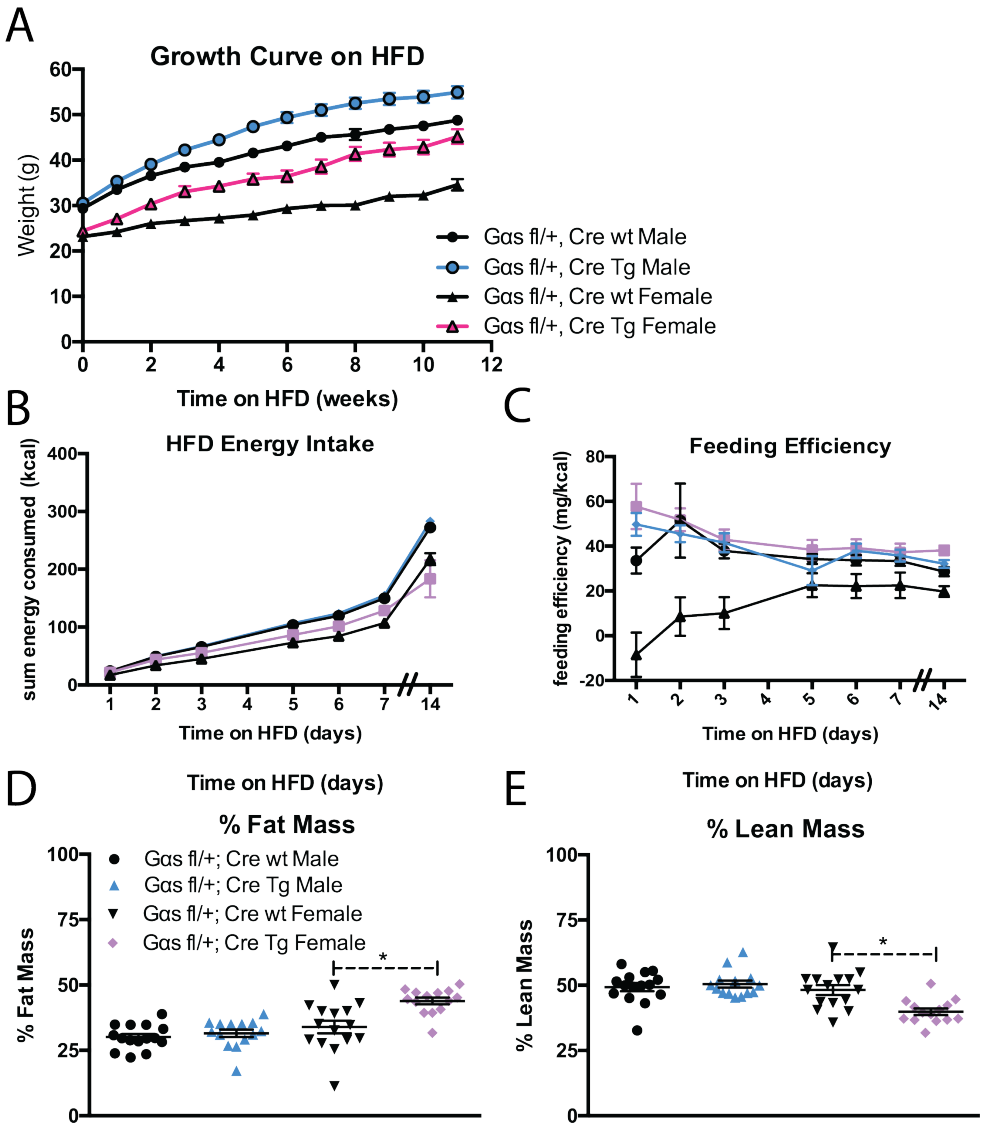

Figure 2-2. Obesity by increase in %fat mass in female mice with heterozygous loss of Gαs function in MC4R cells.

A) Diet induced obesity (DIO) growth curves of male and female mice on high fat diet (HFD) for 12 weeks in Gαs $^{fl/+}$; MC4R-Cre Tg and control genotype Gαs $^{fl/+}$; MC4R-Cre wt. Fed HFD from 8 to 20 weeks of age. Female Gαs $^{fl/+}$; MC4R-Cre Tg vs. Gαs $^{fl/+}$; MC4R-Cre wt *P < 0.05, one way ANOVA with multiple comparisons and by multiple t-tests with significant difference beginning at 5 weeks – 12 weeks on HFD. B) HFD energy intake as measured by sum of kcal consumed/day. NS difference in female and male mice consumption over 7 days, multiple t-tests with Holm Sidak's correction. C) Female mice are significantly more efficient than control mice in allocating HFD, while males are NS from 1-14 days on HFD. 2-way ANOVA with multiple comparisons 95% CI of diff 15.3 to 44.2, P****. D) %Fat mass and %lean mass in male and female groups. Female Gαs $^{fl/+}$; MC4R-Cre Tg vs. Gαs $^{fl/+}$; MC4R-Cre wt %fat mass **P = 0.0013, %lean mass ** P = 0.0011. Multiple t-tests. (n = 14-21/group, *P<0.05, **P<0.005, ***P<0.0005, ****P< 0.0001).

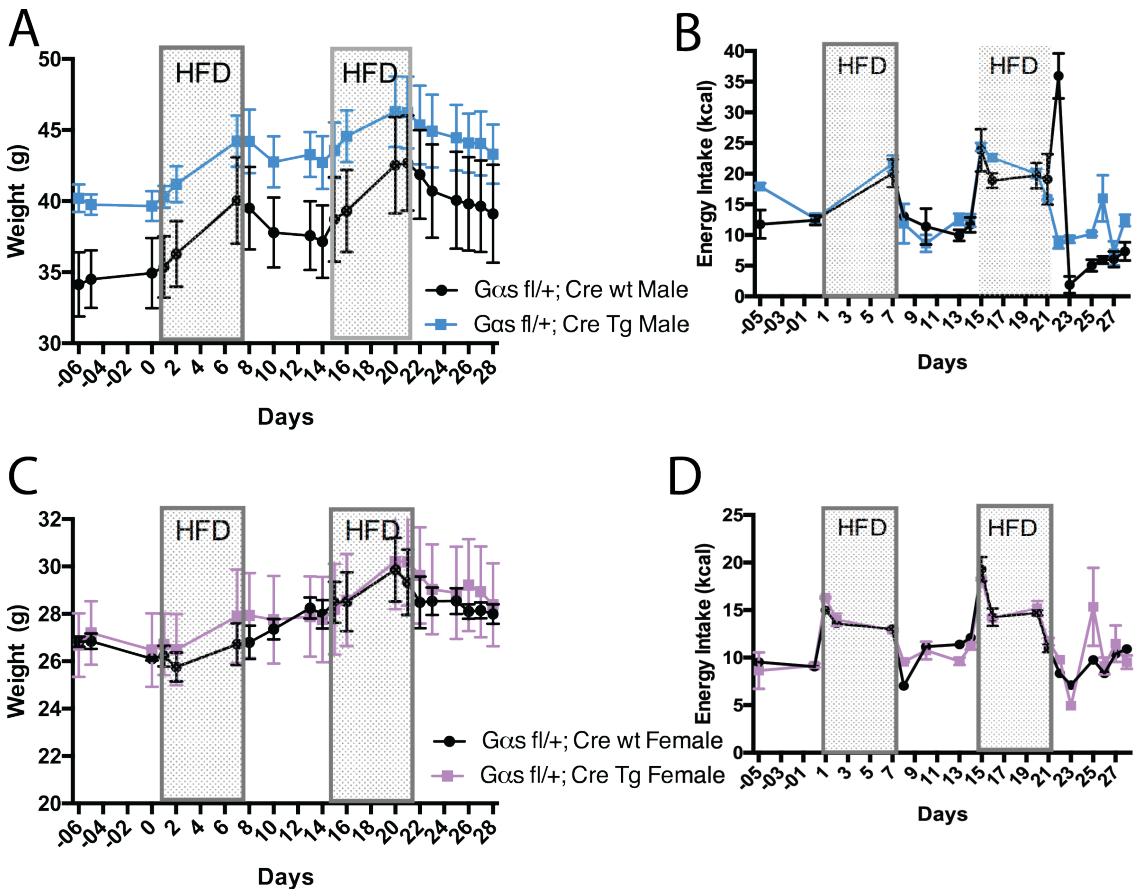

Figure 2- 3. Gαs$^{fl/+}$; MC4R-Cre^{Tg} respond normally to acute fluctuations in dietary fat from cycling chow diet and HFD
Normal chow diet and HFD switched every 7 days for 2 cycles in group housed Gαs$^{fl/+}$; MC4R-Cre^{Tg} and control Gαs$^{fl/+}$; MC4R-Cre^{wt} mice. No significant difference in growth curves of change in weight in A) male and C) female experimental and control groups. No significant difference in energy intake in kcal indicating week to week fluctuations in consumption from chow to HFD in B) male and D) female mice. One way ANOVA with multiple comparisons. (n = 10- 15 animals /group, *P<0.05, **P<0.005, ***P<0.0005, ****P< 0.0001).

HFD is known to challenge energy homeostasis and drive imbalance toward metabolic syndrome. To test the efficiency of Gαs$^{fl/+}$; MC4R-Cre^{Tg} animals in responding glucose after sustained dietary conditions of caloric excess, glucose utilization was tested by IPGTT in DIO mice on HFD for 20 weeks. After a 10 hour fast, a dose of 2 mg/kg glucose, adjusted in proportion to lean mass, was administered to mice and glucose levels were measured from 0-120 minutes (Fig 2-4.A). At 60 -120 minutes post injection, glucose was significantly elevated in female

$G\alpha s^{fl/+}$; MC4R-Cre^{Tg} vs. control mice with p values of P = 0.0006 at 60 minutes and P = 0.0001 at 120 minutes. Likewise area under the curve (AUC) analysis by one-way ANOVA with multiple comparisons confirmed that female $G\alpha s^{fl/+}$; MC4R-Cre^{Tg} had significantly reduced glucose tolerance compared with control littermates (Fig2-4.B). In agreement with prior characterization of response to HFD, no significant difference was observed in males. These physiologic characterization data from heterozygous female mice inconclusively indicate that Gαs in MC4R cells has a role in maintaining proper response to metabolic challenge and that this may be a sexually dimorphic effect.

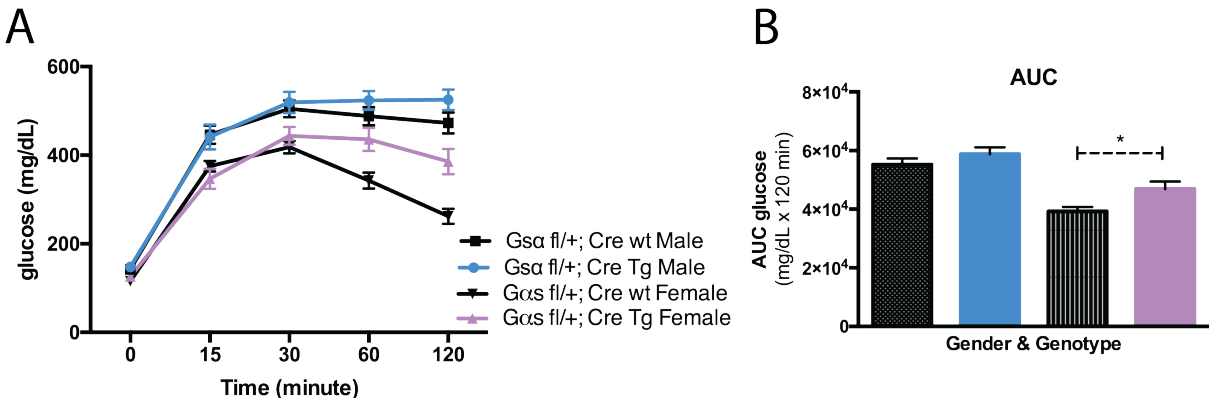

Figure 2-4. Glucose intolerance in female $G\alpha s^{fl/+}$; MC4R-Cre^{Tg} mice on HFD. A) Plasma glucose concentration during intraperitoneal glucose tolerance test (IPGTT) 2 mg/kg glucose, normalized to % lean body mass was administered to each animal. IPGTT was performed after ten hour daytime fast in mice fed HFD for five months in male (blue and black plot) and female (pink and black striated plot) animals. Multiple t-tests with Holm's Sidak correction sig dif in female 60 min **P = 0.0006 and 120 min ****P = 0.0001. B) Comparison of the % difference in total AUC shows that $G\alpha s^{fl/+}$; MC4R-Cre^{Tg} differed significantly from control $G\alpha s^{fl/+}$; MC4R-Cre^{wt} mice in females. (n = 6-11/group, *P<0.05, **P<0.005, ***P<0.0005, ****P<0.0001 one-way ANOVA with Tukey's multiple comparisons test).

PYY response

Post-prandial release of PYY is part of a hormonal feedback loop contributing to satiety. Peripheral administration of α-MSH or MC4R agonist has been shown to induce PYY and GLP1 release from intestinal L-cells and this is known to be driven by cAMP release, an intracellular signaling protein downstream of Gαs activation. Heterozygous loss of Gαs in MC4R cells did not alter PYY release as measured by plasma ELISA. Thus MC4R function is able to compensate for the maternally inherited heterozygous loss of Gαs.

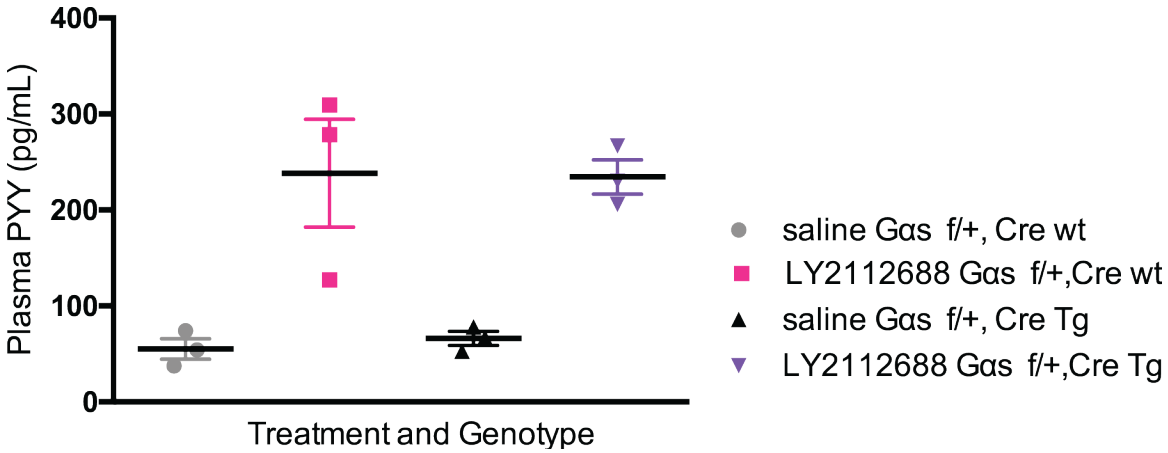

Figure 2-5. Normal melanocortin-stimulated PYY release in Gαs$^{fl/+}$; MC4R-Cre^{Tg} mice.
Female 27-30 week old Gαs$^{fl/+}$; MC4R-Cre^{Tg} and control Gαs$^{fl/+}$; MC4R-Cre^{wt} mice were injected with 3 mg/kg saline or LY2112688 intraperitoneally after a 6 hour daytime fast. 15 minutes following the injection, blood was collected and plasma prepared. Plasma was then assayed for peptide YY (PYY) using ELISA (Luminex). Points indicate mean PYY concentrations determined in duplicate from individual mouse serum samples, bars indicate means from multiple mice. Significant induction of PYY response with LY2112688, mimicking postprandial induction of PYY. (n=3-4/group, *P<0.05, student's t-test).

Summary and Conclusions

Global deletion and haploinsufficiency of MC4R results in a rapid onset obesity phenotype, and studies from Podyma et al. who have deleted Gαs specifically from MC4R cells, indicate loss of G-protein dependent signaling pathway through the Gαs subunit recapitulates the majority of the MC4R knockout phenotype. Here

we show that in our hands the same model causes P0 lethality, and that maternally inherited heterozygous loss of Gαs (Gαs$^{fl/+}$; MC4R-Cre^{Tg}) has a minor obesigenic effect observable by DIO. Because Gαs flox allele is passed from maternally inherited floxed alleles it will be preferentially expressed (ie Gαs deletion) in maternal imprinted regions like PVN. The Weinstein group has shown that Sim-1-Cre, Gαs maternal flox/wt reduced PVN Gαs expression to 30% of control compared to Gαs paternal flox/wt which reduced expression to 70% of control. Thus in critical nuclei like the PVN, our Gαs$^{fl/+}$; MC4R-Cre^{Tg} may have more complete transmission of Gαs knockdown. However our difficulty in generating an experimental colony of mice with homozygous deletion of Gαs indicates that the development and function of native PVN MC4R cells with Gαs deletion should be assessed and more rigorously. A developmental defect has not been ruled out.

Podyma et al. have shown that complete deletion of Gαs in MC4R cells causes rapid weight gain due to an increase in both lean and fat mass on chow diet from 4-12 weeks of age due to hyperphagia and reduced energy expenditure [94]. The Weinstein maternal inherited Gαs $^{fl/+}$;MC4R-Cre^{Tg,} had lesser, yet still significant weight mainly in males with most of the weight stored as an increase in fat mass. Our results differ in that we observed no obesigenic effect on chow diet. Furthermore we observe significant weight gain, driven by loss of Gαs, in DIO females exclusively (Fig 2-2.A), which appears to be due to changes in energy expenditure as there was no consistent change in HFD intake (Fig 2-2.B) yet feed efficiency was elevated in Gαs $^{fl/+}$;MC4R-Cre^{Tg,} females (Fig 2-2.C). In contrast to Podyma (and Weinstein), loss of Gαs was more deleterious to energy homeostasis in females than males as shown by significant increase in percent fat mass at and percent lean mass (Fig 2-2.D-E) and reduced glucose tolerance in females (Fig 2-4). MC4R is required for acute homeostatic responses to fluctuations in dietary fat [144], however Gαs $^{fl/+}$;MC4R-Cre^{Tg,} males and females are unaffected and drop weight and energy intake during chow exposure as expected (Fig 2-3). Complete deletion of Gαs resulted in abnormal glucose metabolism as measured by both elevated GTT and ITT on chow fed animals [94]. Furthermore when Podyma et al.

repeated these assays in maternally inherited Gαs $^{fl/+}$;MC4R-Cre^{Tg} mice (the same as our model), insulin induction is normal and glucose utilization is still impaired although at a ~30% decrease from the effect in Gαs $^{fl/fl}$ (no mention to gender of animals tested). In our hands after Gαs $^{fl/+}$;MC4R-Cre^{Tg} animals had matured on HFD, a glucose tolerance was administered to test glucose utilization. Similar to the aforementioned, glucose metabolism was impaired by loss of Gαs, although this was only observed in females (Fig 2-4). This confirms that Gαs may augment MC4R signaling to integrate the insulin hormone pathway through the ANS.

Our studies indicate that haploinsufficiency of Gαs does not contribute to a notable obesigenic phenotype. However, the variable results between labs, and the possibility the Gαs deletion produces a developmental defect in MC4R neurons suggest the need for further study.

CHAPTER 3

KIR7.1 CRISPR KNOCKOUT EMBRYONIC LETHALITY

Introduction

Kir7.1 has been detected in a wide variety of cells and tissue types, however it plays a common role in these locations—maintaining resting membrane potential near the potassium equilibrium potential [206]. This is accomplished by its inward rectifying potassium current, whose proper function and dysfunction, as detected by mutations in protein coding motifs by genome sequencing, is implicated in a number of physiologic processes. In humans *KCNJ13* is found on chromosome 2, in mice *Kcnj13* is on chromosome 3. The Kir7.1 sequence is highly conserved and the mouse gene is comprised of 1349 nucleotides with three exons, two coding and one noncoding. This gene is translated into a 360 amino acid protein ~40.5 kDa. The channel subunit is comprised of two transmembrane segments and cytoplasmic amino and carboxy terminals predicted to be 360- amino acids protein with very low sequence structural homology to even its nearest Kir channel family member. These subunits combine into a homo- or heterotetramer to form the channel, although it is unknown what type of tetramer Kir7.1 preferentially forms or if there is variability in different tissues.

After the discovery of a role for Kir7.1 in G-protein independent regulation of MC4R signaling, we immediately set out to develop whole body and site-specific transgenic models for reduced or ablated *Kcnj13* expression in the mouse for further physiologic characterization or Kir7.1 in the melanocortin system [104]. Because CRISPR-Cas9 is an efficient and expedient method for generating gene specific mosaic mice, we utilized this system to study the physiologic effects of whole animal *Kcnj13* knockout [262] [263]. CRISPR guide RNAs or crRNAs specific to a target region of the gene of interest that is predicted to cause loss of function (LOF) are injected with Cas9, an RNA-guided DNA endonuclease into zygotes. These editing primed zygotes are then implanted into pseudo-pregnant dams. When the target

DNA is found, Cas9 binds to the DNA and cuts it at a random site within or near the target sequence. Thus, pups born will have a mosaic variety of unique deletions, and following germline transmission they can then be sequenced and characterized for predicted changes in protein function.

While initial reports disputed the presence of Kir7.1 in kidney, improvements in methodology and reagents have confirmed the presence of Kir7.1 in the kidney. Herein its unusual properties such as low single channel conductance (50fS), low sensitivity to blockade by external Ba^{2+} or Cs^{+}, very low dependence on conduction on external K^{+}, localization close to Na-K-ATPase channel suggest it may be involved in a number of processes. Historically the role of Kir7.1 in the kidney has been muddled by conflicting reports of subcellular localization. For example some reports have ascertained that Kir7.1 may be involved in K+ recycling across basolateral membranes or it may facilitate renal K^{+} excretion under the condition of K^{+} overload [264]. Kidney expression profiles from PCR and Western blot in guinea pig, human, and micro-dissected rat nephron kidney have identified Kir7.1 in several regions. Immunostaining has shown Kir7.1 along the basolateral membrane of cell types along the nephron including distal convoluted tubule and principal cells. Recently the most thorough characterization to date by Kir7.1-HA has identified Kir7.1 in the inner medulla, but not the cortex or outer medulla of the kidney [223]. Furthermore Kir7.1 was observed in inner medulla collecting ducts, but not thin limbs of the loop of Henle in isolated tubules.

Loss of *Kcnj13* function has been published in zebrafish and humans (Table 1-3), however to our knowledge, no known metabolic defects have been observed. In 2015 Zhong et al. described F0 CRISPR *Kcnj13* mosaic mice used to study RPE function where mutations in Kir7.1 expression are known to cause congenital blindness such as LCA and SVD [250]. F0 animals were used rather than germline transmitted F1—Fx mice because it was determined that homozygous deletion of *Kcnj13* caused P0 embryonic lethality. This is an unanticipated finding, meriting further understanding of *Kcnj13* mutation penetrance in other organ systems of affected humans. Our studies were conducted before publication of Zhong et al and are focused on the metabolic phenotype of *Kcnj13*. Although *Kcnj13 -/-* was post-

natal lethal with our mutant alleles as well, we used heterozygous mice to study the physiologic phenotype in pathways commonly mediated by MC4R. Because the tissue and cellular location, tetramer construction, and regulating signaling partners can each impact channel function, this CRISPR knockout mouse model will be a useful tool, however future studies will also need to be conducted in a model where *Kcnj13* is specifically ablated in MC4R cells produce viable animals for study.

Results

Generation of CRISPR Kir7.1 loss of function mouse strains

In order to generate a *Kcnj13* specific knockout model, guide RNAs honing into the *Kcnj13* sequence just before the transmembrane 1 domain (TM1) (cDNA 146-159) were injected into zygotes along with guide RNA for the *Tyrosinase* gene (Fig 3-1.B) [265]. Small mutations that are either an insertion or deletion (INDEL) in this region of *Kcnj13* are predicted to cause frameshifts resulting in loss of function (LOF). Genetic mutations in *Tyrosinase* do not introduce deleterious effects on organ systems other than coat color pigmentation, which serves as a positive indicator of CRISPR-Cas9 genome editing in the animal. There were 27 live P0 mosaic pups born, 27 of which survived through weaning. At least seven (six female, one male) carried *Kcnj13* mutations (29%) as determined by Surveyor assay for positive *Kcnj13* mutation. All of these pups also displayed coat pigmentation variability due to variable penetrance of tyrosinase from the original black coat color, from albino to piebald, to seal-point, and gray or brown (Fig 3-1.A). Of the seven *Kcnj13* mutant pups, three females with different frameshift mutations were successful breeders with germline transmission and an efficient genotyping strategy (12.5%). The mutant alles are described below (Fig 3-1.C): Mouse 6 mutant allele: heterozygous for a 1-base deletion in the CRISPR target sequence. Mouse 10A/B mutant allele: compound heterozygote for two mutations. One allele has a 4-base deletion in the CRISPR target sequence. Second allele has a 3-base deletion in the CRISPR target and also a 1-base deletion nine bases downstream from CRISPR target sequence (4-bases total deleted). Mouse 22 mutant allele: heterozygous for a

1-base deletion in the CRISPR target sequence. Only mutant alleles 6, 10B, and 22 were efficiently transmitted and detected by PCR. During the course of breeding experimental animals, one homozygous male *Kcnj13*$^{22/22}$ was born and survived to adulthood, however we were unable to further transmit this allele to homozygosity. Sanger sequencing of an ear tissue sample from animal and a heterozygous *Kcnj13*$^{22/+}$ littermate confirmed the presence of the mutant allele (Fig 3-1.D).

Autopsy determined mechanism of homozygous lethality

Upon discovery of *Kcnj13* $^{-/-}$ mice in all mutant alleles generated from heterozygous crossings, we set out to understand the time and origin of peri-natal lethality. This was the case no matter the breeding pairs combination, be it a homozygous allele deletion (example $^{22/+}$ x $^{22/+)}$ or compound heterozygote deletion (example $^{10B/+}$ x $^{22/+}$). Dissection of pregnant dams from staged bred pairs determined that *Kcnj13* null embryos develop *in utero* with expected Mendelian ratios, but did not survive at expected ratios (Table 3.1).

Table 3-1. Allelic Distribution and Chi-Squared Analysis for Kir7.1 LOF Heterozygous Breeding Pairs

Pup Genotype (P0)	Kir7.1 LOF -/-	Kir7.1 LOF -/+	Kir7.1 LOF wt	Total Pups (16 litters)
Number (actual)	2	67	34	103
Ratio (actual)	0.019	0.65	0.33	**X^2 = 29.214**
Number (expected)	25.75	51.5	25.75	**df = 2**
Ratio (expected)	0.25	0.50	0.25	**P = >0.0001**

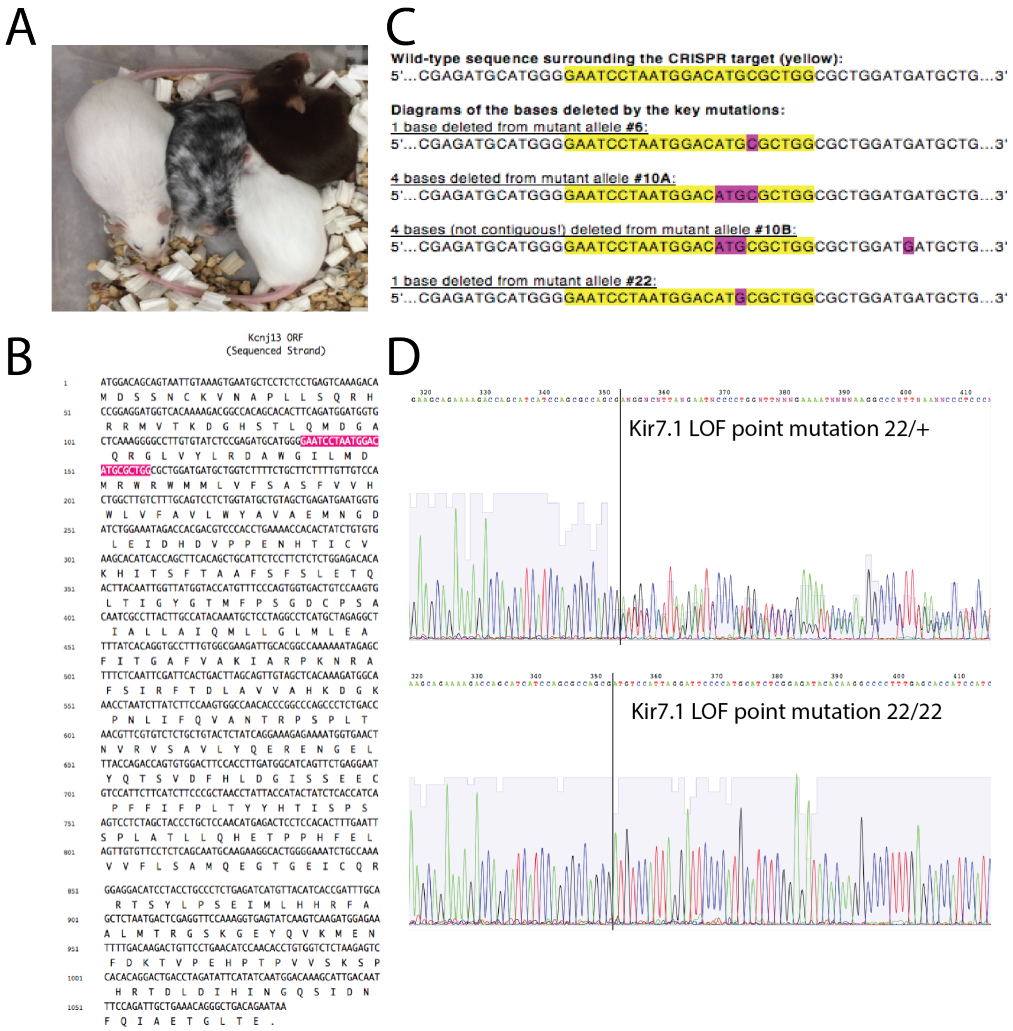

Figure 3-1. Generation of CRISPR Kir7.1 Loss of Function mouse strains.
A) Four founder mice from CRISPR- Cas9 genomic deletion strategy to generate Kir7.1 LOF mutant alleles. Color variation due to guide RNA for random insertion of tyrosinase with Kir7.1 guide RNA. B) DNA sequences of wildtype (wt) CRISPR Kir7.1 target highlighted in yellow and corresponding mutations of four strains, 6, 10A, 10B, and 22, in pink as determined by sequencing. C) *Kcnj13* open reading frame (ORF) showing CRISPR target in pink predicted to cause LOF and or protein degredation. D) Sanger sequencing for Kir7.1 heterozygous mutant 22/+ and one surviving Kir7.1 homozygous mutant 22/22.

Gross histological analysis of deceased P0 *Kcnj13* $^{-/-}$ pups determined the likely cause of death was suffocation by respiratory failure, as the lungs were not inflated. Just recently, defective tracheal tubogenesis has been repeated in a homozygous *Kcnj13* mutant mouse [266]. Additionally abnormalities in both the brain and spinal cord were observed, possibly due to abnormal migration of cells during development or perhaps due to defects in choroid plexus formation. These defects are also noted by Villanueva et al. and indeed lung developmental retardation is reported as the main cause of post-natal lethality in their *Kcnj13* knockout model [224].

Kidney pathology

Briefly, changes in structural morphology of P0 CRISPR *Kcnj13* pups was examined in collaboration with Dr. Jerod Denton. Changes in renal tubule integrity as described by Cornejo et al. were confirmed [223]. Additionally, *Kcnj13* -/- kidney capsular surface was lobular rather than a normal smooth, thin membranous surface indicating surface development was affected [267] [268] [269]. Sagittal slice dissection of kidney showed that renal papilla had a disorganized papillary vascular network and irregular duct patterning. This phenotype may be linked to respiratory system development failure [270]. The presence of Kir7.1 in renal papilla has been shown where it is found in the inner medullary collecting duct [223]. Its papillary presence has led to speculation that Kir7.1 function may contribute to the urinary concentration process. This has been supported by a recent single cell transcriptomic analysis that reveals high expression of Kir7.1 in intercalated rather than principal cells of mouse kidney collecting ducts [271].

Heterozygote phenotype on chow diet and A^y effect

In order to study potential metabolic defects with loss of Kir7.1, heterozygous experimental mice were bred and for the majority of experiments are represented by the alleles *Kcnj13* $^{22/+}$ or *Kcnj13* $^{10B/+}$(hets). Ex vivo slice studies have shown that the AgRP is effective at hyperpolarizing MC4R cells through Kir7.1.

We used the Agouti (A^y) mouse to study whether continuous ectopic endogenous overexpression of agouti, exhibits reduced activity in mice with haploinsuffcient Kir7.1 [31]. Agouti mice are known for their brilliant yellow-orange coat color due to antagonism of MC1R and subsequent follicular production of pheomelanin [272]. Likewise they exhibit obesity and hyperinsulinemia, insulin resistance, hyperglycemia, increased linear growth, and hyperleptinemia due to action of agouti both centrally and peripherally and this phenotype is worsened by loss of MC4R [35]. We crossed Kir7.1 hets with A^y to determine if loss of Kir7.1 further exacerbates agouti driven obesity.

By measuring the growth curve of male and female mice in four genotypes: Kir7.1 het; A^y Tg/+ and its control Kir7.1 wt; A^y Tg/+, followed by Kir7.1 het; A^y wt and its control Kir7.1 wt; A^y wt, from 5 to 27 weeks of age we observed that ectopic expression of A^y does lead to accelerated weight gain on chow diet in both males and females (Fig 3-2.A,C). Haploinsuffienciency of Kir7.1 does not adversely effect males (Fig 3-2.A), however, we observe a significant increase in Kir7.1 het; A^y Tg/+ female weight gain compared to Kir7.1 wt; A^y Tg/+ as measured by one-way ANOVA. This was not due to an increase in chow consumption as both sets of male (Fig 3-2.B) and female (Fig 3-2.D) experimental and control group were not significantly different. The only trend observed is an increase in chow intake for Kir7.1 wt; A^y Tg/+ males and females. Additionally, body composition and body length were measured at 27 weeks of age. We did not observe any significant difference in %fat or %lean mass in males (Fig 3-2.E,F) or females (Fig 3-2.H,I) of any genotype. This was surprising in Kir7.1 het; A^y Tg/+ females, however there may be a trend toward an increase in %fat mass in these females hidden due to a low experimental n for Kir7.1 wt; A^y Tg/+ (data for other Kir7.1 wt; A^y Tg/+ animals lost due to technical error). Body length measurements showed that A^y does indeed incur an increase in longitudinal length in both males and females. The loss of Kir7.1 alone leads to a further increase in body length in both males (Fig 3-2.G) $P = 0.003$ and females (Fig 3-2.J) $P = 0.006$. An increase in body length in Kir7.1 het with the presence of A^y is only observed in males $P = 0.044$. These studies indicate that Kir7.1 may have a role in agouti signaling pathways via the MC4R.

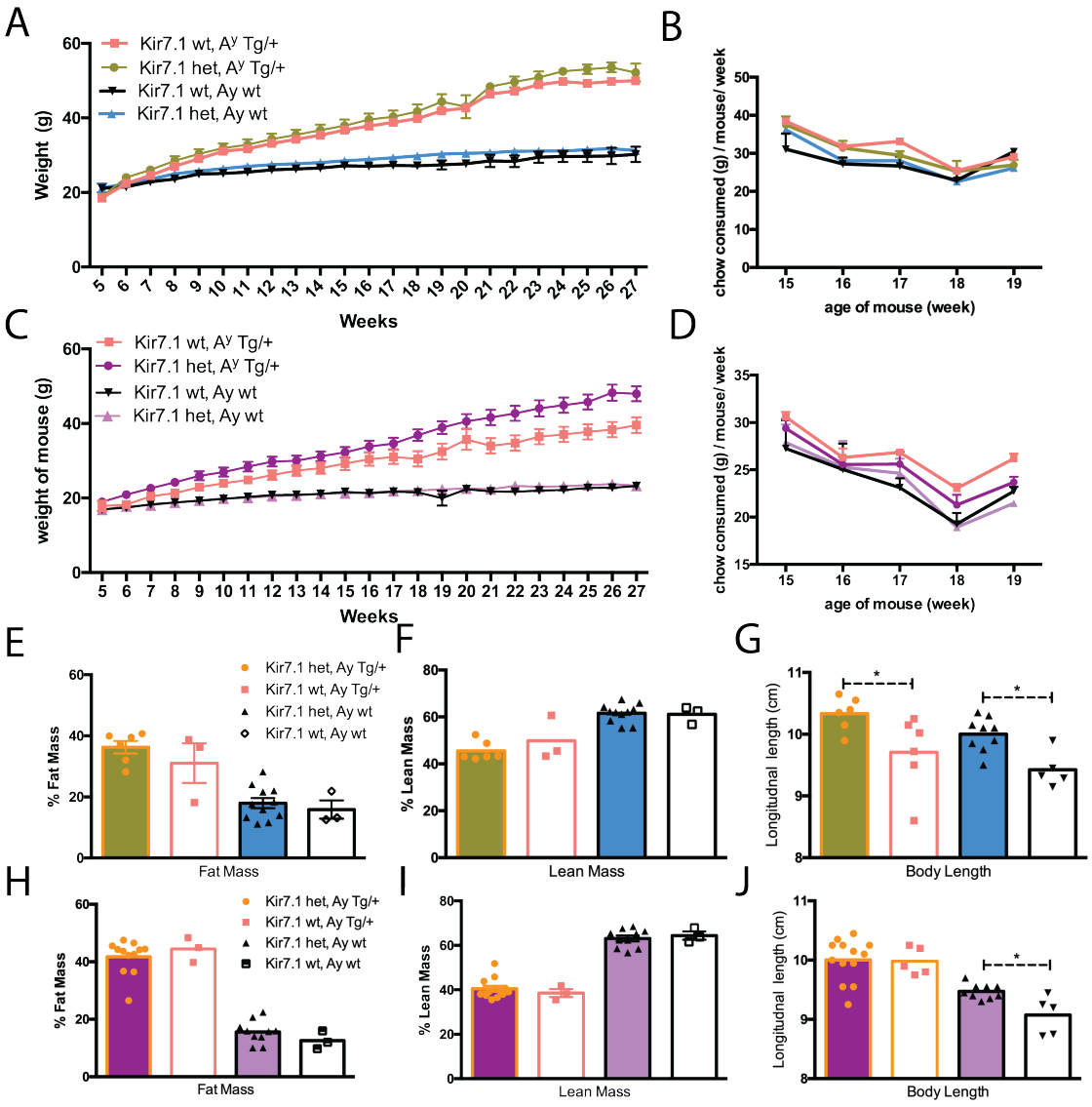

Figure 3-2. Minor physiologic perturbance in response to loss of Kir7.1 function in the presence or absence of A^y on chow diet.

A) Male growth curves and B) chow diet consumption per week . C) Female growth curves and D) chow diet consumption per week. Female Kir7.1 het; A^y Tg/+ versus Kir7.1 wt; A^y Tg/+ * P < 0.05. E) %fat mass, F) % lean mass, and G) length (tip of nose to base of tail) of male mice. H) %fat mass, I) %lean mass, and J) length of female mice. Body composition and body length at 27 weeks of age. All conditions tested in four genotypes: Kir7.1 het; A^y Tg/+, Kir7.1 wt; A^y Tg/+, Kir.1 het; A^y wt, and Kir7.1 wt; A^y wt. (A-D) One way ANOVA with multiple comparisons. (E-J) Multiple t-tests with Holms-Sidak multiple comparisons test. (n = 12-21/group for growth curves from 2 cohorts interspersed across age, n= 4-14 body composition and body length *P<0.05, **P<0.005, ***P<0.0005, ****P< 0.0001).

Heterozygote fasting-induced re-feed

A hallmark role of MC4R is to assimilate peripheral and central feedback of energy stores, intake, and expenditure and orchestrate responses affecting multiple organ systems to maintain energy homeostasis. Global deletion and haploinsufficiency of MC4R effect caloric preference, meal size, and meal duration. To study the role of Kir7.1 in mediating MC4R response to endogenous melanocortin, we used a fast-induced refeeding model. After fasting, AgRP neurons increase production and release of AgRP, GABA, and NPY onto MC4R neurons. We studied the kinetics of refeeding by chow consumption after a 16 hour overnight fast in male and female Kir7.1 het and wildtype mice (Fig 3-3). While there was no significant change in the orexigenic response of Kir het males from 1-24 hours post refeeding, there was a trend toward blunted feeding in Kir het females from 1-4 hours, which became significant at 6 hours post refeeding P = 0.0019, as measured by multiple t-tests with Holm's Sidak correction. This reduction in feeding is lost after 6 hours, nevertheless this finding argues that global haploinsufficiency of Kir7.1 may have an effect on AgRP activation on MC4R neurons.

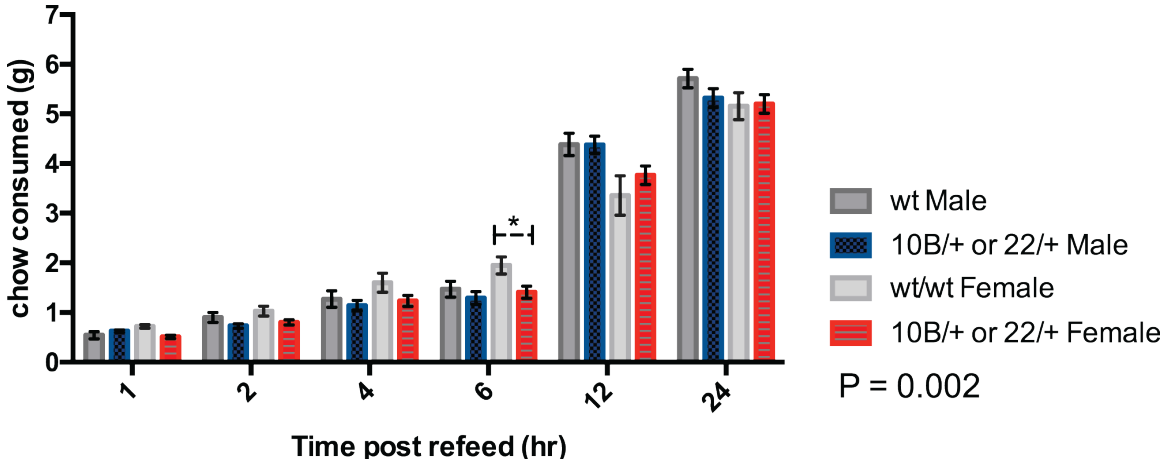

Figure 3-3. Blunted orexigenic response in female Kir7.1 heterozygous mice at six hours after fast-induced reefed.
Feeding response on dark cycle after 16 hour overnight fast in male and female 10B/+ or 22/+ heterozygous mutant mice or wildtype (wt) mice. Female six hour, P = 0.0019 Age of mice 10-11 weeks old. (n = 14-20/group, *P<0.05, Multtiple paired t-tests h multiple comparisons test).

Heterozygote diet induced obesity

Diet induced obesity by high fat diet is a metabolic challenge that is further complicated by loss of MC4R or its pathway signaling partners. Haploinsufficiency of MC4R is sufficient to induce early onset morbid obesity in mice and humans, and high fat hyperphagia in mice [111]. Thus reduction of Kir7.1 expression may also irrevocably alter MC4R response to conditions of caloric fat excess. Dually housed male and female Kir7.1 het and wildtype sibling mice were switched to high fat diet at 10 - 12 weeks of age. Similar to previous studies, there was no significant difference in weight gain of male Kir7.1het mice compared to Kir7.1 wildtype. However, female Kir7.1 het (which reflects either 10B or 22/+) gain significantly more weight on HFD compared to wildtype controls as measured by one-way ANOVA with multiple comparisons. This suggests, in agreement with prior analysis, that reduction in Kir7.1 may augment MC4R signaling *in vivo* and whereas these effects were not observable on chow diet in males or females, the challenge of HFD unmasks the physiologic action of Kir7.1.

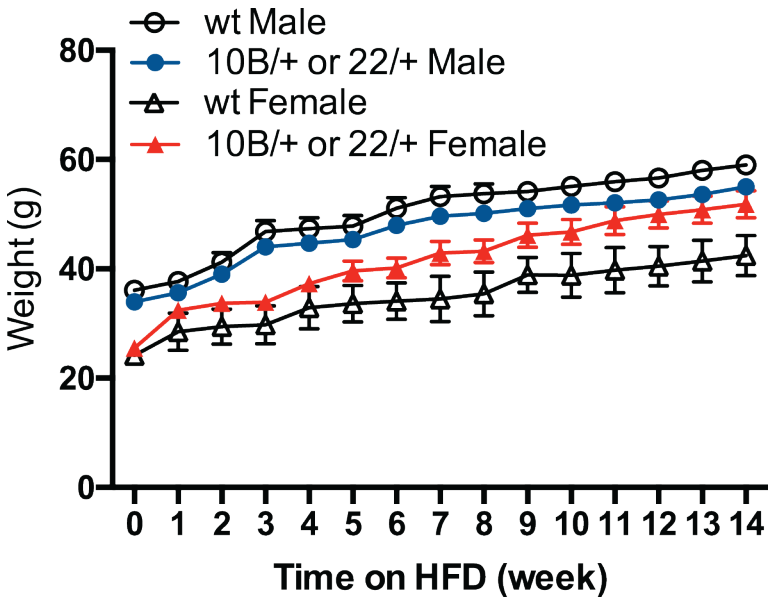

Figure 3-4. Obesity in female Kir7.1 LOF heterozygous mice on high fat diet. Growth curve on high fat diet from male and female mice in genotypes Kir7.1 10B or 22/+ and wildtype (wt). Female Kir7.1 10B or 22/+ versus female wildtype (wt) *P<0.05. One way ANOVA with multiple comparisons.. (n = 5-12 / group,)

Summary and Conclusions

Using a CRISPR-Cas9 global deletion model, we have confirmed the discovery, recently published by other labs, that global deletion of Kir7.1 is postnatal lethal due to respiratory development defects. It is curious that homozygous nonsense mutations such as one found in a human patient with LCA (Arg166X) do not cause death. This may be due to an incomplete loss of *Kcnj13* function at this sequence location. Therefore it may be the case that *Kcnj13* has a developmentally critical role in mice that is not conserved in humans. Although the CRISPR method is comparatively less arduous than making a conditional loss-of-function transgenic model, in order to study the role of *Kcnj13* more effectively it is necessary to use such an animal model in the future.

We further characterized kidney defects, alluded to by the presence of lacZ expression marker in Kir7.1-HA, in E20 and P0 mice [223]. Kir7.1. The main function of Kir7.1 in the kidney may in renal papilla due to observable defects in disorganized renal papilla and irregular duct patterning. The subcellular localization of Kir7.1 in epithelial cells is unknown, however Kir7.1 expression has been detected in papilla IMCD isolated tubules. Kir7.1 most likely contributes to urine concentration or to acid-base balance as it is regulated by intracellular and extracellular pH [273].

By using a haploinsufficient model of Kir7.1, we show Kir7.1 does contribute to some physiologic responses typical for MC4R signaling. Ectopic expression of agouti is a proxy for AgRP, which induces an orexigenic physiologic state. Because Kir7.1 in the slice and *in vitro* results in channel opening, we originally hypothesized that Kir7.1 hets would gain weight, which would be driven further by agouti expression, however we did not observe significant changes. We also observed a minor and sexually dimorphic phenotype. Kir het; A^y Tg/+ females have increased growth (Fig3-2). Interestingly, Kir het; A^y Tg/+ males and Kir het; A^y wt males and females also exhibited increased linear growth. MC4R deficient linear growth is proposed to be driven by hyperphagia, which induces hyperinsulinaemia and may

promote growth by suppressing the growth hormone-insulin-like-growth- factor-1 axis [274]. Despite an absence of hyperphagia with reduced Kir7.1 expression, it appears Kir7.1 may be involved in regulating linear growth. Additionally, in a fast-induced refeeding model of MC4R agonist regulated signaling we observe that female Kir7.1 have a reduced kinetic response to energy intake by chow consumption after a prolonged fast (Fig 3-3). This effect is lost after six hours, nevertheless this may be indicative of a role for Kir7.1 in sustained response to pharmacotherapy with melanocortin agonists. Exposure to high fat diet induces more rapid weight gain in female Kir7.1 het mice (Fig 3-4), arguing for a role of Kir7.1 in maintaining energy balance.

Much remains to be understood regarding the role of G-protein independent MC4R signaling through the Kir7.1 channel. A multiplicity of physiologies further complicates these efforts to deconvolute MC4R biology, however this work confirms the place of Kir7.1 as a player in MC4R neurocircuitry and merits further studies in the localization of Kir7.1 and MC4R coexpression, pharmacologic responses, and mechanism for MC4R -Kir7.1 intracellular cascades.

CHAPTER 4

CONDITIONAL KNOCKOUT OF KIR7.1 IN MC4R

Introduction

Haploinsufficiency of the MC4R in humans is the most common monogenic cause of severe obesity known, accounting for approximately 2% of cases [275] [276]. The composite prevalence of obesity-causing deleterious alleles in the human population has been demonstrated to be approximately 1/1500 [123]. Recent reports provide a detailed clinical picture of the syndrome [120] [277]. Remarkably, the syndrome is virtually identical to that reported for the mouse [278] [279] [280] with increased adipose mass, lean mass, linear growth, hyperinsulinemia, and severe hyperphagia. Genome-wide association studies have also identified SNPs adjacent to the MC4R gene that are associated with obesity [281] [282] [283]. These non-coding changes support the notion that small changes in the expression level of the MC4R may impact adiposity. Humans with haploinsufficiency, or even homozygous null status at the MC4R are relatively normal outside of the obesity syndrome, with only mild hypotension and hyperinsulinemia reported. Another unique feature of the central melanocortin system are the gene dosage effects for MC4R [71] [280], a highly unusual finding for G protein coupled receptor signaling systems.

Thus, the Melanocortin-4 receptor (MC4R) is a well-validated target for the treatment of common obesity (8, 9), and cachexia [284] [285] [286] [287]. Other studies suggest potential applications in diabetes [279] [175] [288] and metabolic syndrome [289] [290], depression related anorexia and anhedonia [291], and obsessive-compulsive disorder [292]. The MC4R appears to be at the heart of the adipostat, in that administration of melanocortin agonists inhibits food intake [71] and increases energy expenditure [293]. Chronic administration of potent

melanocortin agonists has produced significant weight loss in model systems from rodents, to primates [294]. However, clinical trials of potent small molecule orthosteric agonists of the MC4R have failed due to target-mediated pressor effects. Despite the target-mediated pressor response resulting from most melanocortin agonists, two peptide analogues of the native MC4R ligand, α-MSH, have been demonstrated to cause weight loss without a pressor response [295] [296] [297]. One of these compounds, setmelanotide, has been used successfully in a clinical trial in two patients with compound heterozygous mutations in proopiomelanocortin (POMC), the preprohormone precursor for α-MSH and in a clinical trial in patients with homozygous mutations in the gene encoding the leptin receptor [150] [187]. There is no data available explaining why some MC4R agonists are capable of inducing weight loss without the target-mediated pressor response, although biased agonism must be considered in the event that multiple signaling pathways are activated downstream of MC4R.

In this regard, it is already appreciated that MC4R exhibits different signaling modalities on the cellular level *in vivo*. The MC4R couples to $G\alpha_S$ in all cells tested, and it has been demonstrated that deletion of $G\alpha_S$ from MC4R neurons recapitulates the phenotype seen in MC4R knockout mice [237]. However, the complexity of MC4R signaling *in vivo* is also clear. α-MSH activates IML neurons via a putative non-specific cation channel [298], whereas it inhibits MC4R neurons in the dorsal motor nucleus of the vagus nerve via activation of a K_{ATP} channel [176]. Recently, using hypothalamic slice preparation in the mouse, we demonstrated that α-MSH appears to depolarizes and activate MC4R neurons in the PVN via a G protein independent mechanism involving inhibition of the inward rectifier Kir7.1 [45]. This is a highly unusual finding, requiring further validation *in vivo*. Furthermore, a better understanding of the role(s) of variant MC4R signaling modalities *in vivo* might lead to a rationale pharmacological approach to the development of small molecule biased agonists of MC4R that could discriminate between weight loss and pressor activities. Aiming toward these two goals, we

specifically deleted the inward rectifier Kir7.1 from MC4R neurons in the mouse, and conducted pharmacological and physiological studies of the resulting animals.

Results

Constructs and breeding process

Global and tissue-specific deletion of *Kcnj13*

In order to analyze the potential roles of Kir7.1 in MC4R neurons *in vivo*, we developed a versatile, transgenic mouse strategy (Fig. 4-1) using the Knockout Mouse Project (KOMP) mutant allele repository. After germ line transmission, the first generation mutant was a homozygous, global null mouse (*Kcnj13*^{KO}). As previously reported using a Velocigene method, we confirmed the *Kcnj13*^{KO} resulted in early (P0) postnatal lethality (Fig 4-S1) [224]. Pathological analyses indicated retardation of lung and kidney development and failure to suckle as likely sources of lethality. We next derived a floxed line by crossing these animals with a flippase recombinase transgenic C57Bl/6NJ line. Mice expressing *Kcnj13* flanked by loxP sequences (*Kcnj13* $^{fl/fl}$) were confirmed by genotyping. Tissue specific *Kcnj13* knockout mice were then derived using the Cre-loxP method. Kcnj13$^{fl/fl}$ mice were crossed with mice expressing the alleles *Kcnj13* $^{fl/fl}$ and MC4R-t2A-Cre Tg/+ (MC4R^{Cre}) to generate a MC4R cell specific *Kcnj13* knockout experimental animal, hereafter referred to as *Kcnj13*ΔMC4R^{Cre} (Table 4-1).

Table 4-1. Nomenclature of mouse strains used in this study.

	MGI name	Common name
Global knockout	C57BL/6J-*Kcnj13*$^{tm1a(KOMP)Wtsi}$	*Kcnj13* ^{KO}
Floxed allele	C57BL/6J-*Kcnj13*$^{tm1c(KOMP)Wtsi}$	*Kcnj13* $^{fl/fl}$
Cell-specific knockout	C57BL/6J-*Kcnj13*$^{tm1d(KOMP)Wtsi}$	*Kcnj13*ΔMC4R^{Cre}
Cre driver	Tg: C57BL/6J-MC4R-t2a-Cre	*Kcnj13*$^{+/+}$;MC4R^{Cre}

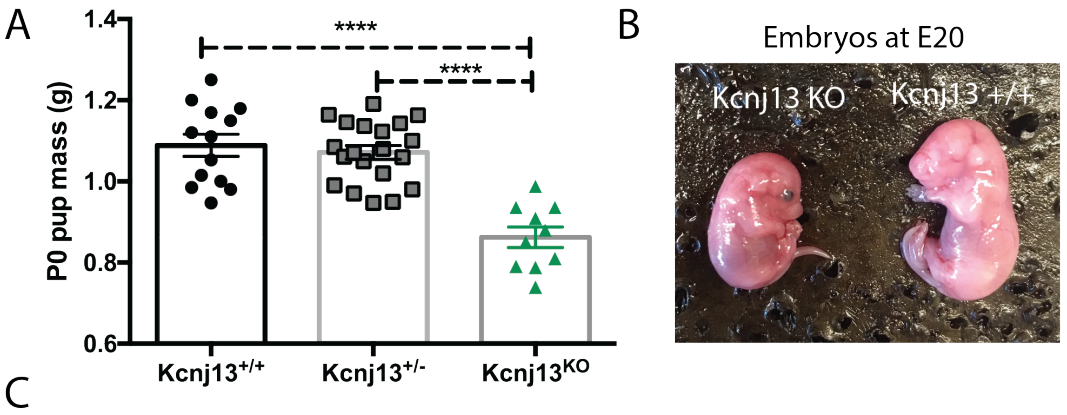

C

Pup Genotype (P0)	Kcnj13 KO	Kcnj13+/-	Kcnj13+/+	Total Pups (10 litters)
Number	22	44	20	86
Ratio	0.26	0.51	0.23	

Fig. 4-S1. P0 lethality from homozygous deletion of Kir7.1 in mice
(A) Mass of P0 pups with genotypes *Kcnj13*$^{+/+}$, *Kcnj13*$^{+/-}$, and *Kcnj13*^{KO} (B) Representative gross pathology of *Kcnj13*^{KO} and *Kcnj13*$^{+/+}$ E20 embryos (C) Genotype distribution of offspring from *Kcnj13*$^{+/-}$ intercrosses examined by PCR (n = 10-20, ****P<0.0001, one-way ANOVA with Tukey's multiple comparisons test).

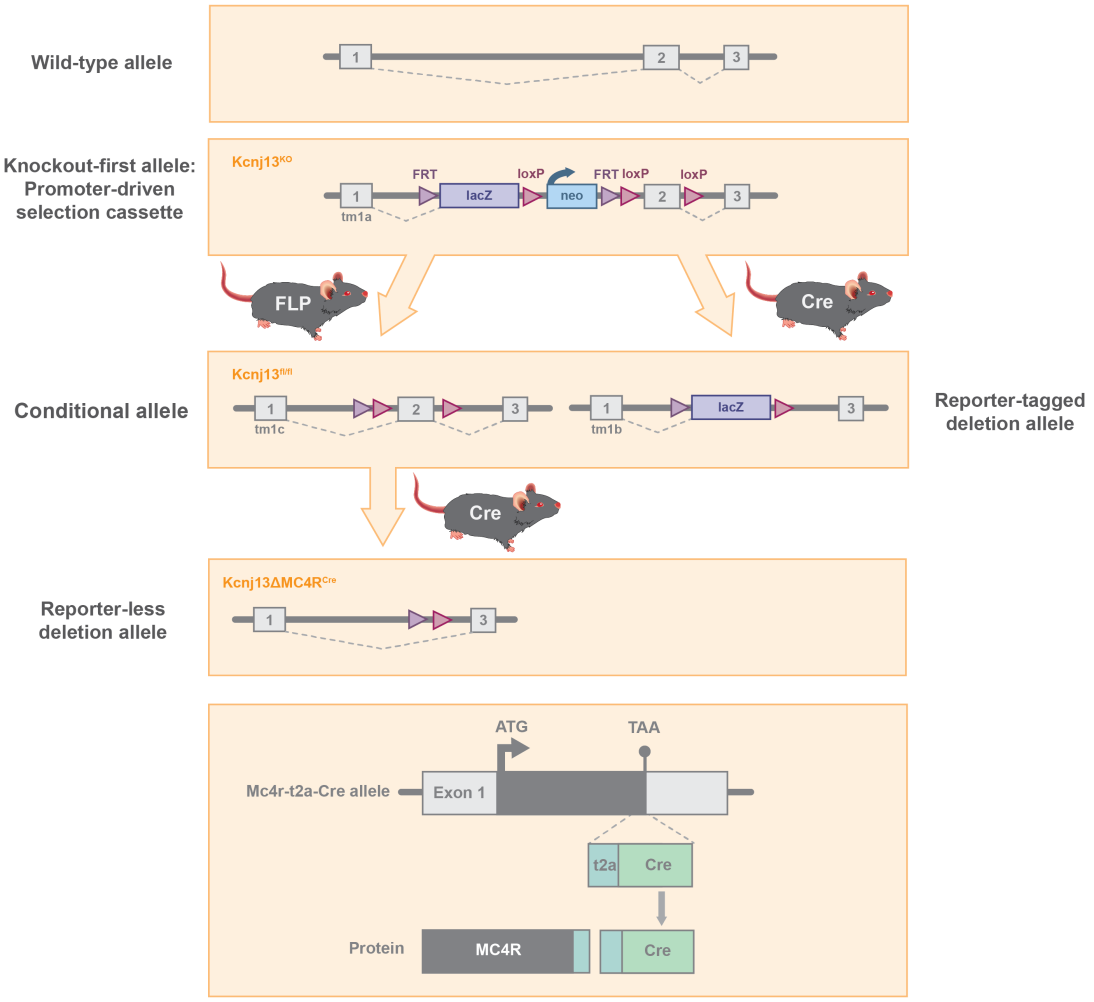

Fig. 4-1. Creation of global and tissue-specific *Kcnj13* knockout mice.
Transgene construct and breeding strategy for promoter-driven, knockout-first, *Kcnj13* targeted selection germline transmissible line (*Kcnj13*^{KO}), crossed with Flp recombinase transgenic mice and then with MC4R-t2a-Cre recombinase mutant mice to generate a MC4R-Cre site-specific *Kcnj13* knockout (*Kcnj13*ΔMC4R^{Cre}) line.

Electrophysiology recordings

Defective α-MSH-induced depolarization of MC4R PVN neurons from *Kcnj13*ΔMC4R^{Cre} mice

Kcnj13 is expressed at low levels in the sparsely distributed MC4R neurons in the CNS [45]. Thus, it is challenging to demonstrate tissue specific deletion of *Kcnj13* using mRNA expression. However, we had previously developed a functional assay of Kir7.1 in a hypothalamic slice preparation [45]. In this assay, Kir7.1 was demonstrated pharmacologically to be required for α-MSH-induced depolarization of MC4R neurons in the paraventricular nucleus of the hypothalamus. We chose to use this assay to test for Kir7.1 activity in MC4R neurons in *Kcnj13*ΔMC4R^{Cre} mice. In order to characterize the necessity of Kir7.1 for α-MSH induced depolarization of MC4R-expressing neurons within the paraventricular nucleus (PVN), electrophysiological slices were prepared from control *Kcnj13*$^{+/+}$;MC4R^{Cre} and *Kcnj13*ΔMC4R^{Cre} mice, in which MC4R neurons are transgenically labeled with GFP. Whereas a 250nM bath application of α-MSH successfully depolarized PVN MC4R neurons in recordings from control mice (Fig 4-2A), depolarization did not occur in recordings from PVN MC4R neurons from *Kcnj13*ΔMC4R^{Cre} mice (Fig 4-2B). These data show the absence of a characterized Kir7.1 response, thereby supporting the argument that Kir7.1 is not expressed in mutant *Kcnj13*ΔMC4R^{Cre} PVN neurons. Furthermore, these findings indicate that Kir7.1 is required for α-MSH induced depolarization in this electrophysiological slice assay.

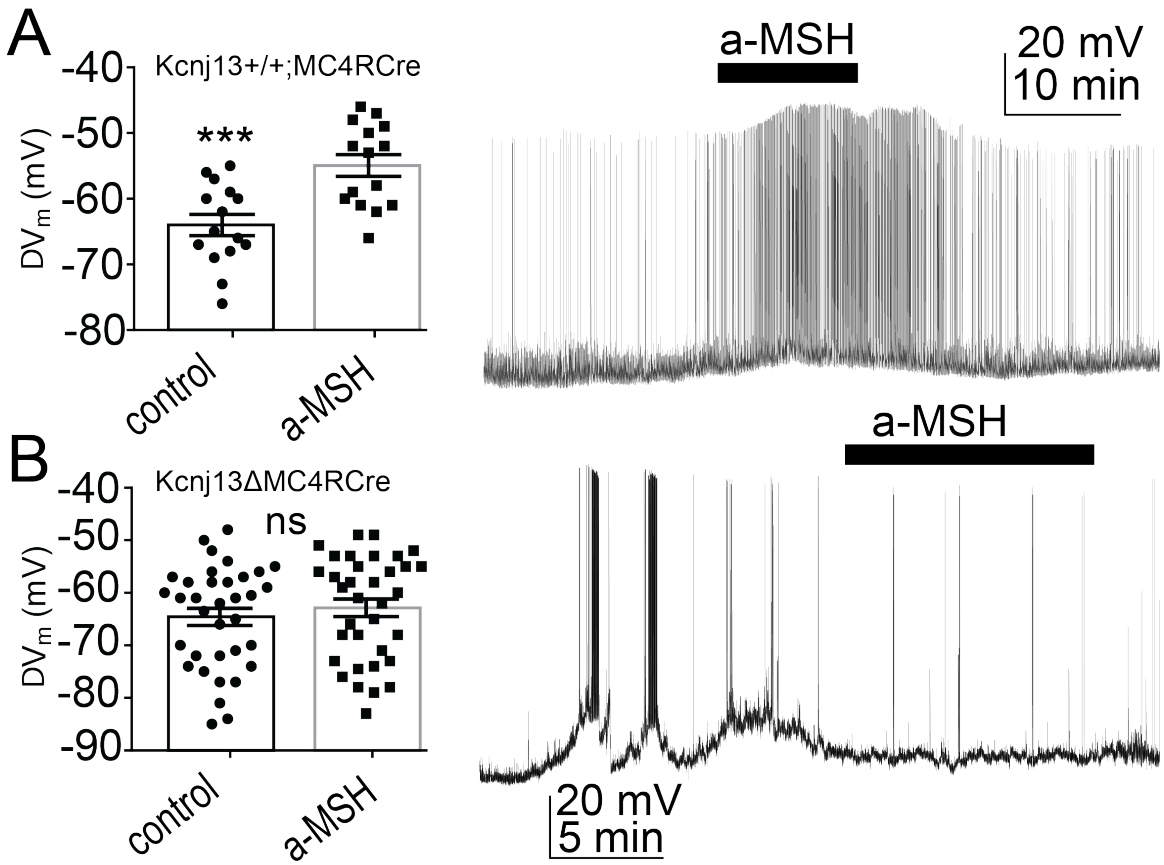

Fig. 4-2. Defective α-MSH-induced depolarization of MC4R PVN neurons in *Kcnj13*ΔMC4R^{Cre} mice.

Slice electrophysiology of PVN MC4R-GFP positive neurons recorded in current clamp with bath application of 250nM α-MSH. (A) Recordings from *Kcnj13*$^{+/+}$;MC4R^{Cre};MC4R-GFP mice in response to vehicle or α-MSH showing induction of action potential differed significantly between and control and α-MSH in bath and a representative depolarizing response of a PVN MC4R neuron (B) Recordings from *Kcnj13*ΔMC4R^{Cre};MC4R-GFP mice, , ns response to α-MSH, P=0.11, and a representative lack of depolarizing response in a PVN MC4R neuron. Bar graph represents mean +/- SEM of 15-35 cells. (***P<0.0001, paired t-test). V_m, membrane potential in millivolts (mV).

LY2112688 response

Defective anorexic response to melanocortin peptides in *Kcnj13*ΔMC4R^{Cre} mice

Because the absence of Kir7.1 disrupted α-MSH induced neuronal depolarization in PVN MC4R neurons in an *ex vivo* slice preparation, we hypothesized that feeding behavior in response to α-MSH administration might also be adversely affected. To investigate the physiological effect of an MC4R agonist on MC4R neurons in the absence of Kir7.1 *in vivo*, we administered the potent α-MSH analogue, LY2112688, at the beginning of the dark cycle, after a 16-24 hour fast, and measured food intake. Despite powerful drivers to restore energy stores resulting from a state of nutritional deficit, LY2112688 blunts the fasting-induced refeeding response in control genotype groups, however in *Kcnj13*ΔMC4R^{Cre} male (Fig 4-3A) and female (Fig 4-3B) mice the duration of LY2112688 action is reduced. Notably, from three hours post refeeding in males and four hours post refeeding in females to twelve hours later, mice with MC4R specific deletion of Kir7.1 show a significantly reduced anorectic response to LY2112688 compared to *Kcnj13*$^{fl/fl}$ in males and *Kcnj13*$^{fl/fl}$ and *Kcnj13*$^{+/+}$;MC4R^{Cre} control groups in females. Additionally, at 13 and 24 hours there is no significant difference between the action of saline or LY2112688 administered to *Kcnj13*ΔMC4R^{Cre} males, while feeding in control *Kcnj13*$^{fl/fl}$ animals injected with LY2112688 remains suppressed.

This study paradigm was repeated using male mice following bilateral lentiviral *Kcnj13* shRNA knockdown, or administration of a scrambled control lentivirus in the PVN (sc shRNA). After 3 weeks recovery mice were acclimated to handling and injection before beginning the fast-induced refeeding study (Fig 4-3C). Similar to genetic deletion of Kir7.1, viral knockdown of Kir7.1 exclusively in the PVN also reduced the duration of the anorectic activity of LY2112688. LY2112688 was no longer effective at reducing food intake compared to saline in Kir7.1 knockdown animals from 12 hours post refeeding through 40 hours. Conversely, LY2112688 significantly reduced chow consumption in mice with intact Kir7.1 for the duration of the study. Successful targeting and delivery of *Kcnj13* shRNA or sc shRNA lentiviral vectors were confirmed by GFP expression localized to the PVN in post-

mortem mice(not shown). Taken together these data show that Kir7.1 expression is required for the extended duration of anorectic response to a melanocortin peptide.

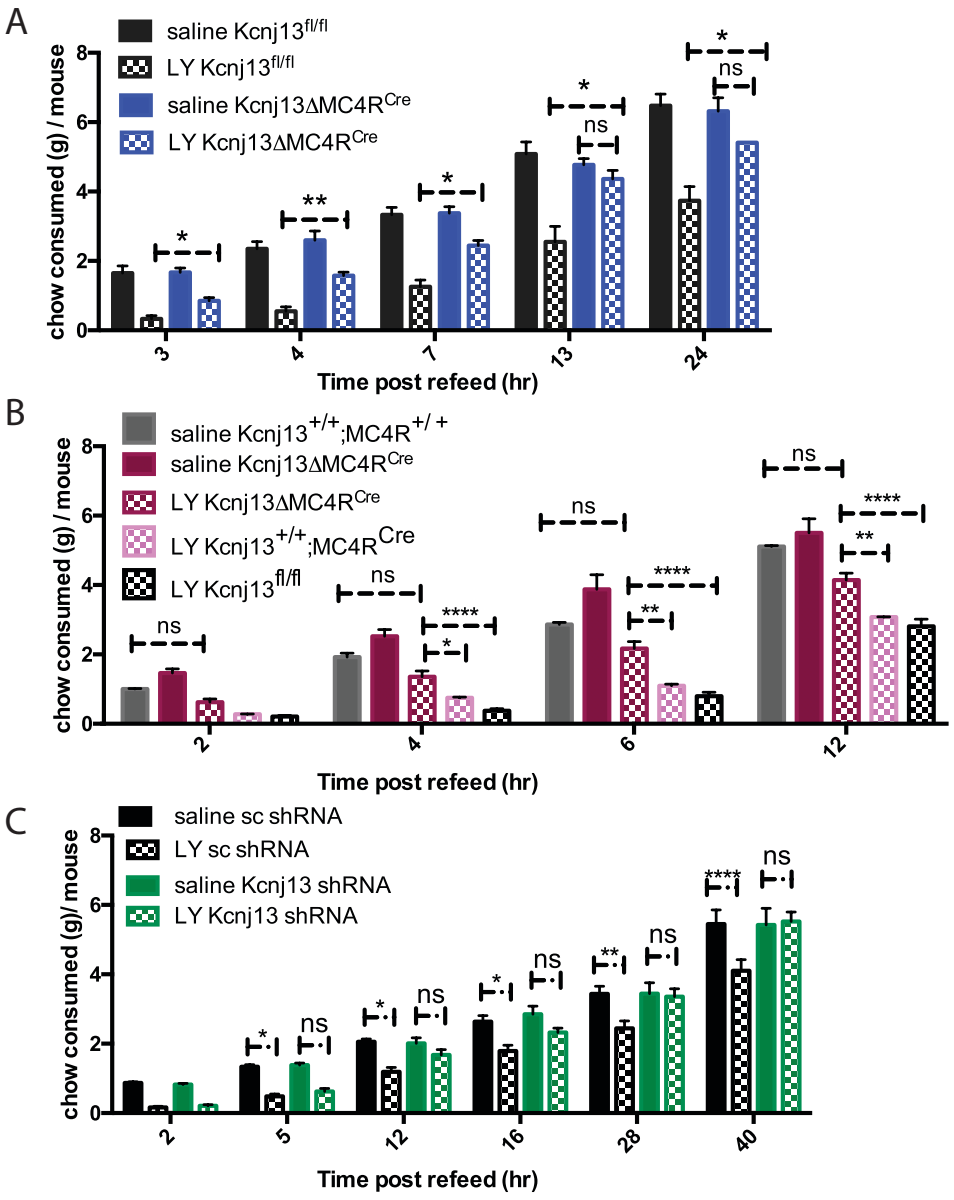

Fig. 4-3. Defective anorexic response to melanocortin agonist LY2112688 in *Kcnj13*ΔMC4R^{Cre} mice.

Feeding response on dark cycle after IP injection of saline or LY2112688 in male (A), female (B) *Kcnj13*ΔMC4R^{Cre}, *Kcnj13*$^{fl/fl}$, and/or *Kcnj13*$^{+/+}$;MC4R^{Cre}, *Kcnj13*$^{+/+}$;MC4R$^{+/+}$ and male (C) *Kcnj13* shRNA or sc shRNA lentiviral knockdown mice following 16-24hr fast. Dose of 10mg/kg (n = 4-9/group, *P<0.05, **P<0.005, ****P<0.0001, 2-way ANOVA with multiple comparisons test).

AgRP response

We have previously shown the role of Kir7.1 in mediating a G-protein independent MC4R response in both hypothalamic slices and in cells transfected with MC4R and Kir7.1 [45]. These electrophysiological and pharmacological experiments also demonstrated that AgRP appeared to open Kir7.1 channels in a MC4R-dependent manner [45]. To study whether Kir7.1 is necessary for AgRP-induced stimulation of food intake we delivered AgRP intracerebrventricularly (ICV) to mice in a fed state. Cannulas were implanted in the lateral ventricle of *Kcnj13*$^{fl/fl}$*Kcnj13*$^{+/+}$;MC4R^{Cre}, and *Kcnj13*ΔMC4R^{Cre} male mice, and animals were allowed to recover for 5 days. Two days after a saline injection to establish baseline conditions, 1 μg of the peptide AgRP was injected ICV during light cycle. While *Kcnj13*ΔMC4R^{Cre} had a slight trend in lower food intake, we observed no sustained significant difference in central AgRP induced feeding initiation or duration between genotypes (Fig 4-4A). This suggests Kir7.1 is not required for the orexigenic response to AgRP. Likewise, all genotypes responded to AgRP with an increase in body weight in proportion to the increase in food intake (Fig 4-4B). There was no significant difference in change in body weight between genotypes.

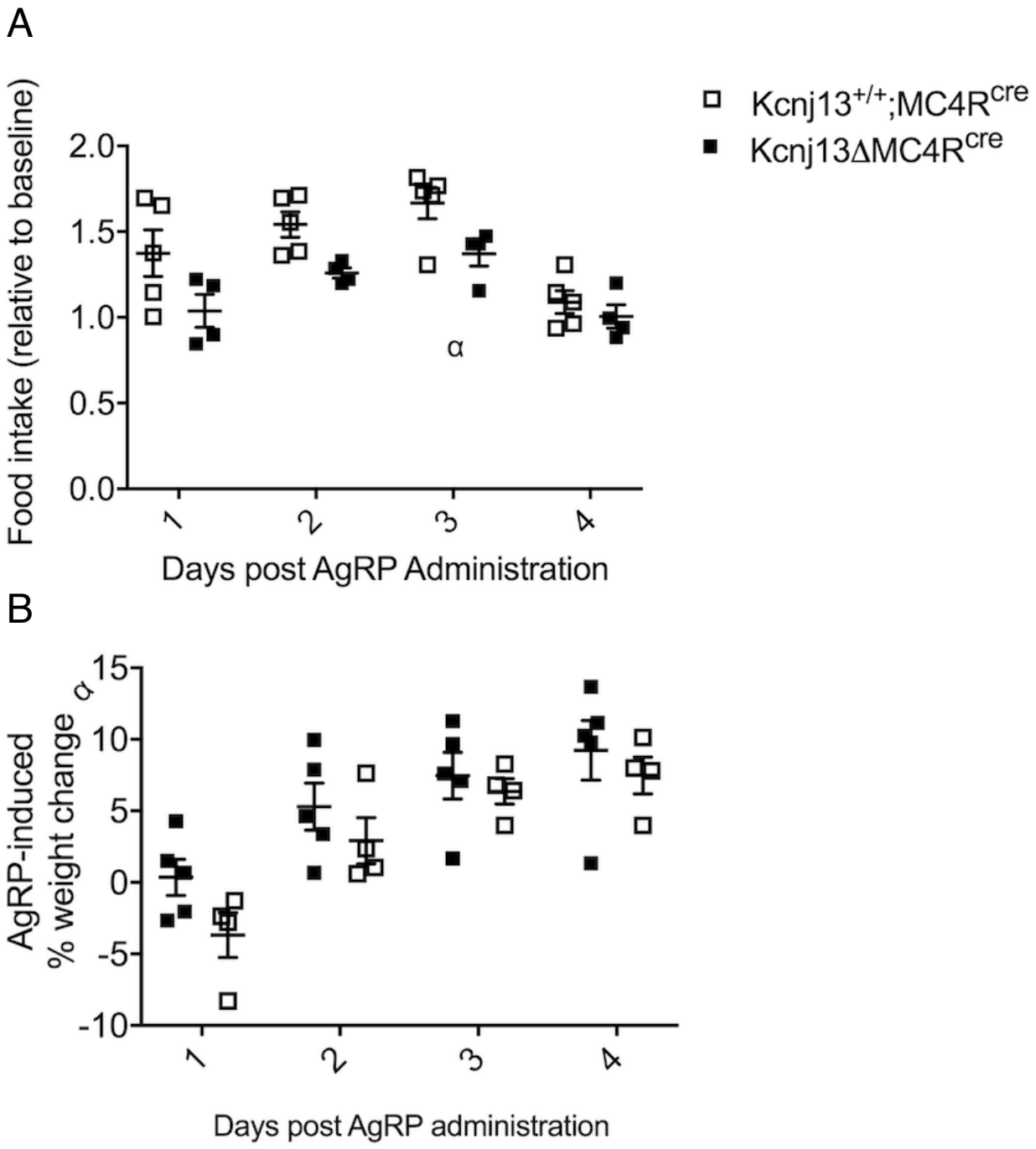

Fig. 4-4 Normal orexigenic response to AgRP in *Kcnj13*ΔMC4R^{Cre} mice.
Change in chow consumption (A) and change in body weight (B) from day 0 central administration of AgRP at a dose of 2nmol. (A) Chow consumption differed significantly between *Kcnj13*ΔMC4R^{Cre} and *Kcnj13*$^{+/+}$;MC4R^{Cre} mice at day 2. (B) NS in change in body weight at any time between *Kcnj13*ΔMC4R^{Cre} and *Kcnj13*$^{+/+}$;MC4R^{Cre} mice. (n = 2-5/group, *P<0.05, **P<0.005, 2-way ANOVA with multiple comparions test).

PYY response

Normal melanocortin-stimulated PYY release in *Kcnj13*ΔMC4R^{Cre} mice

Whereas MC4R is expressed in many brain nuclei, peripheral expression has also been mapped. Notably, MC4R is expressed in enteroendocrine L cells, and peripheral administration of α-MSH has been demonstrated to induce MC4R-dependent release of PYY and GLP1 from these cells [82]. Thus, the function of MC4R on L cells can be assessed using an assay for increased plasma PYY following peripheral administration of an MC4R agonist. We next examined the requirement for Kir7.1 in MC4R-mediated PYY release from L cells. The absence of Kir7.1 in MC4R cells does not interfere with the release of the satiety factor PYY into plasma (Fig. 4-5). Thus, the role of Kir7.1 in MC4R function appears to be important in neurons of the PVN, but not enteroendocrine L cells.

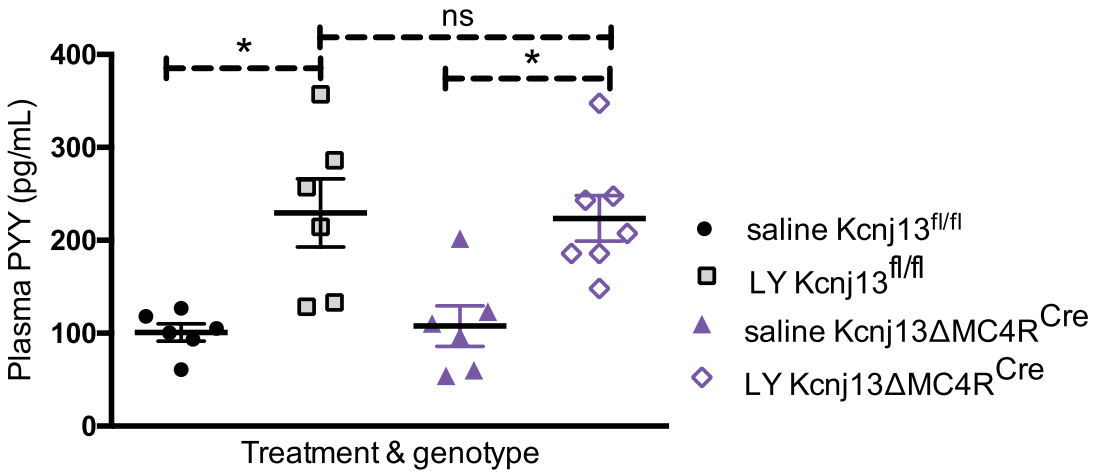

Fig. 4-5 Normal melanocortin-stimulated PYY release in *Kcnj13*ΔMC4R^{Cre} mice. Male and female C57BL/6J *Kcnj13*ΔMC4R^{Cre} and *Kcnj13*$^{fl/fl}$ control mice were administered saline or saline containing 5mg/kg LY2112688 intraperitoneally. 15 minutes following treatment, blood was collected, and plasma prepared. Plasma was then assayed for peptide YY (PYY) using ELISA (Luminex). Points indicate mean PYY concentrations determined in duplicate from individual mouse serum samples, bars indicate means from multiple mice. (n=6-7/group, *P<0.05, student's t-test).

Chow diet response

Phenotypic characterization of *Kcnj13*ΔMC4R^{Cre} mice

Global deletion of MC4R in the mouse can produce measurable increases in adipose mass as early as 5 weeks of age [280]. To determine the effects of Kir7.1 ablation on MC4R signaling, we studied body weight, body composition, feeding behavior, and glucose tolerance in *Kcnj13*ΔMC4R^{Cre} and control *Kcnj13*$^{fl/fl}$, *Kcnj13*$^{+/+}$;MC4R^{Cre} , and *Kcnj13*$^{+/+}$;MC4R$^{+/+}$ mice. At 20 weeks of age, we did not observe differences in body weight in the four strains maintained on normal mouse chow (Fig. 4-6A-B). Moreover, when lean and fat mass accrual was compared in young 12 week old mice and mature, no significant difference was detected in lean or fat mass between groups (Fig 4-6F-G). However, by 26 weeks of age in female and 50 weeks of age in male *Kcnj13*ΔMC4R^{Cre} showed significantly greater weight compared with all three control strains (Fig 4-6A, B). One-way ANOVA analysis showed *Kcnj13*ΔMC4R^{Cre} male and female mice gained significantly more weight over the time course than the control genotypes. No significant difference was observed in daily chow consumption between groups (Fig 4-6 E). At 28 weeks of age female *Kcnj13*ΔMC4R^{Cre} mice weight were observed to have significantly more absolute and %fat mass compared to control genotypes (Fig. 4-6F, H), while lean mass was unchanged (Fig. 4-6G, I). Both male and female 30 week *Kcnj13*ΔMC4R^{Cre} animals also exhibited significant increased length compared to controls (Fig. 4-6C-D).

Glucose utilization was assessed by IP glucose tolerance test (GTT) in female mice at 28 weeks of age. The 2mg/kg dosage of glucose was adjusted in proportion to lean body mass. Whereas all genotypes initially responded to the bolus of glucose similarly (Fig. 4-6J), *Kcnj13*ΔMC4R^{Cre} mice showed impaired glucose metabolism from 45-120 minutes (Fig. 4-6L). No significant difference was detected from 0-120 minutes (Fig. 4-6K).

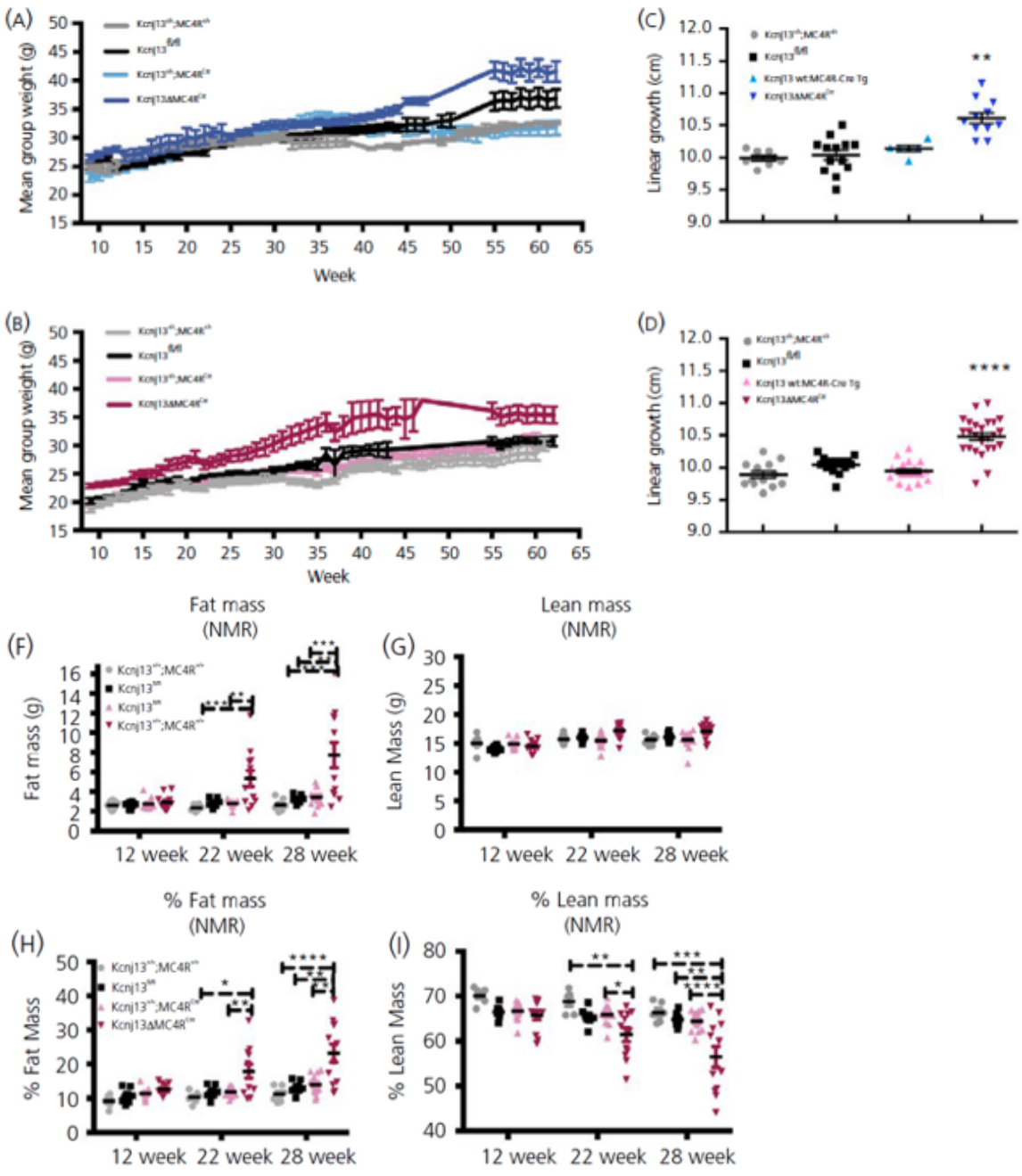

Fig. 4-6. Late onset obesity develops in chow fed *Kcnj13*ΔMC4R^{Cre}mice.
(A-I) Growth curves on chow diet of (A) male and (B) female mice interspersed across 3 age cohorts from 9 to 58 weeks (C) male and (D) female linear length measured from snout to anus in euthanized mice at approximately 30 weeks. Each dot represents the snout-anus distance of one individual animal (n = 6-25 per group) (E) Daily chow consumption per mouse during week of mouse age indicated One-way ANOVA test with Tukey's multiple comparisons. Absolute fat (F) and lean (G) mass and %fat (H) and %lean (I) mass body composition of 12wk, 22wk, and 28wk female mice. Multiple t-tests with Holms-Sidak multiple comparison test.

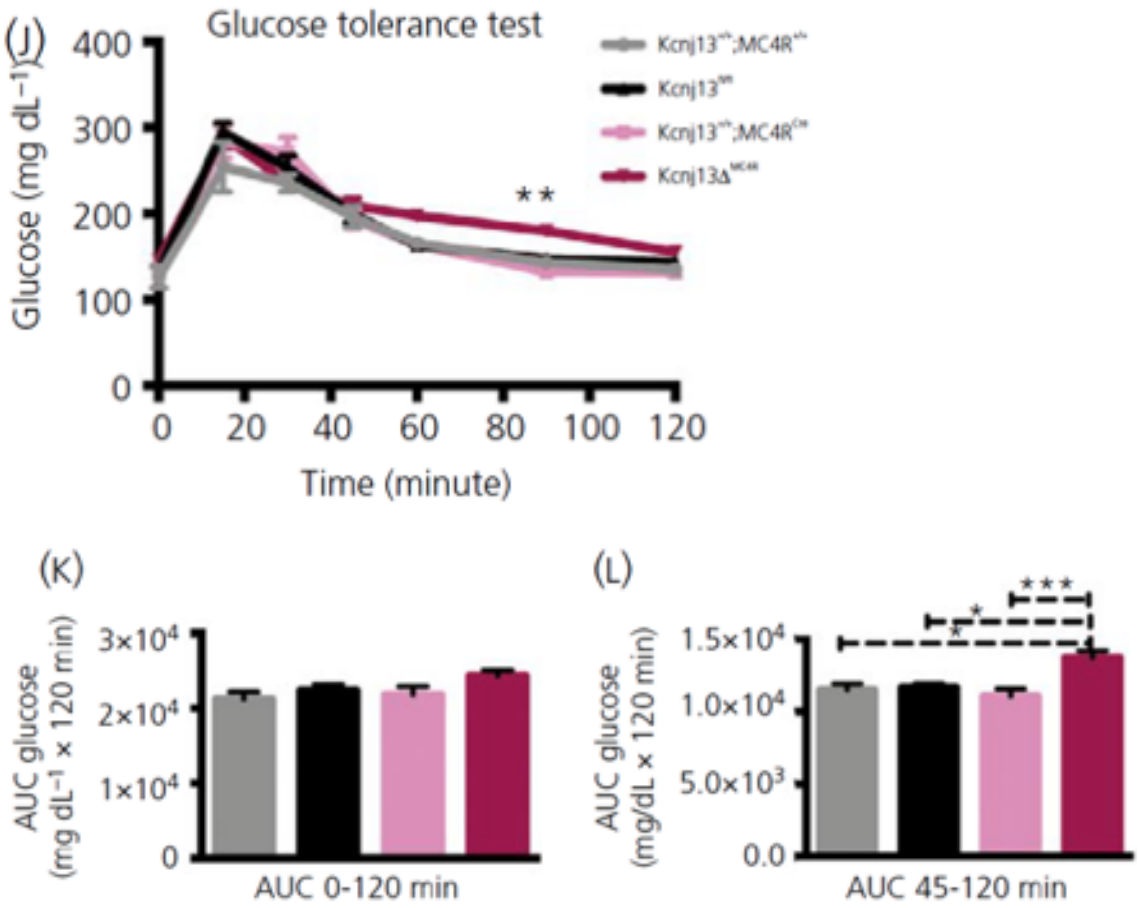

Fig. 4-6. Late onset obesity develops in chow fed *Kcnj13*ΔMC4R^{Cre}mice.
(J-L) Plasma glucose concentration during intraperitoneal glucose tolerance test (IPGTT) 2g/kg glucose, normalized to % lean body mass was administered to each animal. IPGTT was performed after six hour daytime fast in 28wk female animals (H) female animals. Comparison of the % difference in total AUC shows (K) AUC from 0-120 is similar, whereas *Kcnj13*ΔMC4R^{Cre} differed significantly from control genotypes from (L) 45-120min. (J) multiple t-tests (K-L) One-way ANOVA with multiple comparisons. (n = 6-12/group, *P<0.05, **P<0.005, ***P<0.0005, ****P< 0.0001).

Diet-induced obesity response

To attempt to accelerate the differences in growth, male and female animals of all four genotypes were placed on high fat chow (HFD). Mice were acclimated to single housing at 8-10 weeks old and switched from chow to HFD at 10-13 weeks of age, during which time intake and growth were monitored weekly for 3 months. A clear

obesogenic effect of the Cre transgene was apparent under these conditions, perhaps due to reduction of functional MC4R resulting from the method of Cre expression, requiring cleavage of an MC4R-Cre fusion protein under the control of the endogenous MC4R promoter. Nonetheless, increased growth of male and female *Kcnj13*ΔMC4R^{Cre} was apparent, when compared with MC4R-Cre controls. A mixed linear effect statistical model, an alternative to ANOVA with repeated measures, was used to analyze the growth curves. This modeling tool determined that while the *Kcnj13*$^{+/+}$;MC4R^{Cre} male and female control weight gain profiles are significantly different than the non-Cre expressing *Kcnj13*$^{fl/fl}$ control genotype, the male *Kcnj13*ΔMC4R^{Cre} weight gain profile (Fig 7A) is also significantly different than the *Kcnj13*$^{+/+}$;MC4R^{Cre} control. Female weight gain is significantly different from 70-84 days on HFD as determined by multiple student's t-tests (Fig 7C). We were unable to measure an effect of any genotype on food intake (Fig 7B, D). After consuming high fat diet for 3 months there was a significant increase in fat mass in both *Kcnj13*ΔMC4R^{Cre} and *Kcnj13*$^{+/+}$;MC4R^{Cre} groups (Fig 7E-H), however we were unable to measure an effect of Kir7.1 deletion, probably due to the significant background effect of the Cre transgene (Fig 7E-H).

Glucose tolerance

We next tested glucose utilization by IP glucose tolerance test (GTT). Glucose doses were adjusted in proportion to lean mass. Despite the lack of difference in adipose mass between *Kcnj13*ΔMC4R^{Cre} and *Kcnj13*$^{+/+}$;MC4R^{Cre} mice, male and female *Kcnj13*ΔMC4R^{Cre} mice had significantly reduced glucose tolerance compared with all control strains, including *Kcnj13*$^{+/+}$;MC4R^{Cre} (Fig 7I-L).

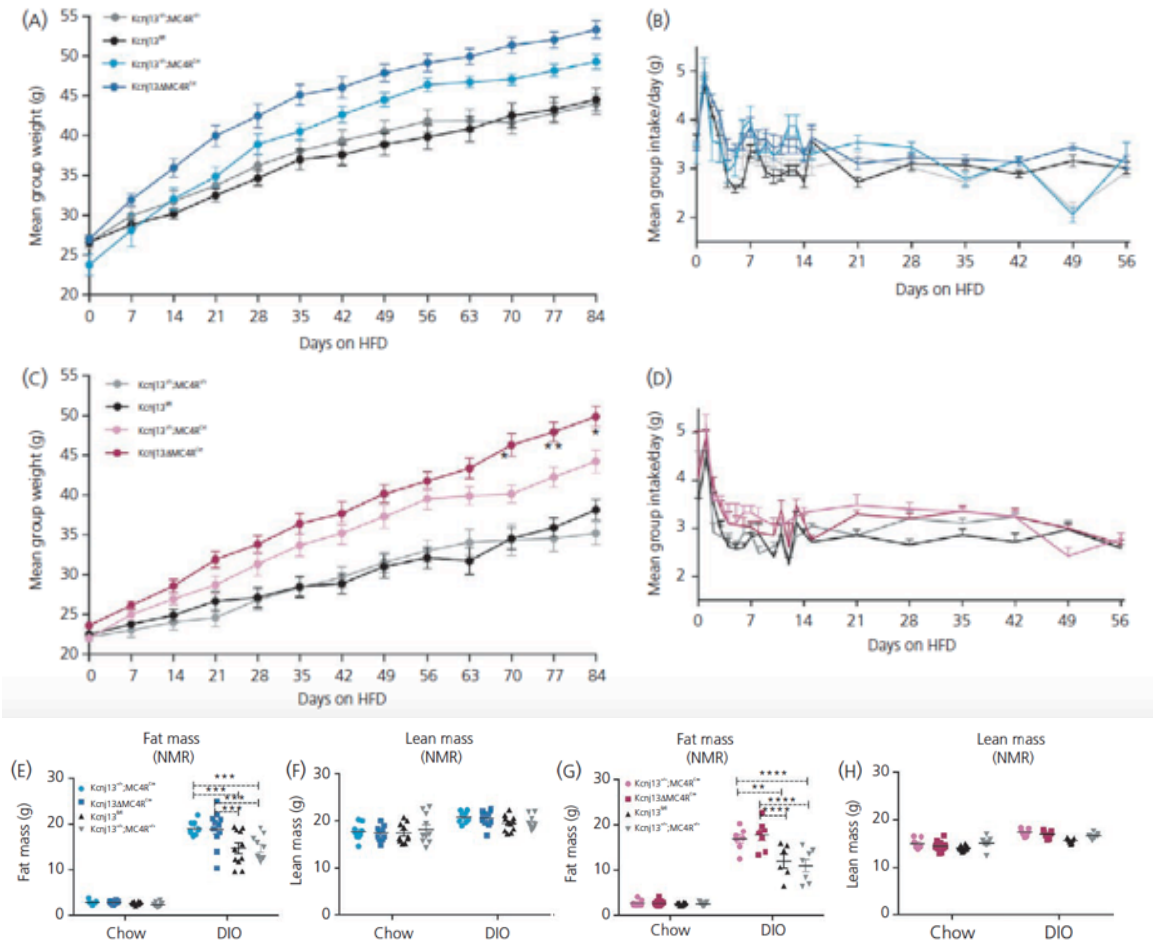

Fig. 4-7. Obesity and glucose intolerance in *Kcnj13*ΔMC4R^{Cre} mice on high fat diet.

(A-H) Growth curves on high fat diet from (A) male and (C) female mice (n = 7-11/group, Mixed linear effect model of DIO male *Kcnj13*$^{+/+}$;MC4R^{Cre} vs. *Kcnj13*$^{fl/fl}$ P value < 1.1e-6, female P value < 2.2e-16. *Kcnj13*$^{+/+}$;MC4RCre vs. *Kcnj13*ΔMC4R^{Cre} male P value = 0.01, female P value = 0.8). (*P<0.05, **P<0.005 via multiple students t-test *Kcnj13*$^{+/+}$;MC4R^{Cre} vs. *Kcnj13*ΔMC4R^{Cre}). Daily high fat diet consumption of (B) male and (D) female mice. One-way ANOVA test. (E-H) Fat and lean mass body composition of male (E-F) and female (G-H) on chow vs HFD. Two-way ANOVA with Tukey's multiple comparison test.

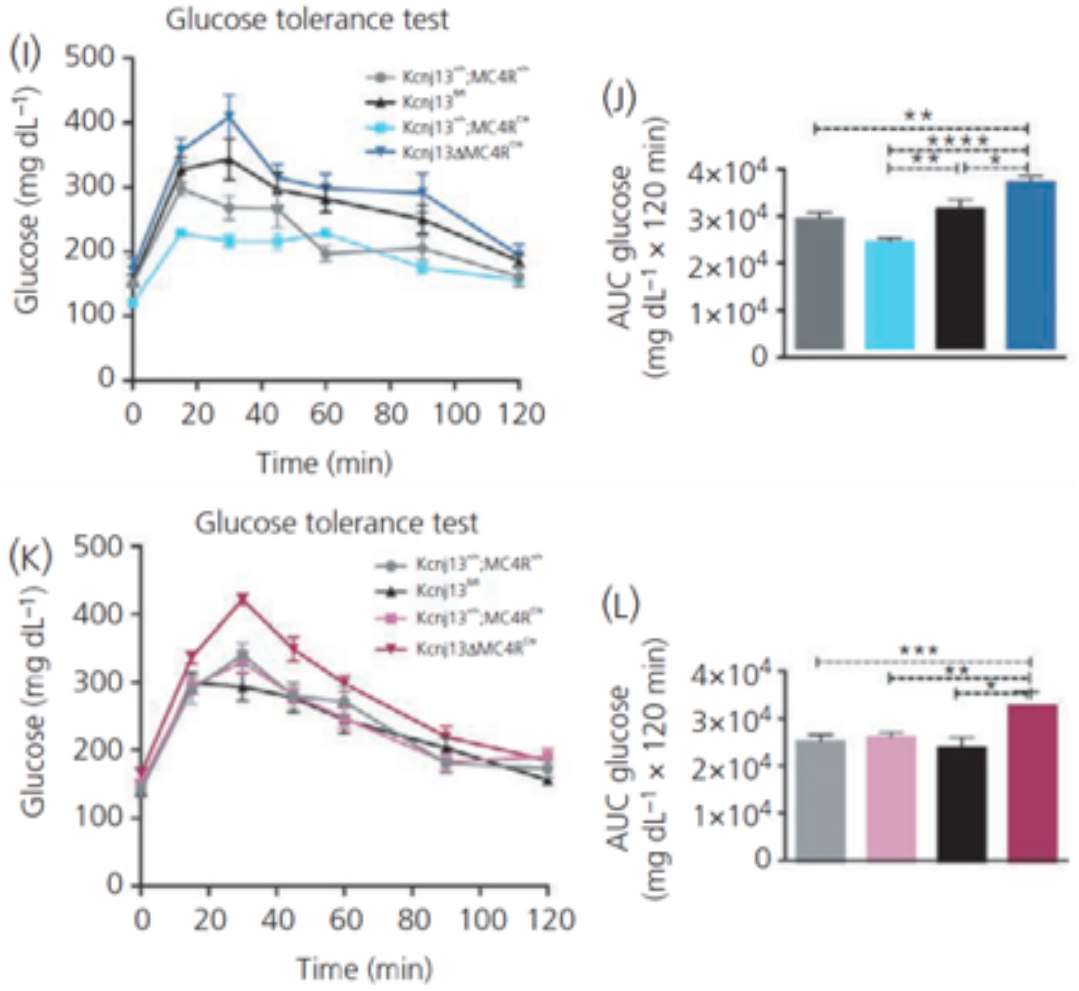

Fig. 4-7. Obesity and glucose intolerance in *Kcnj13*ΔMC4R^{Cre} mice on high fat diet.

(I-L) Plasma glucose concentration during intraperitoneal glucose tolerance test (IPGTT) 1g/kg glucose, normalized to % lean body mass was administered to each animal. IPGTT was performed after eight hour daytime fast in mice fed HFD for five months in (I) male and (K) female animals. Comparison of the % difference in total AUC shows that *Kcnj13*ΔMC4R^{Cre} differed significantly from control genotypes in (J) males and (L) females. (n = 6-8/group, *P<0.05, **P<0.005, ***P<0.0005, one-way ANOVA with Tukey's multiple comparisons test).

Summary and Conclusions

MC4R is known to signal through the Gαs-cAMP signaling pathway in cell assays and *in vivo*. However, our data on MC4R signaling in a hypothalamic slice preparation from the mouse suggested that the MC4R depolarizes neurons in the PVN via G protein independent regulation of the inward rectifier Kir7.1. To assess the potential physiological role of this MC4R-Kir7.1 signaling pathway, we used Cre-loxP technology to delete Kir7.1 from MC4R-expressing cells in the mouse, and investigated the consequences on MC4R signaling as well as on MC4R-mediated physiological responses.

Homozygous loss of Kir7.1 is known to cause degenerative eye diseases such as snowflake vitreoretinal degeneration (SVD) and Leber congenital amaurosis (LCA) [242] [244] in humans, and a pigmentary defect in the *jaguar* zebrafish [233], and thus we anticipated being able to conduct our studies in the global Kir7.1 knockout mouse. Surprisingly, however, we discovered that homozygous deletion of Kir7.1 in the mouse caused perinatal lethality. Histological analysis demonstrated stunted lung and kidney development as well as reduced body mass (Fig 4-S1), and this same finding was reported by another laboratory [299]. It is unclear why Kir7.1 is an essential developmental gene in the mouse but not zebrafish or humans, although the observation suggests variable physiological functions of this channel in different species.

After proceeding through a breeding strategy to obtain animals with a floxed *Kcnj13* allele, we generated animals with MC4R-site specific deletion of Kir7.1. Because Kir7.1 is expressed at very low levels in the sparsely distributed MC4R neurons [45], we were unable to readily validate the absence of Kir7.1 mRNA from MC4R neurons. Recording from MC4R labeled cells in the PVN is a well-established tool for characterizing MC4R firing activity [300]. Likewise, the depolarization signature of MC4R cells via closure of Kir7.1 has been defined in the slice preparation. Using this functional assay, we observed depolarization of *Kcnj13*$^{+/+}$;MC4R^{Cre} cells in response to α-MSH (Fig 4-2A). By contrast, with the deletion of Kir7.1 in *Kcnj13*ΔMC4R^{Cre} cells, α-MSH induced depolarization was no

longer observed (Fig 4-2B), supporting the hypothesis that Kir7.1 is required for α-MSH-induced depolarization of PVN MC4R neurons in the slice preparation. We have not surveyed this requirement for Kir7.1 in other MC4R neurons depolarized by α-MSH. Furthermore, we do not know how depolarization of PVN MC4R neurons in the slice preparation correlates with the physiological sequelae of MC4R activation *in vivo*. Interestingly, although administration of MC4R agonists rapidly inhibits food intake (Fig 4-2), inhibition of food intake via opotogenetic or chemogenetic activation of POMC neurons has a latency of several hours. Thus, it is possible that activation of MC4R neurons in a slice preparation reflects pharmacological but not necessarily physiological activation of MC4R.

To investigate the role of Kir7.1 in mediating the pharmacological response to α-MSH *in vivo*, we began by quantifying the feeding response on regular chow in response to an anorexigenic dose of exogenously administered α-MSH analogue, LY2112688. No significant difference is observed in baseline daily chow consumption in control vs *Kcnj13*ΔMC4R^{Cre} mice (Fig 4-6D). Although food intake was potently inhibited by IP delivery of LY2112688 in animals with intact Kir7.1 in MC4R cells, male and female animals lacking Kir7.1 exhibited a reduced responsiveness to LY2112688 throughout the study, and also exhibited a greatly reduced duration of response. Specifically, animals lacking Kir7.1 in MC4R cells lost LY2112688 responsiveness typically by 12 hours, whereas control strains sustained responsiveness for 24-40 hours (Fig 4-3A-C). These results suggest that sustained activity of an administered MC4R agonist requires Kir7.1. Experiments using viral knockdown of Kir7.1 in the PVN produced very similar findings, indicating that the effect is a result of the acute loss of function of Kir7.1 in PVN neurons, rather than a developmental defect.

This study parallels prior work using a Tl^+ flux assay in HEK293 cells expressing MC4R and Kir7.1 to characterize the regulation of ion flux through Kir7.1 mediated by MC4R [103]. These data suggested that the G-protein mediated cAMP response peaks rapidly after α-MSH exposure, whereas inhibition of Tl+ flux through Kir7.1 continued long after cAMP response ebbed [45]. Although our data clearly demonstrated pharmacological defects in response to melanocortin agonists in the

absence of Kir7.1, whereby stimulation causes rapid inhibition of food intake, chronic stimulation of ARC POMC neurons using opto- or chemogenetic methods reduces food intake only after several hours [63] [70]. This indicates that Kir7.1 may also be important for the anorexigenic effects of endogenous melanocortins released by POMC neurons, and suggests that it would be interesting to examine the effects of chronic stimulation of POMC neurons in the *Kcnj13*ΔMC4R^{Cre} mouse.

AgRP engages the MC4R at high affinity, but does not couple the receptor to G proteins or stimulate arrestin recruitment [301]. Thus, when we determined that AgRP stimulates MC4R-dependent opening of Kir7.1 [33}, we predicted that AgRP was a biased agonist, signaling specifically via Kir7.1. We anticipated that the *Kcnj13*ΔMC4R^{Cre} would have reduced physiologic response to the inverse agonist AgRP as well. However, a preliminary study demonstrated that exogenous ICV delivery of AgRP to the hypothalamus induced similar hyperphagia and 4 days of weight gain in *Kcnj13*ΔMC4R^{Cre} and control mice (Fig 4-4A-B). Thus in contrast to our hypothesis, AgRP may not require Kir7.1 for normal signaling. Of course, these studies were also limited by virtue of being pharmacologic in nature, and additional studies will need to be conducted to determine if a compensatory signaling pathway has been activated in this knockout model, such as AgRP activation of ERK phosphorylation. Other explanations include the possibility that a) AgRP functions exclusively as an inverse agonist and competitive antagonist of MC4R driven Gαs signaling, or b) AgRP also signals via an as yet unidentified mechanism [302] [303] [304].

Not only is MC4R widely expressed in the CNS, but also sites of peripheral expression have been detected, namely in the peripheral nervous system and enteroendocrine L-cells [77] [305] [26] [82]. Transcriptional profiling of L cell negative and L cell positive populations from both intestinal ileum and colon determined that whereas MC4R is enriched in L-cells, *Kcnj13* expression values are similar in these populations (correspondence with Arora Tulika using ArrayExpress database accession numbers E-MTAB-6322 and E-MTAB-6324) [306]. Using an assay for detecting MC4R-dependent L-cell release of PYY in response to exogenous administration of the α-MSH analogue LY2112688, we found that the absence of

Kir7.1 in MC4R cells has no effect on PYY release (Fig 4-5). These data clearly show that MC4R induces PYY release in a Kir7.1 independent manner, emphasizing the point that there are multiple modes of MC4R signaling, and that some physiological signaling events are Kir7.1 independent. Elevation of cAMP in L cells has been demonstrated to stimulate PYY release [82].

Deletion and haploinsufficiency of MC4R results in a rapid onset of phenotypes, most prominently early onset obesity characterized by both hyperphagia, reduced energy expenditure, hyperinsulinemia, and protection from obesity associated hypertension, observable by 8 weeks of age [307] [280] [83]. To address the physiological phenotype(s) of site-specific loss of Kir7.1 in MC4R cells we investigated the weight gain profile, caloric consumption, body mass composition, linear growth, and glucose metabolism of *Kcnj13*ΔMC4R^{Cre} mice maintained on normal mouse chow. Initially, at the 9-15 week time points, we observed no change in body weight, body composition, or metabolism in these mice. However, because mice were measured beyond 15 weeks, we observed the *Kcnj13*ΔMC4R^{Cre} mice tended to gain more weight than control genotypes, particularly in females. At 1 year of age, we observed weight gain in *Kcnj13*ΔMC4R^{Cre} male and female mice compared to *Kcnj13*$^{fl/fl}$, *Kcnj13*$^{+/+}$;MC4R^{Cre}, and *Kcnj13*$^{+/+}$;MC4R$^{+/+}$ mice, moreover female *Kcnj13*ΔMC4R^{Cre} mice gained weight more rapidly than males. (Fig 4-6A, B). It was interesting to note a large effect of Kir7.1 loss on linear growth at 30 weeks of age (Figure 4-6C-D), reminiscent of an effect seen on MC4R deletion. The late onset obesity was not accompanied by any measurable hyperphagia (Fig. 4-6E). By the 28 week time point female *Kcnj13*ΔMC4R^{Cre} mice gained significantly more fat as measured by absolute mass (Fig. 4-6F) and %fat mass (Fig. 4-6H) than control genotypes. There was no concordant change in absolute lean mass (Fig. 4-6J) although %lean mass was altered reciprocally (Fig. 4-6I). Thus the late onset weight gain was clearly a result of increased adipose mass and not lean mass.

The lean mass adjusted, low dose glucose tolerance test indicates deterioration of peripheral glucose metabolism in *Kcnj13*ΔMC4R^{Cre} mice, associated with significant fat accrual (Fig. 4-6J-L). MC4R signaling regulates glucose homeostasis in addition to excess adipose mass animals, both of which may have contributed to defective glucose utilization shown here [279]. It is possible that hyperphagia exists, although it is too small to be detected in parallel with the very slow, late onset obesity.

To potentially accelerate the effects of Kir7.1 deletion, we conducted similar experiments, placing mice on high fat diet. Notably, the expression of MC4R-t2a-Cre-recombinase alone in the *Kcnj13*$^{+/+}$;MC4R^{Cre} control genotype has an obesigenic effect on high fat diet fed mice (Fig 4-7A, C). Given the morbid early onset obesity arising from a 50% reduction in MC4R expression in mice or humans, even a very small reduction of MC4R mRNA production, or reduced production or function of the MC4R protein resulting from, for example, inefficient cleavage of the t2a site needed for release of Cre recombinase from the MC4R-Cre fusion protein could explain the obesity seen in *Kcnj13*$^{+/+}$;MC4R^{Cre} mice fed high fat chow. Similarly, it is possible that the 18-22 amino acid carboxy-terminal extension on the MC4R protein, resulting from cleavage of MC4R and Cre-recombinase, produced an MC4R with slightly reduced activity. However, these remain hypotheses because there is no data available regarding the MC4R mRNA or protein made by the MC4R-t2a-Cre-recombinase construct.

Nonetheless, When Kir7.1 is ablated from MC4R cells, male and female mice are more sensitive to diet induced weight gain than the *Kcnj13*$^{+/+}$;MC4R^{Cre} controls (Fig 4-7A, C). This does not appear to be due to the result of a sustained hyperphagic response (Fig 4-7B, D). A comparison of body mass composition by NMR reveals a significant increase in fat mass in both male and female *Kcnj13*ΔMC4R^{Cre} animals compared to *Kcnj13*$^{+/+}$;MC4R$^{+/+}$ and *Kcnj13*$^{fl/fl}$ controls, but not compared to *Kcnj13*$^{+/+}$;MC4R^{Cre} (Fig4-7 E-H). Given the significant increase in total weight, we hypothesize that the lack of a difference in fat mass in *Kcnj13*ΔMC4R^{Cre} animals vs controls by be the result of a lack of sensitivity of the whole animal NMR method. This phenotype diverges from global loss of MC4R, which manifests a

rapid obesigenic response to high fat diet, while *Kcnj13*ΔMC4R^{Cre} mice display milder, delayed onset obesity [308]. Likewise MC4R deletion results in an increase in both lean and fat mass [76]. The obesigenic effect of the MC4R^{Cre} allele is clearly problematic, and a MC4R-Cre allele with no background activity is clearly needed to advance the field.

After mice had matured on high fat diet, a glucose tolerance test was conducted to test glucose utilization. A low glucose dose (1 mg/kg) adjusted to lean mass was used as mice on high fat diet already have compromised glucose homeostasis [309, 310]. Here the Cre-driver line had no intermediate phenotype, whereas the *Kcnj13*ΔMC4R^{Cre} male and female mice had perturbed tolerance to glucose as confirmed by a significant increase in area under the curve (Fig 4-7I-L). The autonomic nervous system governs central glycemia via its two arms: ChAT^{Mc4r} expressing sympathetic neurons and Phox2b^{Mc4r} expressing parasympathetic neurons [307]. Mice lacking MC4R present with hyperglycemia and hyperinsulinemia that is further exacerbated during fat accrual into maturity. Although parasympathetic nervous system outflow stimulates insulin release, sympathetic nervous system outflow via ChAT^{Mc4r} neurons has been demonstrated to modulate glycemic tone [175]. The deteriorating weight maintenance and glucose intolerance in *Kcnj13*ΔMC4R^{Cre} mice suggests that Kir7.1 may also augment MC4R signaling in autonomic nervous system pathways regulating glucose homeostasis.

The data presented here show a measurable requirement for Kir7.1 in MC4R neurons for pharmacological responses to melanocortin agonists, but not antagonists. In particular, Kir7.1 may be required for sustained responses to pharmacotherapy with melanocortin agonists such as setmelanotide. It will be informative to determine if the delayed anorexigenic effect of optogenetic stimulation of POMC neurons requires Kir7.1. Likewise, given the apparent role of Kir7.1 in sustained anorexia, it may be informative to investigate the role of Kir7.1 in mediating the demonstrated role of MC4R signaling in disease cachexia in the

mouse. Similarly, other physiological responses to melanocortins, such as those involved in the control of glucose homeostasis, may depend on Kir7.1. Importantly, these data do not prove a physiologically relevant direct coupling of MC4R to the channel, since, of course, the loss of this channel could alter the function of MC4R neurons in a non-specific manner. Furthermore, we provide a direct example of a physiologically mediated MC4R pathway, PYY release, from L cells, that appears Kir7.1 independent. Likewise, we found no evidence for a compromised response to AgRP.

Given the requirement of Kir7.1 in α-MSH induced depolarization of PVN MC4R neurons, we were anticipating a larger obesity phenotype in the *Kcnj13*ΔMC4R^{Cre} mice. We were surprised to note the very modest effect of Kir7.1 on body weight, as well as the divergence of the phenotype from that seen in MC4R knockout mice and patients with MC4R mutations. Indeed, all mutations leading to defective MC4R signaling, including mutations in MC4R, POMC, deletion of Gαs in MC4R cells and even overexpression of AgRP, lead to a similar melanocortin obesity phenotype characterized by early onset obesity, with hyperphagia, increased linear growth, and increased lean mass. A very different phenotype, involving modest late onset obesity, with no measurable hyperphagia, increased linear growth, and no increase in lean mass, was instead observed in mice lacking Kir7.1 in MC4R cells. There are many potential explanations for these findings, including changes that compensate early on for the absence of Kir7.1. Recently, a rather dramatic example was reported illustrating the tremendous compensatory plasticity of the melanocortin circuits in response to early developmental gene knockout [311]. Deletion of leptin receptor from AgRP neurons is found to produce only a minor obesity and disease phenotype relative to global leptin receptor deletion [312]. By contrast, CRISPR-mediated deletion of the gene in AgRP neurons in adult animals produced a morbid obesity syndrome almost paralleling that seen in the *db/db* mouse [312]. Even more relevant to the present study, leptin hyperpolarizes neurons by opening the K_{ATP} channel [313]. Although global deletion of the Kir6.2 subunit of this channel had a limited effect on glucose homeostasis and no

obesogenic effect, CRISPR-mediated mutagenesis of Kir6.2 in AgRP neurons alone yielded a morbid obesity syndrome with diabetes [312] [314] [315]. Thus, it is possible that a wholly different phenotype may be seen upon deletion of Kir7.1 in the adult mouse.

Alternatively, the results reported in the present study may indicate that Kir7.1 plays a very specific and limited role in the physiological functioning of MC4R. Additionally, the data obtained do not rule out the possibility that the phenotype results from a minor developmental alteration in a subset of MC4R neurons. Furthermore, we proved a direct example of a physiologically-mediated MC4R pathway. PYY release, from L-cells, which appears to be Kir7.1-independent. Interestingly, irrespective of the physiological role(s) for Kir7.1 in MC4R signaling, the present study demonstrates a significant pharmacological effect of Kir7.1 *in vivo* and in the slice preparation. These data may thus be important for the ongoing challenge with respect to the development of therapeutics acting at the MC4R, further highlighting the complexities of MC4R signaling that remain to be solved.

CHAPTER 5

DISCUSSION AND FUTURE DIRECTIONS

Through the studies undertaken in this work a novel understanding of MC4R signaling partners, Gαs, and in particular Kir7.1, in regulating energy homeostasis has been elucidated. This is the first description of Kir7.1 in whole animal metabolic physiology. This work shows that Kir7.1 global haploinsufficient animals have a heightened response to weight gain on high fat diet, have increased linear growth, and are more responsive to MC4R antagonist agouti. To hone in on the effect of Kir7.1 specifically in MC4R cells, a Cre-loxP model shows that Kir7.1 is required for MC4R signaling as *ex vivo* PVN cells exposed to α-MSH fail to depolarize in the absence of Kir7.1, confirming and further implicating Kir7.1 in resistance to sustained anorexic effect of exogenously delivered α-MSH analogue. Furthermore, late onset obesity on chow confirms a heightened response to high fat diet, as well as reduced glucose tolerance. Other MC4R-mediated pathways do not appear to be adversely affected by Kir7.1 deletion including centrally delivered AgRP-induced stimulation of food intake and induction of PYY release from intestinal L-cells. Thus Kir7.1 mediates the magnitude and kinetics of the overall response to α-MSH, whereas the response attributed to AgRP does not appear to be significantly altered, at least in the limited AgRP analysis conducted herein. These findings have putative implications for development of biased pharmacotherapies.

Role of Kir7.1 in MC4R signaling *in vivo*

Since the initial description of the prominent role of MC4R as the rheostat of energy homeostasis, much effort has been spent on understanding MC4 and its corresponding signaling and regulatory partners. Kir7.1 is an apparent contributor to this pantheon of players albeit with a comparatively modest, late onset role. In these the interaction of MC4R and Kir7.1 is most profoundly pharmacological and pertaining to the POMC arm of MC4R. However there is also a clear effect on linear

growth which recapitulates a MC4R phenotype. The dampened and late onset phenotype observed herein may be due to modes of signaling controlled primarily by G-protein or due to developmental compensatory effect from Cre-lox mutagenesis. Because energy intake is a highly protected function with many central cell and nuclei type specific neuronal circuits feeding into the behavioral manifestation of eating, Kir7.1 may have a role in energy intake that is currently masked by compensatory effects in this developmental knockout model. This would be similar to initial studies of AgRP driven food intake, where knockout of *AgRP* displayed a late onset lean phenotype including reduced adiposity and increased metabolic after 6 months of age [316]. Likewise developmental deletion of *Npy* results in compensatory adaptations [317]. Using a centrally delivered adeno-associated virus CRISPR model in adult mice the Kong group recently confirmed developmental compensatory effect had obscured leptin signaling pathways through AgRP neurons in mice [311]. Additionally, the Gαs story is far from concluded. A notable gap that remains to be addressed is whether neurons lacking *GNAS* remain fully functional, have normal projections, and whether the Cre obesigenic phenotype background also affects the model of MC4R specific deletion Gαs. Thus while my data shows a clear pharmacological role for Kir7.1 in MC4R cells, the physiologic role may better be determined via site specific deletion system such as CRISPR or hormone inducible-Cre in adults an approach that would also be useful for further study of Gαs signaling in MC4R.

Single cell-specific pull down and transcriptome analysis could elucidate if *Kcnj13* is co-expressed with MC4R in other nuclei known to contribute to autonomic energy expenditure such as the hindbrain DMX. Future studies using a viral or inducible knockdown of *Kcnj13* could be used to further explore the mechanism of *Kcnj13* in MC4R cells. These types of models would be ideal because it would limit the mutation opportunities for compensatory changes during development.

While the absence of clinically noted metabolic deficiencies in humans with *Kcnj13* mutations is surprising, it is also indicative of complexities in Kir7.1. Furthermore, late onset obesity probably would not have been noted in the few cases of Kir7.1 blindness reported. It is known that Kir7.1 can form homo- or

heteromeric assemblies, however it is unknown what combination or combinations of tetramer exist in the PVN or in other regions of Kir7.1 expression. These protein adaptations may confer distinct properties to Kir7.1 that are site specific or compensatory. This may explain the absence of death and metabolic dysfunction in patients with Kir7.1 mutation channelopathies leading to SVD or LCA. Some mutations may therefore be tolerated. Perhaps in the future genomic screening of patient cohorts with obesity or metabolic syndrome will lend further understanding of what, if any *Kcnj13* mutations contribute to these syndromes. Mutations might alter ion channel function either due to defective trafficking to the membrane, defective channel opening and closure, less ion selectivity, and/or reduced / heightened interaction with intracellular signaling partners. Molecular understanding for the functional abnormalities associated with a specific mutation need to be established. Severity in pathological consequence is perhaps directly linked to severity of the outcome of mutation.

Until additional tools are developed, obesity-linked variants of the human MC4R can be examined for defective MC4R- Kir7.1 signaling. Some alleles with normal G-protein cAMP activity yet an obese phenotype are already known and may be linked to changes in Kir7.1 coupling. With this knowledge future therapies could circumvent pathologies driven by obesity through drugs or gene or cell therapy

MC4R and targeted drug therapies

The discovery of a G-protein independent pathway for MC4R signaling opened potential avenues for development of biased pharmacotherapies that would avoid harmful cardiopressor effects, which have been the bane of marketable MC4R, targeted compounds. By characterizing the physiologic phenotype and pharmacologic action of Kir7.1 in multiple animal models and experimental assays indicative of MC4R function, we have shown that Kir7.1 is indeed a downstream intracellular mediator of MC4R ligand bound activity. In particular Kir7.1 appears to be important in regulating energy expenditure under metabolic challenge and response to agonist. It remains to be fully understood which molecule, Gαs or

Kir7.1, mediates different processes regulated by MC4. Our studies in combination with Podyma et al. seem to indicate that in at least some MC4R processes, Gαs and Kir7.1 act in harmonious synergy where some physiologic functions are maintained by influence from Kir7.1 (for example linear growth) and other by Gαs (for example hyperphagia). It is reasonable that many phenotypes require input from both pathways, yet these studies foreshadow potential avenues for drug therapies. Specifically, Kir7.1 impacts the length of MC4R response to ligand, which may prove important for MC4R pharmacology. Indeed, 30-50% of catalogued MC4R human mutations, such as MC4R H76R, have been shown to traffic and interact normally with G-protein pathway yet still manifest in clinical obesity. The deleterious mechanism of these mutations may be related to Kir7.1-MC4R signaling. Isolating a biased ligand would still be useful to provide insight into obesity pathogenesis and pharmacology of neural MC4Rs and of course ultimately as a therapy [318]. In the meantime a knockin model for mutation(s) like MC4R H76R could further elucidate features of this signaling modality.

Several attempts have been made to crystallize MC4R, however MC4R constitutive activity and extremely hydrophobic characteristics are likely hindering its purification and crystallization. As future efforts are undertaken, a crystal structure of either inactive ligand-free, ligand bound complex, or complex with even partial bound Gαs or Kir7.1 would be a tremendous breakthrough in understanding MC4R function. While MC4R and Kir7.1 can be co-immunoprecipitated, no data yet proves they interact directly.

Finally, a pitfall of MC4R drug development has been that stimulation of MC4R causes a cardiovascular pressor response. Thus it is critical to determine the effects of Kir7.1 on pressor response. During these studies, I began examining pressor response via telemetry and blood pressure tail cuff, yet because the weight loss was gradual and more modest, ultimately these studies were forestalled until full analysis of cardiovascular profile can occur in model system unhindered by developmental compensation and/or in acute studies with greater granularity. It

would certainly be meaningful if there were a differential effect of body weight and the pressor effect due to Kir7.1 function in MC4R.

Overall many advances have been made in understanding MC4R and its therapeutic potential (Fig 5-1). Now with novel insight in the roles for Kir7.1 in this process, scientific progress through inquiry can continue unraveling the complexities of energy homeostasis.

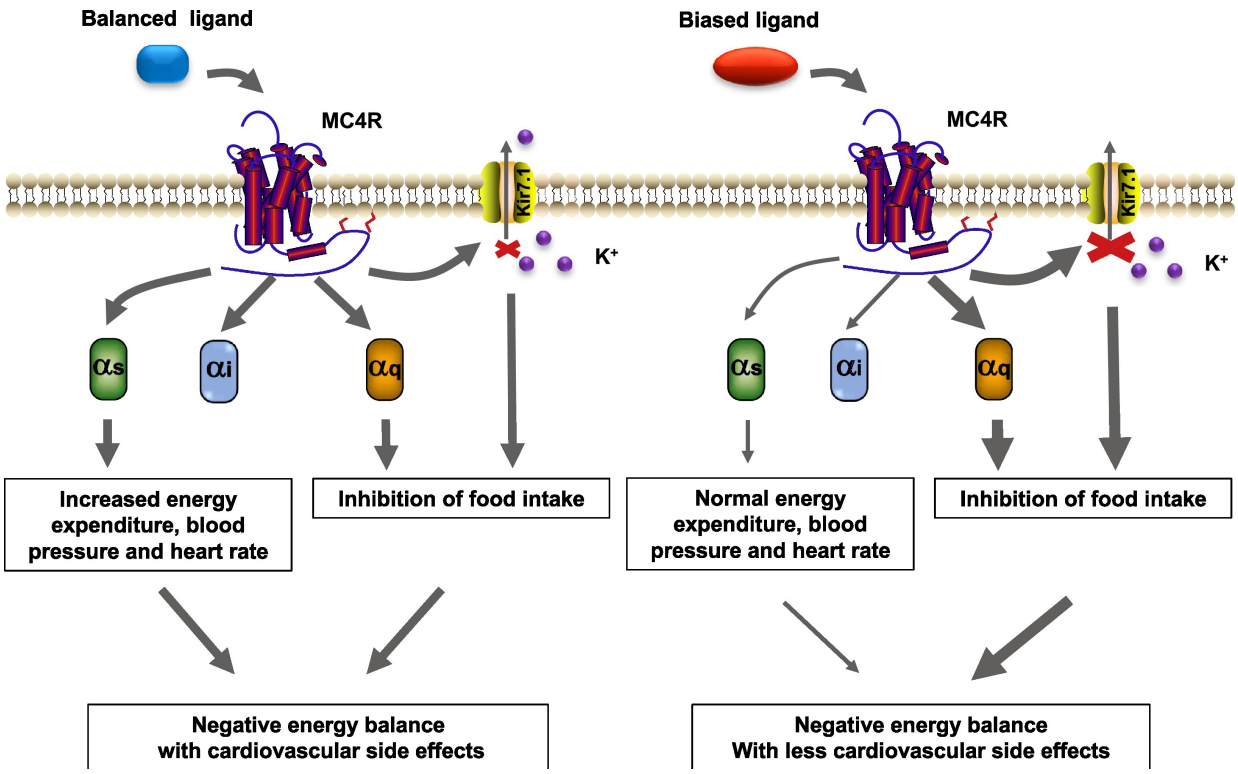

Figure 5-1. Biased signaling at neural MC4R in regulation of energy homeostasis.
Therapeutic relevance of biased signaling at neural MC4R. The MC4R could couple to Gs, Gq and Kir7.1. Normal balanced agonist activates MC4R and non-selectively induces Gs and Gq signaling and closure of Kir7.1, resulting in a negative energy balance with side effects. However, biased ligand activates MC4R and selectively induces Gq signaling and closure of Kir7.1, resulting in negative energy balance without side effects. Modified from (Yan, LK et al., 2017).

CHAPTER 6

METHODS

Mouse Husbandry

Mouse Handling

All mice were housed in standard, infection–free housing conditions at 25°C, in a facility on a 12 hr light:12 hr dark cycle. Strictly pathogen-free quality of the mouse colonies was maintained through quarterly serology, quarterly histopathologic exams, and daily veterinarian monitoring of the general health and welfare of animals. Male and female mice were used for these experimental procedures. Mice were weaned at four weeks of age and kept with 4-5 mice per cage, unless animals were used for feeding studies. Animals used in feeding analysis were singly housed for acute studies and dually housed for long term feeding studies. Unless otherwise described, all mice were fed a standard chow diet (Lab Diet; St. Louis, MO; S-5LOD - 13.5 kcal% fat, 32.98 kcal% Protein, 56.7 kcal% Carbohydrate). Diet induced obesity was promoted by high fat diet (Research Diets; New Brunswick, NJ; D12492 - 60 kcal% fat, 20 kcal% Protein, 20 kcal% Carbohydrate). Post mortem studies were conducted by giving animals a dose of 5mg/kg tribromoethanol in order to deeply anesthetize the mice before sacrifice via decapitation. Tissues of interest were rapidly excised and flash frozen by liquid nitrogen. All procedures were carried out with approval from the Institutional Animal Care and Use Committee of Vanderbilt University Medical Center.

Mouse Lines

Mouse Strains and Genotyping

We used promoter-driven, knockout-first, *Kcnj13* targeted selection clones from the Knockout Mouse Project (KOMP) Repository at UCDavis for the generation of our transgenic mice. Embryonic stem cell (ESC) clones expressing the mutant allele

Kcnj13$^{tm1a(KOMP)wtsi}$ were expanded at Vanderbilt's Transgenic Mouse / ES Cell Shared Resource (TMESCSR), where chimeric mice were generated on the C57BL/6N background. Germ line transmission was confirmed by crossing chimeric male mice to wildtype C57BL/6N females. Genotyping confirmed the presence of the mutant allele, *Kcnj13*$^{tm1a(KOMP)wtsi}$, in progeny. This allele also carries an En2 splice acceptor sequence and a poly-A transcription termination signal, which disrupts *Kcnj13* gene function. Following the KOMP breeding strategy for mutant allele generation, *Kcnj13*$^{tm1a(KOMP)wtsi}$ mice were bred to mice expressing the recombinase flippase to generate the *Kcnj13*$^{tm1c(KOMP)wtsi}$ allele. The expression of FLP recombinase excised the promoter driven Neo cassette, converting allele *tm1a* into conditional mutant allele *tm1c*. Mutant *Kcnj13*$^{tm1c(KOMP)wtsi}$ mice were mated to sibling mice in order to build a colony of *Kcnj13*^{tm1c} mice (referred to as *Kcnj13*$^{fl/fl}$ mice). The *Kcnj13*$^{fl/fl}$ colony was crossed with a MC4R-t2A-Cre Tg/+ line (kindly provided by Dr. Bradford Lowell) to generate a MC4R cell specific *Kcnj13* knockout experimental animal (referred to as *Kcnj13*ΔMC4R^{Cre}). This allele is referred to as *Kcnj13*^{tm1d} in KOMP nomenclature. All mouse lines were maintained on a C57BL/6NJ background with annual backcrosses to wild type C57BL/6NJ mice (Jackson Laboratory; Sacramento, California - Jax Stock No: 005304).

Mc4r-tau-Sapphire mice for electrophysiological studies were obtained from the Jackson Laboratory (Jax Stock No: 008323).

Primers for genotyping *Kcnj13*$^{fl/fl}$ or *Kcnj13*$^{+/+}$ alleles were:
*Kcnj13*_ttR CCAGAGGGTGAGGCTTATAATTTGTGC
*Kcnj13*_F GGTCAGTGAGATATGGCCTAGTGGG

Primers designed to amplify CRISPR *Kcnj13* mutant alleles

Blue=bases that are 3' to the deleted bases.

6-F1	GGAATCCTAATGGACATGG	TM=52.4
10A-F1	GGAATCCTAATGGACGCT	TM=53.7

10A-F2	GGGGAATCCTAATGGACG	TM=54.1
10B-F1	GGGGAATCCTAATGGACC	TM=53.6
22-F1	GGGAATCCTAATGGACATC	TM=52.1

Forward primers paired in Platinum PCR SuperMix High Fidelity (Invitrogen) with the reverse primer:

Kcnj13-R1	CAGACTTGTCTTAACCAAC	TM=51.0

Electrophysiology

Hypothalamic Slice Electrophysiology

Mc4r-tau-Sapphire mice, backcrossed onto the C57BL/6J background, were previously characterized by dual immunohistochemistry and *in situ* hybridization to validate that GFP-positive neurons in the PVN expressed MC4R RNA [79]. Randomly selected MC4R-GFP male and female mice, 8–16 weeks of age, were deeply anaesthetized with isoflurane before decapitation. The brain was entirely removed and immediately submerged in ice-cold, gassed (95% O_2, 5% CO_2) artificial cerebrospinal fluid (aCSF), containing (in mM): 126.2 NaCl, 3.1 KCl, 2 $CaCl_2$, 1 $MgCl_2$, 1 NaH_2PO_4, 26.2 $NaHCO_3$, 10 glucose and 11 sucrose (320 mosm per kg, pH 7.39 when gassed with 95% O_2, 5% CO_2 at room temperature). Brain blocks of containing hypothalamus were made by trimming the whole brains while immersed in oxygenated, near-freezing aCSF and glued to a dental-cement cast customized to the size of the block mounted on a plate with adjustable angle. Brain slices of 200-μm thicknesses were then cut at angle range between 44° and 49° in reference to horizontal plane and transferred to a glass beaker containing oxygenated ACSF at 31 °C. After an incubation period lasting at least one hour, a slice was transferred to a recording chamber (~2.0 ml in volume), then submerged and immobilized with nylon strands drawn taut across a C-shaped platinum wire (1 mm outer diameter), and perfused with warmed (31–32 °C) oxygenated ACSF at a rate of 2–3 ml min^{-1}. EGFP-fluorescent neurons were

unambiguously identified and patched using combined epifluorescence and IR-DIC optics. Fluorescent neurons of healthy IR-DIC appearance but of every level of fluorescence brightness were chosen for electrophysiological recordings. Drugs were added to aCSF and bath applied to the slice via the perfusion system for extracellular applications. The small volume of the recording chamber relative to the flow rate assured a complete exchange of solution occurring in less than 1 min. The persisting effects of a peptide were therefore due to prolonged effects rather than a slow wash out.

In this study, whole-cell patch-clamp recordings were used to obtain information about action potential firing activity, and membrane potentials and currents. Unless stated otherwise, whole cell recordings were performed using patch pipettes of 3.4 MΩ to 5 MΩ resistance when filled with a solution containing (in mM); 125 K gluconate, 8 KCl, 4 $MgCl_2$, 10 HEPES, 5 NaOH, 4 Na_2ATP, 0.4 Na_3GTP, 5 Na_2-creatine phosphate, 7 sucrose and 7 KOH which resulted in a pH ~7.23 and osmolality of 295–300 mosmol per kg. The permeability of the α-MSH regulated channels was investigated by replacing K gluconate and KCl with 130 RbCl and 4 KCl, but otherwise similar condition. The examination of effects of Mg^{2+}-free internal solution on the α-MSH-induced current was conducted in voltage clamp mode from PVN neurons held at −55 mV. The Mg^{2+}-free internal solution contained 103 K-gluconate, 30 KCl, 10 HEPES-KOH, 0.5 $CaCl_2$, 5.5 EDTA-KOH, pH 7.23, with osmolality 304 mosmol per kg. The ATP free solution contained 83 K-gluconate, 30 KCl, 10 HEPES-KOH, 0.5 $CaCl_2$, 4 $MgCl_2$, 5.5 EGTA-KOH, pH 7.2 and osmolality 298 mosmol per kg.

Neuronal integrity was assessed by all of the following: small holding current (≤30 pA at −70 mV) when voltage-clamped, large amplitude rebound spikes, the ability to fire and lack of obvious morphological deterioration (that is, lack of blebbing and nucleus not visually present).

In order to quantify the action potential firing and amplitude of depolarization induced by α-MSH, current clamp recordings were performed in continuous mode while the membrane potential of neurons were held between −55 and −60 mV to prevent continuous spontaneous action potential firing. The firing frequency and membrane potential of neurons was measured during a 3-min period before the application of the peptides, and for another 3-min period 7–11 min after administration of peptide, and results compared.

Data were acquired at 10 kHz using a MultiClamp 700A amplifier (2,000× gain, –3 dB filter frequency 5 kHz) and Clampex 10.0.1 software (Axon Instruments, Union City, CA). GraphPad Prism 5.0 (Graphpad Software, Inc., San Diego, CA) and Excel 2010 (Microsoft) were used for data analysis. Statistical tests used included the paired *t*-test, when examining response of the same neurons before and after treatment with a compound, and the unpaired *t*-test when comparing the responses of different sets of neurons.

Fast-induced Re-feeding

Age and litter matched male and female mice were used for this study from young (not shown) and mature, 35-45 weeks of age, cohorts. Studies were repeated at least three times across multiple cohorts. One week before the study, mice were singly housed and accustomed to handling with IP injections of 100µl saline while provided with ab libitum standard chow and water. One day before the study mice were moved to clean cages with fresh bedding to minimize coprophagia. Mice were food deprived for 16-24 hours, before drug was administered at the beginning of dark cycle.

Mice were food deprived for 16 h before drug treatment, starting shortly before the beginning of the dark cycle. Experiments were blinded; drug compounds were prepared and coded the morning of the injections by an individual who would not be conducting the experiment. The randomly selected experimental groups

consisted of animals given vehicle, 10.0 mg/kg saline or 10.0 mg/kg LY2112688 (LY). For repeated studies, animals rested at least seven days between fasting periods and opposite treatments were given. Numbers needed to achieve significant inhibition of food intake by a melanocortin compound versus saline were based on prior experience. Food intake was measured at multiple time points after injection, beginning at 2 hours and extending as far as 40 hours after injection. In viral knockdown studies a ground feeding cylinder canister with a wire mesh bottom was used rather than the cage hopper. Mice were accustomed to the presence of the canister in their cage for one week before the experiment. The reduced accessibility of this apparatus is reflected in the reduced chow consumption in viral knockdown mice compared to cell specific genetic deletion mice studies. Statistical significance was established using two-way ANOVA and Tukey's post-hoc with a $P < 0.05$ significance value.

shRNA Lentiviral Design and Injection

Plasmids and recombinant lentiviruses

Mouse *Kcnj13* shRNA and scramble shRNA were constructed using the vector pSico (Addgene).

Kcnj13 shRNA plasmid (TRCN0000262099) was from Sigma, MO with sequence:
CCGGCGCCTTACTTGCCATACAAATCTCGAGATTTGTATGGCAAGTAAGGCGTTTTTG

Scramble shRNA (plasmid# 1864) was purchased from Addgene.

Scramble shRNA construct in pLKO.1 vectors was subcloned into pLL3.7 (Addgene, plasmid #:11795), which also encodes GFP. pLL3.7 plasmid with shRNA (scramble vs. *Kcnj13*). *Kcnj13* shRNA was cloned into pLKO.1 expressing mCherry.

293T cells were transfected with 12,6 µg of plasmids containing the shRNA (scramble vs. *Kcnj13*), and 6,3 µg each of the following plasmids: pRSV-Rev, pVSVG, and pMDLp/g (gift of Dr. Roger Colbran) using Lipofectamine 2000 (Invitrogen, CA) on 15 cm dishes. 96 hours post-transfection, culture medium from five 15cm-plates per shRNA clone were collected, and filtered through a 0.45µm filter. Viral particles were isolated by ultracentrifugation at 4˚C, 26000 rpm for 2 hours using a SW32Ti rotor. The pellet was resuspended in sterile PBS, aliquoted and frozen at -80 ˚C until further use.

Viral titer was quantified as follows: 100,000 293T cells were plated on 24-well plates. Cells were transduced by ten-fold serial dilutions of the viral particles with dilution range between 1:10 – $1:10^5$ using polybrene. GFP (for scramble shNA) or mCherry (for shRNA against *Kcnj13*) positive cells were counted in triplicate.

Purified lentivirus suspended in 550-600 nl artificial CSF was injected bilaterally and infused over 15 minutes into the PVN using a stereotactic frame and the coordinates of 0.82 mm posterior to bregma, 0.31 mm lateral to the midline of the brain and 4.68 mm below the surface of the skull, via a 26-gauge guide cannula and a 33-gauge internal injector (Plastics One, Roanoke, VA) connected to a 2 µl Hamilton syringe.

Cannulation Surgery and Intracerbroventricular Injection

To study the effect of ICV injection of MC4R neuropeptide, mice were anesthetized with isoflurane and a stainless-steel cannula (Plastics One, Roanoke, VA) was surgically implanted into the right lateral ventricle using the stereotaxic coordinates of 0.46 mm posterior to the bregma, 1.0 mm lateral to the midline, and 2.2 mm below the surface of the skull. Mice were allowed to recover for approximately 5 days while monitoring food intake and body weight with acclimatization to handling and manipulation of the dummy cannula. After recovery, cannula placement was verified by injecting 10 ng angiotensin II (Sigma, MO) diluted in 0.5 µl sterile saline.

Animals that did not exhibit drinking response within 30 minutes were excluded from the study. A day later experimental procedures were initiated during the light cycle. Peptides (AgRP, kindly provided by Glenn Millhauser) or vehicle were infused in a 0.5 µl volume over a 1-min period with a 2.0 µl Hamilton syringe (Plastics One, Roanoke, VA) coupled to an injection cannula by a polyethylene tubing. After injection the injector was kept in place for 1-min to ensure diffusion from the injector tip. Food intake and body weight was monitored after injection. When experimental procedures concluded, cannula placement was also verified histologically.

Post-Prandial Hormone EMSA

Male and female experimental mice (*Kcnj13*ΔMC4R^{Cre}; *Kcnj13*$^{fl/fl}$) age 25-27 weeks were acclimated to scruffing and injections for up to 5 days prior to blood collection. The day of the study, postprandial plasma PYY was reduced to baseline levels by 6 h daytime fast. Mice were randomly selected to receive intraperitoneal injection of vehicle (saline) or 5 mg/kg of LY2112688 in 100-200 uL volumes according to body weight. Numbers chosen based on prior experience suggesting significance can be achieved with 6 animals per treatment. At 10 min post-injection, approximately 200 µl of blood was collected via submandibular bleeding in conscious mice or by decapitation under anesthesia for trunk bleed. Blood was collected into vials containing appropriate volumes of EDTA and protease inhibitor cocktail for mammalian tissues (Sigma P8340) to prevent degradation of PYY and kept on ice. Upon collection of all blood samples, the vials were spun at 3000 X G at 4°C for 30 minutes. Plasma was removed and spun at 10000 × G at 4°C for 1 minute to pellet remaining blood cells. Plasma was frozen at −80°C until PYY was assayed. Plasma hormones were assayed in 10 µL duplicate samples using the MilliplexMAP Mouse Metabolic Hormone - Magnetic Bead Panel Immunoassay (Millipore MMHMAG-44K 1-plex kit for total PYY), with undiluted plasma to detect PYY (total). The assay was read on a Luminex 100 analyzer. Results were analyzed against a standard curve and concentrations were determined using Milliplex Analyst 5.1 software. Values

were plotted and analyzed using GraphPad Prism. Statistical analyses were conducted using multiple t-tests.

Growth Phenotyping

Male and female mice were dually housed with same sex, same genotype animals of similar weight to collect weekly food intake (standard chow or DIO) and growth data. Mouse lean and fat mass body composition was obtained by NMR (mq10 Minispec; Bruker; Billericia, Massachusetts).

Glucose Tolerance Test

Glucose tolerance testing was conducted as previously described [319]. Three days prior to GTT, body composition was obtained to determine lean body mass. Mice were then habituated to consecutive, daily handling sessions. On the study day, mice were fasted for 6 h from 8am- 3pm. Mice were scruffed to obtain a basal glucose read by tail nick, then injected with 1(DIO) to 2 (chow) mg/kg lean mass dose of glucose in sterile PBS. Glucose readings were obtained by tail vein bleed at 15, 30, 45, 60, 90, and 120 min following injections. Lean mass was determined by NMR body composition scan (mq10 Minispec; Bruker; Billericia, Massachusetts). Repeated sampling by tail vein bleeding was done at least 1 week apart to allow for complete recovery from blood loss. Area under the curve (AUC) was calculated by the trapezoidal rule.

Statistics

Sample size for growth curve studies was chosen using the power equation ($\alpha < 0.05$, $\beta = 0.1$, $\Delta\mu = 25\%$ $\sigma = 5$), whereas sample sizes for remaining studies were estimated based on previous publications. All statistical tests were conducted using GraphPad Prism 6 software (Scientific Software; La Jolla, California). Data is presented as mean ±standard error of the mean. All data with $P<0.05$ was considered statistically

significant. Statistical nomenclature: * =P < 0.05; **P<0.005; ***P<0.001; ****P<0.0001. Experimental performers were generally blinded for initial studies and partially blinded for genotype identity for repeated studies. Experiments were repeated at least three times with age and litter matched animals across experimental and control groups.

REFERENCES

1. Ogden, C.L., et al., *Prevalence of childhood and adult obesity in the United States, 2011-2012.* JAMA, 2014. **311**(8): p. 806-14.
2. Finkelstein, E.A., et al., *Annual medical spending attributable to obesity: payer- and service-specific estimates.* Health Aff (Millwood), 2009. **28**(5): p. w822-31.
3. Cone, R.D., *Anatomy and regulation of the central melanocortin system.* . Nat Neurosci,, 2005. **8**(5): p. 571-8.
4. Mountjoy, K.G., et al., *The cloning of a family of genes that encode the melanocortin receptors.* Science, 1992. **257**: p. 543-546.
5. Cone, R.D., *Studies on the physiological functions of the melanocortin system.* Endocr Rev, 2006. **27**(7): p. 736-49.
6. Roselli-Rehfuss, L., et al., *Identification of a receptor for gamma melanotropin and other proopiomelanocortin peptides in the hypothalamus and limbic system.* Proc Natl Acad Sci U S A, 1993. **90**(19): p. 8856-60.
7. Mountjoy, K.G., *Distribution and Function of Melanocortin Receptors within the Brain.* Adv Exp Med Biol. **681**: p. 29-48.
8. Begriche, K., et al., *Genetic Dissection of the Functions of the Melanocortin-3 Receptor, a Seven-transmembrane G-protein-coupled Receptor, Suggests Roles for Central and Peripheral Receptors in Energy Homeostasis.* J Biol Chem. **286**(47): p. 40771-81.
9. Mountjoy, K.G., et al., *The cloning of a family of genes that encode the melanocortin receptors.* Science, 1992. **257**(5074): p. 1248-51.
10. Gantz, I., et al., *Molecular cloning, expression, and gene localization of a fourth melanocortin receptor.* J Biol Chem, 1993. **268**(20): p. 15174-9.
11. Renquist, B.J., et al., *Physiological roles of the melanocortin MC(3) receptor.* Eur J Pharmacol, 2011. **660**(1): p. 13-20.
12. Lippert, R.N., K.L. Ellacott, and R.D. Cone, *Gender-specific roles for the melanocortin-3 receptor in the regulation of the mesolimbic dopamine system in mice.* Endocrinology, 2014. **155**(5): p. 1718-27.
13. Bagnol, D., et al., *Anatomy of an endogenous antagonist: relationship between Agouti-related protein and proopiomelanocortin in brain.* J Neurosci, 1999. **19**(18): p. RC26.
14. Chen, A.S., et al., *Inactivation of the mouse melanocortin-3 receptor results in increased fat mass and reduced lean body mass.* Nat Genet, 2000. **26**(1): p. 97-102.
15. Butler, A.A., et al., *A unique metabolic syndrome causes obesity in the melanocortin-3 receptor-deficient mouse.* Endocrinology, 2000. **141**(9): p. 3518-21.
16. Versteeg, D.H., et al., *Melanocortins and cardiovascular regulation.* Eur J Pharmacol, 1998. **360**(1): p. 1-14.
17. Renquist, B.J., et al., *Melanocortin-3 receptor regulates the normal fasting response.* Proc Natl Acad Sci U S A, 2012. **109**(23): p. E1489-98.
18. Vanni Caruso, e.a., *Synaptic changes induced by melanocortin signalling.* Nature Reviews Neuroscience, 2014. **15**.

19. Mountjoy, K.G., et al., *Localization of the melanocortin-4 receptor (MC4-R) in neuroendocrine and autonomic control circuits in the brain.* Mol. Endo., 1994. **8**: p. 1298-1308.
20. Gantz, I., et al., *Molecular Cloning, Expression, and Gene Localization of a Fourth Melanocortin Receptor.* J. Biol. Chem., 1993. **268**: p. 15174-15179.
21. Magenis, R.E., et al., *Mapping of the ACTH, MSH, and neural (MC3 and MC4) melanocortin receptors in the mouse and human.* Mammalian Genome, 1994. **5**: p. 503-508.
22. Gantz, I., et al., *Molecular Cloning of a Novel Melanocortin Receptor.* J. Biol. Chem., 1993. **268**: p. 8246-8250.
23. Mountjoy, K.G., et al., *Melanocortin receptor-mediated mobilization of intracellular free calcium in HEK293 cells.* Physiol Genomics, 2001. **5**(1): p. 11-9.
24. Konda, Y., et al., *Interaction of dual intracellular signaling pathways activated by the melanocortin-3 receptor.* Journal of Biological Chemistry, 1994. **269**(18): p. 13162-6.
25. Kim, C.S., et al., *Identification of domains directing specificity of coupling to G-proteins for the melanocortin MC3 and MC4 receptors.* J Biol Chem, 2002. **277**(35): p. 31310-7.
26. Mountjoy, K.G., et al., *Localization of the melanocortin-4 receptor (MC4-R) in neuroendocrine and autonomic control circuits in the brain.* Mol Endocrinol, 1994. **8**(10): p. 1298-308.
27. Chen, W., et al., *Exocrine gland dysfunction in MC5-R-deficient mice: evidence for coordinated regulation of exocrine gland function by melanocortin peptides.* Cell, 1997. **91**(6): p. 789-98.
28. Vergoni, A.V., R. Poggioli, and A. Bertolini, *Corticotropin inhibits food intake in rats.* Neuropeptides, 1986. **7**(2): p. 153-8.
29. Poggioli, R., A.V. Vergoni, and A. Bertolini, *ACTH-(1-24) and alpha-MSH antagonize feeding behavior stimulated by kappa opiate agonists.* Peptides, 1986. **7**(5): p. 843-8.
30. Shimizu, H., et al., *Effects of MSH on food intake, body weight and coat color of the yellow obese mouse.* Life Sci, 1989. **45**(6): p. 543-52.
31. Lu, D., et al., *Agouti protein is an antagonist of the melanocyte-stimulating hormone receptor.* Nature, 1994. **371**: p. 799-802.
32. Yen, T.T., et al., *Obesity, diabetes, and neoplasia in yellow A(vy)/- mice: ectopic expression of the agouti gene.* FASEB Journal, 1994. **8**(8): p. 479-88.
33. Fan, W., et al., *Role of melanocortinergic neurons in feeding and the agouti obesity syndrome.* Nature, 1997. **385**: p. 165-168.
34. Hruby, V.J., et al., *Cyclic lactam α-melanotropin analogues of Ac-Nle^4-c[Asp^4,D-Phe^7, Lys^{10}] α-MSH(4-10)-NH$_2$ with bulky aromatic amino acids at position 7 show high antagonist potency and selectivity at specific melanocortin receptors.* J. Med. Chem., 1995. **38**: p. 3454-3461.
35. Huszar, D., et al., *Targeted disruption of the melanocortin-4 receptor results in obesity in mice.* Cell, 1997. **88**(1): p. 131-141.
36. Ollmann, M.M., et al., *Antagonism of central melanocortin receptors in vitro and in vivo by agouti-related protein.* Science, 1997. **278**(5335): p. 135-8.

37. Graham, M., et al., *Overexpression of Agrt leads to obesity in transgenic mice.* Nat Genet, 1997. **17**(3): p. 273-4.
38. Fong, T.M., et al., *ART (protein product of agouti-related transcript) as an antagonist of MC-3 and MC-4 receptors.* Biochem. Biophys. Res. Commun., 1997. **237**: p. 629-631.
39. Nijenhuis, W.A., J. Oosterom, and R.A. Adan, *AgRP(83-132) acts as an inverse agonist on the human-melanocortin-4 receptor.* Mol Endocrinol, 2001. **15**(1): p. 164-71.
40. Haskell-Luevano, C., et al., *Structure activity studies of the melanocortin-4 receptor by in vitro mutagenesis: identification of agouti-related protein (AGRP), melanocortin agonist and synthetic peptide antagonist interaction determinants.* Biochemistry, 2001. **40**(20): p. 6164-79.
41. Chai, B.X., et al., *Inverse agonist activity of agouti and agouti-related protein.* Peptides, 2003. **24**(4): p. 603-9.
42. Qian, S., et al., *Neither agouti-related protein nor neuropeptide Y is critically required for the regulation of energy homeostasis in mice.* Mol Cell Biol, 2002. **22**(14): p. 5027-35.
43. Wortley, K.E., et al., *Agouti-related protein-deficient mice display an age-related lean phenotype.* Cell Metab, 2005. **2**(6): p. 421-7.
44. Wu, Q. and R.D. Palmiter, *GABAergic signaling by AgRP neurons prevents anorexia via a melanocortin-independent mechanism.* European journal of pharmacology, 2011. **660**(1): p. 21-7.
45. Ghamari-Langroudi, M., et al., *G-protein-independent coupling of MC4R to Kir7.1 in hypothalamic neurons.* Nature, 2015.
46. Shutter, J.R., et al., *Hypothalamic expression of ART, a novel gene related to agouti, is up-regulated in obese and diabetic mutant mice.* Genes Dev, 1997. **11**(5): p. 593-602.
47. Padilla, S.L., J.S. Carmody, and L.M. Zeltser, *Pomc-expressing progenitors give rise to antagonistic neuronal populations in hypothalamic feeding circuits.* Nature medicine, 2010. **16**(4): p. 403-5.
48. Cowley, M.A., et al., *Leptin activates anorexigenic POMC neurons through a neural network in the arcuate nucleus.* Nature, 2001. **411**(6836): p. 480-4.
49. Huo, L., H.J. Grill, and C. Bjorbaek, *Divergent regulation of proopiomelanocortin neurons by leptin in the nucleus of the solitary tract and in the arcuate hypothalamic nucleus.* Diabetes, 2006. **55**(3): p. 567-73.
50. Lemus, M.B., et al., *A stereological analysis of NPY, POMC, Orexin, GFAP astrocyte, and Iba1 microglia cell number and volume in diet-induced obese male mice.* Endocrinology, 2015. **156**(5): p. 1701-13.
51. Betley, J.N., et al., *Parallel, redundant circuit organization for homeostatic control of feeding behavior.* Cell, 2013. **155**(6): p. 1337-50.
52. Civelli, O., Birnberg, N., Herbert, E., *Detection and quantitation of pro-opiomelanocortin mRNA in pituitary and brain tissue from different species.* Journal of Biological Chemistry, 1982. **257**: p. 6783-6787.
53. Clark, A.J., et al., *In vitro and in vivo analysis of the processing and fate of the peptide products of the short proopiomelanocortin mRNA.* Mol Endocrinol, 1990. **4**(11): p. 1737-43.

54. Joseph, S.A., W.H. Pilcher, and C. Bennett-Clarke, *Immunocytochemical localization of ACTH perikarya in nucleus tractus solitarius: Evidence for a second opiocortin neuronal system.* Neurosci.Lett., 1983. **38**: p. 221-225.
55. Schwartzberg, D.G. and P.K. Nakane, *ACTH-related peptide containing neurons within the medulla oblongata of the rat.* Brain Res, 1983. **276**(2): p. 351-6.
56. Bronstein, D.M., et al., *Evidence that beta-endorphin is synthesized in cells in the nucleus tractus solitarius: detection of POMC mRNA.* Brain Research, 1992. **587**: p. 269-275.
57. Pinto, S., et al., *Rapid rewiring of arcuate nucleus feeding circuits by leptin.* Science, 2004. **304**(5667): p. 110-5.
58. Padilla, S.L., D. Reef, and L.M. Zeltser, *Defining POMC neurons using transgenic reagents: impact of transient Pomc expression in diverse immature neuronal populations.* Endocrinology, 2012. **153**(3): p. 1219-31.
59. Wang, D., et al., *Whole-brain mapping of the direct inputs and axonal projections of POMC and AgRP neurons.* Frontiers in Neuroanatomy, 2015. **9**: p. 40.
60. van de Wall, E., et al., *Collective and individual functions of leptin receptor modulated neurons controlling metabolism and ingestion.* Endocrinology, 2008. **149**(4): p. 1773-85.
61. Perello, M., R.C. Stuart, and E.A. Nillni, *Differential effects of fasting and leptin on proopiomelanocortin peptides in the arcuate nucleus and in the nucleus of the solitary tract.* Am J Physiol Endocrinol Metab, 2007. **292**(5): p. E1348-57.
62. Balthasar, N., et al., *Leptin Receptor Signaling in POMC Neurons Is Required for Normal Body Weight Homeostasis.* Neuron, 2004. **42**(6): p. 983-91.
63. Aponte, Y., D. Atasoy, and S.M. Sternson, *AGRP neurons are sufficient to orchestrate feeding behavior rapidly and without training.* Nat Neurosci, 2011. **14**(3): p. 351-5.
64. Atasoy, D., et al., *Deconstruction of a neural circuit for hunger.* Nature, 2012. **488**(7410): p. 172-7.
65. Krashes, M.J., et al., *Rapid, reversible activation of AgRP neurons drives feeding behavior in mice.* The Journal of Clinical Investigation, 2011. **121**(4): p. 1424-1428.
66. Krashes, M.J., et al., *Rapid versus delayed stimulation of feeding by the endogenously released AgRP neuron mediators GABA, NPY, and AgRP.* Cell Metab, 2013. **18**(4): p. 588-95.
67. Betley, J.N., et al., *Neurons for hunger and thirst transmit a negative-valence teaching signal.* Nature, 2015. **521**(7551): p. 180-185.
68. Dietrich, M.O., et al., *Hypothalamic Agrp neurons drive stereotypic behaviors beyond feeding.* Cell, 2015. **160**(6): p. 1222-32.
69. Aponte, Y., D. Atasoy, and S.M. Sternson, *AGRP neurons are sufficient to orchestrate feeding behavior rapidly and without training.* Nat Neurosci. **14**(3): p. 351-5.
70. Zhan, C., et al., *Acute and long-term suppression of feeding behavior by POMC neurons in the brainstem and hypothalamus, respectively.* J Neurosci, 2013. **33**(8): p. 3624-32.
71. Fan, W., et al., *Role of melanocortinergic neurons in feeding and the agouti obesity syndrome.* Nature, 1997. **385**(6612): p. 165-8.

72. Koch, M., et al., *Hypothalamic POMC neurons promote cannabinoid-induced feeding.* Nature, 2015. **519**(7541): p. 45-50.
73. Mountjoy, K.G., *Pro-Opiomelanocortin (POMC) Neurons, POMC-Dervied Peptides, Melanocortin Receptors, and Obesity: How Understanding of this System has Changed Over the Last Decade.* Journal of Neuroendocrinology, 2015. **27**: p. 406-418.
74. Kishi, T., et al., *Expression of melanocortin 4 receptor mRNA in the central nervous system of the rat.* J Comp Neurol, 2003. **457**(3): p. 213-35.
75. Cui, H., et al., *Neuroanatomy of melanocortin-4 receptor pathway in the lateral hypothalamic area.* The Journal of comparative neurology, 2012. **520**(18): p. 4168-83.
76. Cone, R.D., *Anatomy and regulation of the central melanocortin system.* Nat Neurosci, 2005. **8**(5): p. 571-8.
77. Tao, Y.X., *The melanocortin-4 receptor: physiology, pharmacology, and pathophysiology.* Endocr Rev, 2010. **31**(4): p. 506-43.
78. Siljee, J.E., et al. , *Melanocrtin 4 receptor distribution in the human hypothalamus.* European Journal of Endocrinology, 2013. **168**: p. 361-369.
79. Liu, H., et al., *Transgenic mice expressing green fluorescent protein under the control of the melanocortin-4 receptor promoter.* J Neurosci, 2003. **23**(18): p. 7143-54.
80. Balthasar, N., et al., *Divergence of melanocortin pathways in the control of food intake and energy expenditure.* Cell, 2005. **123**(3): p. 493-505.
81. Rossi, J., et al., *Melanocortin-4 receptors expressed by cholinergic neurons regulate energy balance and glucose homeostasis.* Cell Metab, 2100. **13**(2): p. 195-204.
82. Panaro, B.L., et al., *The melanocortin-4 receptor is expressed in enteroendocrine L cells and regulates the release of peptide YY and glucagon-like peptide 1 in vivo.* Cell Metab, 2014. **20**(6): p. 1018-29.
83. Garfield, A.S., et al., *A neural basis for melanocortin-4 receptor-regulated appetite.* Nat Neurosci, 2015.
84. Carpenter, B., Nehmé, R., Warne, T., Leslie, A. G. W., & Tate, C. G., *Structure of the adenosine A2A receptor bound to an engineered G protein.* Nature, 2016. **536**(7614): p. 104-107.
85. Srinivasan, S., et al., *Constitutive activity of the melanocortin-4 receptor is maintained by its N-terminal domain and plays a role in energy homeostasis in humans.* J Clin Invest, 2004. **114**(8): p. 1158-64.
86. Kleuss, C., et al., *Mechanism of GTP hydrolysis by G-protein alpha subunits.* Proceedings of the National Academy of Sciences of the United States of America, 1994. **91**(21): p. 9828-31.
87. Rasmussen, S.G.F., DeVree, B. T., Zou, Y., Kruse, A. C., Chung, K. Y., Kobilka, T. S., and B.K. . . . Kobilka, *Crystal Structure of the β(2)Adrenergic Receptor-Gs protein complex.* . Nature, 2011. **477**(7366): p. 549-555.
88. Ho, R.J., & Sutherland, E. W. , *Action of feedback regulator on adenylate cyclase.* . Proc Natl Acad Sci U S A, 1975. **72**(5): p. 1773-1777.

89. Francis, S.H., Turko, I. V., & Corbin, J. D. , *Cyclic nucleotide phosphodiesterases: relating structure and function.* . Prog Nucleic Acid Res Mol Biol, 2001. **65**: p. 1-52.
90. Kim, C., Xuong, N. H., & Taylor, S. S., *Crystal structure of a complex between the catalytic and regulatory (RIalpha) subunits of PKA.* Science, 2005. **307**(5710): p. 690-696.
91. Shen, Y., Fu, W. Y., Cheng, E. Y., Fu, A. K., & Ip, N. Y. , *Melanocortin-4 receptor regulates hippocampal synaptic plasticity through a protein kinase A-dependent mechanism.* J Neurosci, 2013. **33**(2): p. 464-472.
92. Shinyama, H., et al., *Regulation of melanocortin-4 receptor signaling: agonist-mediated desensitization and internalization.* Endocrinology, 2003. **144**(4): p. 1301-14.
93. Glas, E., Muckter, H., Gudermann, T., & Breit, A. , *Exchange factors directly activated by cAMP mediate melanocortin 4 receptor-induced gene expression.* Sci Rep, 2016. **6**(32776).
94. Brandon Podyma, H.S., Eric A. Wilson, Bradley Carlson, Ethan Pritikin,, Oksana Gavrilova, Lee S. Weinstein, and Min Chen, *The stimulatory G protein Gsα is required in melanocortin 4 receptor-expressing cells for normal energy balance, thermogenesis and glucose metabolism.* JBC, 2018.
95. Konda, Y., et al., *Interaction of dual intracellular signaling pathways activated by the melanocortin-3 receotor.* J. Biol. Chem., 1994. **269**: p. 13162-13166.
96. Buch, T.R., et al., *Pertussis toxin-sensitive signaling of melanocortin-4 receptors in hypothalamic GT1-7 cells defines agouti-related protein as a biased agonist.* J Biol Chem, 2009. **284**(39): p. 26411-20.
97. Lei, Q., Jones, M. B., Talley, E. M., Schrier, A. D., McIntire, W. E., Garrison, J. C., & Bayliss, D. A. , *Activation and inhibition of G protein-coupled inwardly rectifying potassium (Kir3) channels by G protein beta gamma subunits.* ProcNatl Acad Sci U S A, 2000. **97**(17): p. 9771-9776.
98. Lei, Q., et al., *Activation and inhibition of G protein-coupled inwardly rectifying potassium (Kir3) channels by G protein beta gamma subunits.* Proc Natl Acad Sci U S A, 2000. **97**(17): p. 9771-6.
99. Ghamari-Langroudi, M., D. Srisai, and R.D. Cone, *Multinodal regulation of the arcuate/paraventricular nucleus circuit by leptin.* Proc Natl Acad Sci U S A, 2011. **108**(1): p. 355-60.
100. Ghamari-Langroudi, M., et al., *Regulation of thyrotropin-releasing hormone-expressing neurons in paraventricular nucleus of the hypothalamus by signals of adiposity.* Mol Endocrinol, 2010. **24**(12): p. 2366-81.
101. Czyzyk, T.A., et al., *Disruption of the RIIÎ² subunit of PKA reverses the obesity syndrome of agouti lethal yellow mice.* Proceedings of the National Academy of Sciences, 2008. **105**(1): p. 276-281.
102. Broberger, C., et al., *The neuropeptide Y/agouti gene-related protein (AGRP) brain circuitry in normal, anorectic, and monosodium glutamate-treated mice.* Proc. Natl. Acad. Sci. USA, 1998. **95**: p. 15043-15048.
103. Litt MJ, C.R., Ghamari-Langroudi M, *Characterization of MC4R Regulation of the Kir7.1 Channel Using the Tl+ Flux Assay.* Methods Mol Biol., 2018. **1684**: p. 211-222.

104. Ghamari-Langroudi, M., et al., , *G-protein-independent coupling of MC4R to Kir7.1 in hypothalamic neurons.* . Nature, 2015.
105. Yeo, G.S., et al., *A frameshift mutation in MC4R associated with dominantly inherited human obesity.* Nat Genet, 1998. **20**(2): p. 111-2.
106. Vaisse, C., et al., *A frameshift mutation in human MC4R is associated with a dominant form of obesity.* Nature Genetics, 1998. **20**: p. 113-114.
107. Zakel, U.A., et al., *[Prevalence of melanocortin 4 receptor (MC4R) mutations and polymorphismsin consecutively ascertained obese children and adolescents from a pediatric health care utilization population].* Klin Padiatr, 2005. **217**(4): p. 244-9.
108. Biebermann, H., et al., *Autosomal-dominant mode of inheritance of a melanocortin-4 receptor mutation in a patient with severe early-onset obesity is due to a dominant-negative effect caused by receptor dimerization.* Diabetes, 2003. **52**(12): p. 2984-8.
109. Rettenbacher, E., et al., *A novel non-synonymous mutation in the melanocortin-4 receptor gene (MC4R) in a 2-year-old Austrian girl with extreme obesity.* Exp Clin Endocrinol Diabetes, 2007. **115**(1): p. 7-12.
110. Tan, K., et al., *Functional characterization and structural modeling of obesity associated mutations in the melanocortin 4 receptor.* Endocrinology, 2009. **150**(1): p. 114-25.
111. Vaisse, C., et al., *Melanocortin-4 receptor mutations are a frequent and heterogeneous cause of morbid obesity.* J Clin Invest, 2000. **106**(2): p. 253-62.
112. Farooqi, I.S., et al., *Dominant and recessive inheritance of morbid obesity associated with melanocortin 4 receptor deficiency.* J Clin Invest, 2000. **106**(2): p. 271-9.
113. Yeo, G.S., et al., *Mutations in the human melanocortin-4 receptor gene associated with severe familial obesity disrupts receptor function through multiple molecular mechanisms.* Hum Mol Genet, 2003. **12**(5): p. 561-74.
114. Gu, W., et al., *Identification and functional analysis of novel human melanocortin-4 receptor variants.* Diabetes, 1999. **48**: p. 635-639.
115. Hinney, A., et al., *Several mutations in the melanocortin-4 receptor gene including a nonsense and a frameshift mutation associated with dominantly inherited obesity in humans.* J. Clin. Endocrinol. Metab, 1999. **84**(4): p. 1483-1486.
116. Lubrano-Berthelier, C., et al., *Molecular genetics of human obesity-associated MC4R mutations.* Ann N Y Acad Sci, 2003. **994**: p. 49-57.
117. Mergen, M., et al., *A novel melanocortin 4 receptor (MC4R) gene mutation associated with morbid obesity.* J Clin Endocrinol Metab, 2001. **86**(7): p. 3448.
118. Santoro, N., et al., *Prevalence of pathogenetic MC4R mutations in Italian children with early onset obesity, tall stature and familial history of obesity.* BMC Med Genet, 2009. **10**: p. 25.
119. Lubrano-Berthelier, C., et al., *A homozygous null mutation delineates the role of the melanocortin-4 receptor in humans.* J Clin Endocrinol Metab, 2004. **89**(5): p. 2028-32.
120. Farooqi, I.S., et al., *Clinical spectrum of obesity and mutations in the melanocortin 4 receptor gene.* N Engl J Med, 2003. **348**(12): p. 1085-95.

121. Lubrano-Berthelier, C., et al., *Melanocortin 4 receptor mutations in a large cohort of severely obese adults: prevalence, functional classification, genotype-phenotype relationship, and lack of association with binge eating.* J Clin Endocrinol Metab, 2006. **91**(5): p. 1811-8.
122. Rong, R., et al., *Identification and functional characterization of three novel human melanocortin-4 receptor gene variants in an obese Chinese population.* Clin Endocrinol (Oxf), 2006. **65**(2): p. 198-205.
123. Alharbi, K.K., et al., *Prevalence and functionality of paucimorphic and private MC4R mutations in a large, unselected European British population, scanned by meltMADGE.* Hum Mutat, 2007. **28**(3): p. 294-302.
124. Stutzmann, F., et al., *Prevalence of melanocortin-4 receptor deficiency in Europeans and their age-dependent penetrance in multigenerational pedigrees.* Diabetes, 2008. **57**(9): p. 2511-8.
125. Roth, C.L., et al., *A novel melanocortin-4 receptor gene mutation in a female patient with severe childhood obesity.* Endocrine, 2009. **36**(1): p. 52-9.
126. Hinney, A., Volckmar, A. L., & Knoll, N., *Melanocortin-4 receptor in energyhomeostasis and obesity pathogenesis. .* Prog Mol Biol Transl Sci, 2013. **114**: p. 147-191.
127. Tao, Y.X., *Mutations in melanocortin-4 receptor and human obesity.* Prog Mol Biol Transl Sci, 2009. **88**: p. 173-204.
128. Greenfield, J.R., et al., *Modulation of blood pressure by central melanocortinergic pathways.* N Engl J Med, 2009. **360**(1): p. 44-52.
129. Panaro, B.L. and R.D. Cone, *Melanocortin-4 receptor mutations paradoxically reduce preference for palatable foods.* Proc Natl Acad Sci U S A, 2013. **110**(17): p. 7050-5.
130. Srisai, D., Gillum, M. P., Panaro, B. L., Zhang, X. M., Kotchabhakdi, N., Shulman, G. I., . and R.D. . . Cone, *Characterization of the hyperphagic response to dietary fat in the MC4R knockout mouse.* Endocrinology, 2011. **152**(3): p. 890-902.
131. van der Klaauw, A.A., Keogh, J. M., Henning, E., Stephenson, C., Kelway, S., Trowse, and F. V. M., I. S., *Divergent effects of central melanocortin signalling on fat and sucrose preference in humans. .* Nat Commun, 2016. **7**(13055).
132. Wang, X.H., Wang, H. M., Zhao, B. L., Yu, P., & Fan, Z. C., *Rescue of defective MC4R cell-surface expression and signaling by a novel pharmacoperone Ipsen 17.* J Mol Endocrinol, 2014. **53**(1): p. 17-29.
133. Granell, S., Serra-Juhe, C., Martos-Moreno, G. A., Diaz, F., Perez-Jurado, L. A., Baldini, and A. G., J. , *A novel melanocortin-4 receptor mutation MC4R-P272L associated with severe obesity has increased propensity to be ubiquitinated in the ER in the face of correct folding. .* PLoS One, 2012. **7**(12): p. e50894.
134. Tao, Y.-X., & Huang, H. , *Ipsen 5i is a Novel Potent Pharmacoperone for Intracellularly Retained Melanocortin-4 Receptor Mutants. .* Frontiers in endocrinology, 2014. **5**(131).
135. Heid, I.M., Vollmert, C., Kronenberg, F., Huth, C., Ankerst, D. P., Luchner, A., . . .Hebebrand, J., *Association of the MC4R V103I polymorphism with the metabolic syndrome: the KORA Study. .* Obesity (Silver Spring), 2008. **16**(2): p. 369-376.

136. Xiang, Z., Proneth, B., Dirain, M. L., Litherland, S. A., & Haskell-Luevano, C., *Pharmacological characterization of 30 human melanocortin-4 receptor polymorphisms with the endogenous proopiomelanocortin-derived agonists, synthetic agonists, and the endogenous agouti-related protein antagonist.* Biochemistry, 2010. **49**(22): p. 4583-4600.
137. Wang, D., Ma, J., Zhang, S., Hinney, A., Hebebrand, J., Wang, Y., & Wang, H. J., *Association of the MC4R V103I polymorphism with obesity: a Chinese case-control study and meta-analysis in 55,195 individuals.* . Obesity (Silver Spring), 2010. **18**(3): p. 573-579.
138. Ste Marie, L., et al., *A metabolic defect promotes obesity in mice lacking melanocortin-4 receptors.* Proc Natl Acad Sci U S A, 2000. **97**(22): p. 12339-44.
139. Huszar, D., Lynch, C. A., Fairchild-Huntress, V., Dunmore, J. H., Fang, Q., Berkemeier, and L. L. R., F. , *Targeted disruption of the melanocortin-4 receptor results in obesity in mice.* Cell, 1997. **88**(1): p. 131-141.
140. Weide, K., et al., *Hyperphagia, not hypometabolism, causes early onset obesity in melanocortin-4 receptor knockout mice.* Physiol Genomics, 2003. **13**(1): p. 47-56.
141. Kleiber, M., *Body size and metabolism.* ENE, 1932. **1**(9).
142. Kaiyala, K.J., & Schwartz, M. W., *Toward a More Complete (and Less Controversial) Understanding of Energy Expenditure and Its Role in Obesity Pathogenesis.* Diabetes, 2011. **60**(1): p. 17-23.
143. Almundarij, T.I., Smyers, M. E., Spriggs, A., Heemstra, L. A., Beltz, L., Dyne, E., . . . and C.M. Novak, *Physical Activity, Energy Expenditure, and Defense of Body Weight in Melanocortin 4 Receptor-Deficient Male Rats.* Sci Rep., 2016. **6**(37435).
144. Butler, A.A., et al., *Melanocortin-4 receptor is required for acute homeostatic responses to increased dietary fat.* Nat Neurosci, 2001. **4**(6): p. 605-11.
145. Sutton, G.M., et al., *Diet-genotype interactions in the development of the obese, insulin-resistant phenotype of C57BL/6J mice lacking melanocortin-3 or -4 receptors.* Endocrinology, 2006. **147**(5): p. 2183-96.
146. Lute, B., Jou, W., Lateef, D. M., Goldgof, M., Xiao, C., Piñol, R. A., . . . Reitman, M. L., *Biphasic Effect of Melanocortin Agonists on Metabolic Rate and Body Temperature.* . Cell metabolism, 2014. **20**(2): p. 333-345.
147. Hwa, J.J., Ghibaudi, L., Gao, J., & Parker, E. M., *Central melanocortin system modulates energy intake and expenditure of obese and lean Zucker rats.* American Journal of Physiology - Regulatory, Integrative and Comparative Physiology, 2001. **281**(2): p. R444-R451.
148. Jonsson, L., Skarphedinsson, J. O., Skuladottir, G. V., Atlason, P. T., Eiriksdottir, V. H., and L. Franzson, & Schioth, H. B. , *Melanocortin receptor agonist transiently increases oxygen consumption in rats.* . Neuroreport, 2001. **12**(17): p. 3703-3708.
149. Chen, K.Y., et al., *RM-493, a melanocortin-4 receptor (MC4R) agonist, increases resting energy expenditure in obese individuals.* J Clin Endocrinol Metab, 2015. **100**(4): p. 1639-45.
150. Kievit P, H.H., Marks DL, Dong JZ, Glavas MM, Sinnayah P, Pranger L, Cowley MA, Grove KL, Culler MD, *Chronic treatment with a melanocortin-4 receptor agonist causes weight loss, reduces insulin resistance, and improves*

cardiovascular function in diet-induced obese rhesus macaques. Diabetes, 2013 **62**(2): p. 490-7.
151. Toshioninui, G.K., Fujino, M. A., Meguid, M. M., & Kasuga, M., *Effects of agouti-related protein, orexin and melanin-concentrating hormone on oxygen consumption in mice. International journal of molecular medicine.* 2002. **10**: p. 523-525.
152. Small, C.J., Liu, Y. L., Stanley, S. A., Connoley, I. P., Kennedy, A., Stock, M. J., & Bloom, S. R., *Chronic CNS administration of Agouti-related protein (Agrp) reduces energy expenditure.* . Int J Obes Relat Metab Disord., 2003. **27**(4): p. 530-533.
153. Shukla, C., Koch, L. G., Britton, S. L., Cai, M., Hruby, V. J., Bednarek, M., & Novak, C. M. , *Contribution of regional brain melanocortin receptor subtypes to elevated activity energy expenditure in lean, active rats.* Neuroscience, 2015. **310**: p. 252-267.
154. Haynes, W.G., et al., *Interactions between the melanocortin system and leptin in control of sympathetic nerve traffic.* Hypertension, 1999. **33**(1 Pt 2): p. 542-547.
155. Voss-Andreae, A., et al., *Role of the central melanocortin circuitry in adaptive thermogenesis of brown adipose tissue.* Endocrinology, 2007. **148**(4): p. 1550-60.
156. Nogueiras, R., et al., *The central melanocortin system directly controls peripheral lipid metabolism.* J Clin Invest, 2007. **117**(11): p. 3475-88.
157. Matsumura, K., Tsuchihashi, T., Abe, I., & Iida, M. , *Central alpha-melanocytestimulating hormone acts at melanocortin-4 receptor to activate sympathetic nervous system in conscious rabbits.* Brain Res., 2002. **948**(1-2): p. 145-148.
158. Ni, X.P., et al., *Central receptors mediating the cardiovascular actions of melanocyte stimulating hormones.* J Hypertens, 2006. **24**(11): p. 2239-46.
159. Hill, C., & Dunbar, J. C. , *The effects of acute and chronic alpha melanocyte stimulating hormone (alphaMSH) on cardiovascular dynamics in conscious rats.* Peptides, 2002. **23**(9): p. 1625-1630.
160. Li, S.J., et al., *Melanocortin antagonists define two distinct pathways of cardiovascular control by alpha- and gamma-melanocyte-stimulating hormones.* J Neurosci, 1996. **16**(16): p. 5182-8.
161. Iwasa, M., Kawabe, K., & Sapru, H. N. , *Activation of melanocortin receptors in the intermediolateral cell column of the upper thoracic cord elicits tachycardia in the rat.* . Am J Physiol Heart Circ Physiol,, 2013. **305**(6): p. H885-893.
162. K Eerola, P.R., A M Penttinen, L Vähätalo, M Savontaus, and E Savontaus, *α-MSH overexpression in the nucleus tractus solitarius decreases fat mass and elevates heart rate.* journal of Endocrinology, 2014. **222**: p. 123-136.
163. Kuo, J.J., A.A. Silva, and J.E. Hall, *Hypothalamic melanocortin receptors and chronic regulation of arterial pressure and renal function.* Hypertension, 2003. **41**(3 Pt 2): p. 768-74.
164. Pavia, J.M., Schioth, H. B., & Morris, M. J. , *Role of MC4 receptors in the depressor and bradycardic effects of alpha-MSH in the nucleus tractus solitarii of the rat.* . Neuroreport,, 2003. **14**(5): p. 703-707.
165. Humphreys, M.H., Ni, X. P., & Pearce, D. , *Cardiovascular effects of melanocortins.* . Eur J Pharmacol., 2011. **660**(1): p. 43-52.

166. Tallam, L.S., et al., *Cardiovascular, renal, and metabolic responses to chronic central administration of agouti-related peptide.* Hypertension, 2004. **44**(6): p. 853-8.
167. Tallam, L.S., da Silva, A. A., & Hall, J. E. , *Melanocortin-4 receptor mediates chronic cardiovascular and metabolic actions of leptin.* . Hypertension, 2006. **48**(1): p. 58-64.
168. Royalty, J.E., et al., *Investigation of safety, tolerability, pharmacokinetics, and pharmacodynamics of single and multiple doses of a long-acting alpha-MSH analog in healthy overweight and obese subjects.* J Clin Pharmacol, 2014. **54**(4): p. 394-404.
169. Tallam, L.S., A.A. da Silva, and J.E. Hall, *Melanocortin-4 receptor mediates chronic cardiovascular and metabolic actions of leptin.* Hypertension, 2006. **48**(1): p. 58-64.
170. Tallam, L.S., et al., *Melanocortin-4 receptor-deficient mice are not hypertensive or salt-sensitive despite obesity, hyperinsulinemia, and hyperleptinemia.* Hypertension, 2005. **46**(2): p. 326-32.
171. do Carmo, J.M., da Silva, A. A., Rushing, J. S., & Hall, J. E. , *Activation of the central melanocortin system contributes to the increased arterial pressure in obese Zucker rats.* . Am J Physiol Regul Integr Comp Physiol, 2012. **302** (5): p. R561-567.
172. Ward, K.R., Bardgett, J. F., Wolfgang, L., & Stocker, S. D. , *Sympathetic response to insulin is mediated by melanocortin 3/4 receptors in the hypothalamic paraventricular nucleus.* Hypertension, 2011. **57**(3): p. 435-441.
173. Shek, E.W., M.W. Brands, and J.E. Hall, *Chronic leptin infusion increases arterial pressure.* Hypertension, 1998. **31**(1 Pt 2): p. 409-14.
174. do Carmo, J.M., et al., *Control of blood pressure, appetite, and glucose by leptin in mice lacking leptin receptors in proopiomelanocortin neurons.* Hypertension, 2011. **57**(5): p. 918-26.
175. Rossi, J., et al., *Melanocortin-4 receptors expressed by cholinergic neurons regulate energy balance and glucose homeostasis.* Cell Metab, 2011. **13**(2): p. 195-204.
176. Sohn, J.W., J.K. Elmquist, and K.W. Williams, *Neuronal circuits that regulate feeding behavior and metabolism.* Trends in neurosciences, 2013.
177. Michael J Litt, G.D.O., Daniel Lark, Isin Cakir, Christy Moore, Mary C Barber, James Atkinson, Josh Fessel, Javid Moslehi, Roger D Cone *Loss of the melanocortin-4 receptor in mice causes dilated cardiomyopathy.* Elife, 2018.
178. Lensing, C.J.F., K. T.; Schnell, S. M.; Speth, R. C.; Zarth, A. T.; Haskell-Luevano, C., *Developing a Biased Unmatched Bivalent Ligand (BUmBL) Design Strategy to Target the GPCR Homodimer Allosteric Signaling (cAMP over β-Arrestin 2 Recruitment) Within the Melanocortin Receptors.* . J. Med. Chem. , 2018.
179. Nickolls, S.A., et al., *Molecular determinants of melanocortin 4 receptor ligand binding and MC4/MC3 receptor selectivity.* J Pharmacol Exp Ther, 2003. **304**(3): p. 1217-27.
180. Sebhat, I.K., et al., *Design and pharmacology of N-[(3R)-1,2,3,4-tetrahydroisoquinolinium- 3-ylcarbonyl]-(1R)-1-(4-chlorobenzyl)- 2-[4-*

cyclohexyl-4-(1H-1,2,4-triazol- 1-ylmethyl)piperidin-1-yl]-2-oxoethylamine (1), a potent, selective, melanocortin subtype-4 receptor agonist. J Med Chem, 2002. **45**(21): p. 4589-93.
181. Wikberg, J.E. and F. Mutulis, *Targeting melanocortin receptors: an approach to treat weight disorders and sexual dysfunction.* Nat Rev Drug Discov, 2008. **7**(4): p. 307-23.
182. Al-Obeidi, F., et al., *Potent and prolonged acting cyclic lactam analogues of a-melanotropin: Design based on molecular dynamics.* J. Med. Chem., 1989. **32**: p. 2555-2561.
183. Hruby, V.J., et al., *Cyclic lactam alpha-melanotropin analogues of Ac-Nle4-cyclo[Asp5, D- Phe7,Lys10] alpha-melanocyte-stimulating hormone-(4-10)-NH2 with bulky aromatic amino acids at position 7 show high antagonist potency and selectivity at specific melanocortin receptors.* J Med Chem, 1995. **38**(18): p. 3454-61.
184. Rosen, R.C., et al., *Evaluation of the safety, pharmacokinetics and pharmacodynamic effects of subcutaneously administered PT-141, a melanocortin receptor agonist, in healthy male subjects and in patients with an inadequate response to Viagra.* Int J Impot Res, 2004. **16**(2): p. 135-42.
185. Diamond LE, E.D., Heiman JR, Rosen RC, Perelman MA, Harning R, *An effect on the subjective sexual response in premenopausal women with sexual arousal disorder by bremelanotide (PT-141), a melanocortin receptor agonist.* . J. Sex Med., 2006. **3**: p. 628–638
186. Gilbert W. Kim, J.E.L., Erik S. Blomain, and Scott A. Waldman, *Anti-Obesity Pharmacotherapy: New Drugs and Emerging*
Targets. Clin Pharmacol Ther. , 2014. **95**(1): p. 53–66.
187. Tinh-Hai Collet, B.D., Jacek Mokrosinski, Hillori Connors, Julia M. Keogh, Edson Mendes de Oliveira, Elana Henning, Christine Poitou-Bernert, Jean-Michel Oppert, Patrick Tounian, Florence Marchelli, Rohia Alili, Johanne Le Beyec, Dominique Pépin, Jean-Marc Lacorte, Andrew Gottesdiener, Rebecca Bounds, Shubh Sharma, Cathy Folster, Bart Henderson, Stephen O'Rahilly, Elizabeth Stoner, Keith Gottesdiener, Brandon L. Panaro, Roger D. Cone, Karine Clément, Sadaf Farooqi, and Lex H.T. Van der Ploeg, *Evaluation of a melanocortin-4 receptor (MC4R) agonist (Setmelanotide) in MC4R deficiency.* Mol Metab. , 2017. **6**(10): p. 1321–1329.
188. Kuhnen, P., et al., *Proopiomelanocortin Deficiency Treated with a Melanocortin-4 Receptor Agonist.* N Engl J Med, 2016. **375**(3): p. 240-6.
189. Clément, K., Biebermann H., Farooqi, S., Lex Van der Ploeg, et al. , *MC4R agonism promotes durable weight loss in patients with leptin receptor deficiency.* Nature Med., 2018. **24**: p. 551–555.
190. Wang ZQ, T.Y., *Functional studies on twenty novel naturally occurring melanocortin-4 receptor mutations.*
.
Biochim Biophys Acta., 2011. **1812**(9): p. 1190-1199.
191. Tao YX, H.H., Wang ZQ, Yang F, Williams JN, Nikiforovich GV. 7, *Constitutive activity of neural melanocortin receptors.* . Methods Enzymol. , 2010. **484**: p. 267–279.

192. Haskell-Luevano C, M.E., *Agouti-related protein functions as an inverse agonist at a constitutively active brain melanocortin-4 receptor.* . Regul Pept 2001. **99**(1): p. 1–7.
193. Hinney A, e.a., *Melanocortin-4 receptor gene: case-control study and transmission disequilibrium test confirm that functionally relevant mutations are compatible with a major gene effect for extreme obesity.* . J Clin Endocrinol Metab. , 2003. **88**(9): p. 4258–4267.
194. Mohammad S, B.G., Granell S, Narducci P, Martelli AM, Baldini G, *Constitutive traffic of melanocortin-4 receptor in Neuro2A cells and immortalized hypothalamic neurons.* J Biol Chem. , 2007 **282**(7): p. 4963-74.
195. Persani L, L.A., Alberti L, Romoli R, Mantovani G, Filetti S, Spada A, Conti M, *Induction of specific phosphodiesterase isoforms by constitutive activation of the cAMP pathway in autonomous thyroid adenomas.* J Clin Endocrinol Metab., 2000. **85**(8): p. 2872-8.
196. Shinozaki H, B.V., Tao YX, Ang KL, Conti M, Segaloff DL, *Desensitization of Gs-coupled receptor signaling by constitutively active mutants of the human lutropin/choriogonadotropin receptor.*
. J Clin Endocrinol Metab. , 2003. **88**(3): p. 1194-204.
197. Swale, D.R., S.V. Kharade, and J.S. Denton, *Cardiac and renal inward rectifier potassium channel pharmacology: emerging tools for integrative physiology and therapeutics.* Curr Opin Pharmacol, 2014. **15**: p. 7-15.
198. Bouyer, K. and R.B. Simerly, *Neonatal leptin exposure specifies innervation of presympathetic hypothalamic neurons and improves the metabolic status of leptin-deficient mice.* J Neurosci, 2013. **33**(2): p. 840-51.
199. Atasoy, D., et al., *A genetically specified connectomics approach applied to long-range feeding regulatory circuits.* Nat Neurosci, 2014. **17**(12): p. 1830-9.
200. Ghamari-Langroudi, M., et al., *G-protein-independent coupling of MC4R to Kir7.1 in hypothalamic neurons.* Nature, 2015. **520**(7545): p. 94-8.
201. Weaver, C.D., et al., *A thallium-sensitive, fluorescence-based assay for detecting and characterizing potassium channel modulators in mammalian cells.* J Biomol Screen, 2004. **9**(8): p. 671-7.
202. Michael J. Litt, R.D.C., Masoud Ghamari-Langroudi, *Characterization of MC4R regulation of the Kir7.1 channel using the Tl+ flux assay.* Methods in Molecular Biology, 2018. **1684**(1064-3745): p. 211-222.
203. Zhang, Z., Li, M., Lu, R., Alioua, A., Stefani, E., & Toro, L. , *The angiotensin II type 1 receptor (AT1R) closely interacts with large conductance voltage- and Ca2+-activated K+ (BK) channels and inhibits their activity independent of Gprotein*
activation. . J Biol Chem., 2014. **289**(37): p. 25678-25689.
204. Raphemot, R., et al., *Discovery, characterization, and structure-activity relationships of an inhibitor of inward rectifier potassium (Kir) channels with preference for Kir2.3, Kir3.x, and Kir7.1.* Front, 2011. **2**: p. 75. Epub 2011 Nov 30.
205. Katz, B., *Les constantes electriques de la membrane du muscle.* Arch. Sci. Physiol. (Paris), 1949. **3**: p. 285-299.

206. Hibino, H., et al., *Inwardly Rectifying Potassium Channels: Their Structure, Function, and Physiological Roles.* Physiological Reviews, 2010. **90**(1): p. 291-366.
207. Furst O, M.B., D'Avanzo N *Phosphoinositide regulation of inward rectifier potassium (Kir) channels.* . Front Physiol, 2014. **4**(404).
208. Hilgemann, D.W. and R. Ball, *Regulation of cardiac Na+,Ca2+ exchange and KATP potassium channels by PIP2.* Science, 1996. **273**(5277): p. 956-9.
209. Pfaffinger PJ, M.J., Hunter DD, Nathanson NM, Hille B *GTP-binding proteins couple cardiac muscarinic receptors to a K channel.* . Nature 1985. **31**(6037): p. 536–538.
210. Tucker SJ, G.F., Proks P, Trapp S, Ryder TJ, Haug T et al *Molecular determinants of KATP channel inhibition by ATP.* . EMBO J, 1998. **17**(12): p. 3290–3296.
211. Ho K , N.C., Lederer WJ , Lytton J , Vassilev PM , Kanazirska MV , Hebert SC, *Cloning and expression of an inwardly rectifying ATP-regulated potassium channel.* Nature, 1993. **362**: p. 31-38.
212. Tateno T, N.N., Hirata Y, Hirose S, *Role of C-terminus of Kir7.1 potassium channel in cell-surface expression.* Cell Biol Int 2006. **30**: p. 270-7.
213. Glowatzki E , F.G., Brandle U , Rexhausen U , Zenner HP , Ruppersberg JP , Fakler B, *Subunit-dependent assembly of inward-rectifier K+ channels.* Proc Biol Sci, 1995. **261**: p. 251-261.
214. Yang J , J.Y., Jan LY . *Determination of the subunit stoichiometry of an inwardly rectifying potassium channel.* Neuron, 1995. **15**: p. 1441-1447.
215. Schram G , M.P., Pourrier M , Wang Z , Nattel S, *Kir2.4 and Kir2.1 K+ channel subunits co-assemble: a potential new contributor to inward rectifier current heterogeneity.* J Physiol, 2002. **544**: p. 337-349.
216. Kuo A , G.J., Antcliff JF , Rahman T , Lowe ED , Zimmer J , Cuthbertson J , Ashcroft FM , Ezaki T , Doyle DA . *Crystal structure of the potassium channel KirBac1.1 in the closed state.* Science, 2003. **300**: p. 1922-1926.
217. Nishida M , C.M., Chait BT , MacKinnon R . *Crystal structure of a Kir3.1-prokaryotic Kir channel chimera.* EMBO J, 2007. **26**: p. 4005-4015.
218. Inanobe A , M.T., Nakagawa A , Kurachi Y, *Structural diversity in the cytoplasmic region of G protein-gated inward rectifier K+ channel.* Channels (Austin), 2007. **1**: p. 39-45.
219. Pegan S , A.C., Zhou W , Kwiatkowski W , Collins A , Slesinger PA , Choe S . *Cytoplasmic domain structures of Kir2.1 and Kir3 1 show sites for modulating gating and rectification.* Nat Neurosci., 2005. **8**: p. 279-287.
220. Nishida M , M.R., *Structural basis of inward rectification: cytoplasmic pore of the G protein-gated inward rectifier GIRK1 at 1.8 A resolution.* Cell, 2002. **111**: p. 957-965.
221. Doring, F., et al., *The epithelial inward rectifier channel Kir7.1 displays unusual K+ permeation properties.* J Neurosci., 1998. **18**(21): p. 8625-36.
222. Nakamura, N., et al., *Inwardly rectifying K+ channel Kir7.1 is highly expressed in thyroid follicular cells, intestinal epithelial cells and choroid plexus epithelial cells: implication for a functional coupling with Na+,K+-ATPase.* Biochem J., 1999. **342**(Pt 2): p. 329-36.

223. Cornejo Isabel, V.S., Burgos Johanna, López-Cayuqueo Karen I., Chambrey Régine, Julio-Kalajzić Francisca, Buelvas Neudo, Niemeyer María I., Figueiras-Fierro Dulce, Brown Peter D., Sepúlveda Francisco V., Cid L. P., *Tissue Distribution of Kir7.1 Inwardly Rectifying K+ Channel Probed in a Knock-in Mouse Expressing a Haemagglutinin-Tagged Protein* Frontiers in Physiology 2018. **9**.
224. Villanueva S, B.J., López-Cayuqueo KI, Lai KM3, Valenzuela DM, Cid LP, Sepúlveda FV, *Cleft Palate, Moderate Lung Developmental Retardation and Early Postnatal Lethality in Mice Deficient in the Kir7.1 Inwardly Rectifying K+ Channel.* PLoS One, 2015. **10**(9).
225. Krapivinsky, G., et al., *A Novel Inward Rectifier K+ Channel with Unique Pore Properties.* Neuron, 1998. **20**(5): p. 995-1005.
226. Hibino, H., et al., *Inwardly rectifying potassium channels: their structure, function, and physiological roles.* Physiol Rev, 2010. **90**(1): p. 291-366.
227. Krapivinsky G , M.I., Eng L , Krapivinsky L , Yang Y , Clapham DE, *A novel inward rectifier K+ channel with unique pore properties.* Neuron, 1998. **20**: p. 995-1005.
228. Partiseti M , C.V., Agnel M , Culouscou JM , Graham D, *Cloning and characterization of a novel human inwardly rectifying potassium channel predominantly expressed in small intestine.* FEBS Lett 1998. **434**: p. 171-176.
229. Boassa, D.Y., Andrea, *Physiological Roles of Aquaporins in the Choroid Plexus.* Current topics in developmental biology, 2005. **67**: p. 181-206.
230. McCloskey, C., et al., *The inwardly rectifying K+ channel KIR7.1 controls uterine excitability throughout pregnancy.* EMBO Mol Med, 2014. **6**(9): p. 1161-74.
231. Conor McCloskey, C.R., Elizabeth Bailey, Samantha McCavera, Hugo A van den Berg, . . . Andrew M Blanks, *The inwardly rectifying K+ channel KIR7.1 controls uterine excitability throughout pregnancy.* EMBO Molecular Medicine, 2014. **6**(9): p. 1161-1174.
232. Crankshaw DJ, C.D., Morrison JJ, *Effects of the KIR7.1 Blocker VU590 on Spontaneous and Agonist-Induced Contractions of Human Pregnant Myometrium.* Reprod Sci., 2017. **24**(10): p. 1402-1409.
233. Iwashita, M., et al., *Pigment pattern in jaguar/obelix zebrafish is caused by a Kir7.1 mutation: implications for the regulation of melanosome movement.* PLoS Genet, 2006. **2**(11): p. e197.
234. Inaba, M., H. Yamanaka, and S. Kondo, *Pigment pattern formation by contact-dependent depolarization.* Science, 2012. **335**(6069): p. 677.
235. Motoko Iwashita, M.W., Masaru Ishii, Tim Chen, Stephen L Johnson, Yoshihisa Kurachi, Norihiro Okada, Shigeru Kondo *Pigment Pattern in jaguar/obelix Zebrafish Is Caused by a Kir7.1 Mutation: Implications for the Regulation of Melanosome Movement.* PLoS Genet, 2006. **2**(11).
236. Maderspacher F1, N.-V.C., *Formation of the adult pigment pattern in zebrafish requires leopard and obelix dependent cell interactions.* Development. , 2003. **130**(15): p. 3447-57.
237. Hejtmancik, J.F., et al., *Mutations in KCNJ13 cause autosomal-dominant snowflake vitreoretinal degeneration.* Am J Hum Genet, 2008. **82**(1): p. 174-80.

238. Sergouniotis, P.I., et al., *Recessive mutations in KCNJ13, encoding an inwardly rectifying potassium channel subunit, cause leber congenital amaurosis.* Am J Hum Genet, 2011. **89**(1): p. 183-90.
239. Sepúlveda, F.V., Cid, L. P., Teulon, J., and Niemeyer, M. I. , *Molecular aspects of structure, gating and physiology of pH-sensitive background K2P and Kir K+-transport channels.* . Physiol. Rev. , 2015. **95**: p. 179–217.
240. Shahi, P.K., Liu, X., Aul, B., Moyer, A., Pattnaik, A., Denton, J., et al. , *Abnormal electroretinogram after Kir7.1 channel suppression suggests role in retinal electrophysiology.* . Sci. Rep. , 2017. **7**.
241. Hirose T , L.K., Schepens CL, *Snowflake degeneration in hereditary vitreoretinal degeneration.* Am J Ophthalmol 1974. **77**: p. 143-153.
242. Pattnaik BR, T.S., Asuma MP, Schroeder T, Sharma A, Mitchell JC, Edwards AO, Pillers DA., *Snowflake Vitreoretinal Degeneration (SVD) Mutation R162W Provides New Insights into Kir7.1 Ion Channel Structure and Function.* PLoS One, 2013. **8**(8).
243. T.J. Hollingsworth, A.K.G., *Defective Trafficking of Rhodopsin and Its Role in Retinal Degenerations.* International Review of Cell and Molecular Biology, 2012.
244. Pattnaik BR, S.P., Marino MJ, Liu X, York N, Brar S, Chiang J, Pillers DA, Traboulsi EI, *A Novel KCNJ13 Nonsense Mutation and Loss of Kir7.1 Channel Function Causes Leber Congenital Amaurosis (LCA16).* Human Mutations, 2015. **36**(7): p. 720-7.
245. Perez-Roustit, S.e.a., *Leber Congenital Amaurosis with Large Retinal Pigment Clumps Caused by Compound Heterozygous Mutations in Kcnj13.* . Retin. Cases Brief Rep., 2016.
246. York N, H.P., Chiu MA, Bird IM, Pillers DM, Pattnaik BR., *Oxytocin (OXT)-stimulated inhibition of Kir7.1 activity is through PIP2-dependent Ca2+ response of the oxytocin receptor in the retinal pigment epithelium in vitro.* Cell Signal, 2017. **37**: p. 93-102.
247. Madonna, M.E., et al., *Agouti-related protein segments outside of the receptor binding core are required for enhanced short- and long-term feeding stimulation.* ACS Chem Biol, 2012. **7**(2): p. 395-402.
248. Hagan, M.M., et al., *Long-term orexigenic effects of AgRP-(83---132) involve mechanisms other than melanocortin receptor blockade.* Am J Physiol Regul Integr Comp Physiol, 2000. **279**(1): p. R47-52.
249. Kumar M., P.B.R., *Focus on Kir7.1: physiology and channelopathy.* Channels (Austin), 2014. **8**(6): p. 488–495.
250. Hua Zhong, Y.C., Yumei Li, Rui Chen, & Graeme Mardon, *CRISPR-engineered mosaicism rapidlyreveals that loss of Kcnj13 function in mice mimics human disease phenotypes.* Sci. Rep. , 2015. **5**.
251. Weinstein LS, X.T., Zhang QH, Chen M., *Studies of the regulation and function of the Gs alpha gene Gnas using gene targeting technology.* Pharmacol Ther., 2007. **115**(2): p. 271-91.
252. Gilman, A.M.K.a.A.G., *Targeted Knockdown of G protein Subunits Selectively prevents Receptor-Mediated Modulation of Effectors and Reveals Complex Changes in Non-targeted Signaling Proteins.* JBC, 2006.

253. Broadie, R.B.R.a.K., *Mutation and Activation of Gs Similarly Alters Pre- and Postsynaptic Mechanisms Modulating Neurotransmission.* J Neurophysiol, 2003. **89**: p. 2620–2638.
254. Yu, S., et al., *Variable and tissue-specific hormone resistance in heterotrimeric Gs protein alpha-subunit (Gsalpha) knockout mice is due to tissue-specific imprinting of the gsalpha gene.* Proc Natl Acad Sci U S A, 1998. **95**(15): p. 8715-20.
255. Chen, M., et al., *Central nervous system imprinting of the G protein G(s)alpha and its role in metabolic regulation.* Cell Metab, 2009. **9**(6): p. 548-55.
256. Weinstein, L.S., *Albright hereditary osteodystrophy, pseudohypoparathyroidism and Gs deficiency*, in *G proteins, receptors, and disease*, A.M. Spiegel, Editor. 1998, Humana Press: Totowa, NJ. p. 23-56.
257. Yu, S., et al., *Paternal versus maternal transmission of a stimulatory G-protein alpha subunit knockout produces opposite effects on energy metabolism.* J Clin Invest, 2000. **105**(5): p. 615-23.
258. Chen M, S.Y., Podyma B, Cui Z, Naglieri B, Sun H, Ho T, Wilson EA, Li YQ, Gavrilova O, Weinstein LS., *Gsα deficiency in the dorsomedial hypothalamus underlies obesity associated with Gsα mutations.* J Clin Invest. , 2017. **27**(2): p. 500-510.
259. Li YQ, S.Y., Pandey M, Chen M, Kablan A, Gavrilova O, Offermanns S, Weinstein LS., *G(q/11)α and G(s)α mediate distinct physiological responses to central melanocortins.* J Clin Invest., 2016 **126**(1): p. 40-9.
260. Min Chen, A.B., Ahmed Kablan, Jiandi Zhang, Oksana Gavrilova, and Lee S. Weinstein, *Gsα Deficiency in the Paraventricular Nucleus of the Hypothalamus Partially Contributes to Obesity Associated with Gsα Mutations.* Endocrinology, 2012. **153**(9): p. 4256–4265.
261. Erika Harno, E.C.C., Anne White, *Metabolic Pitfalls of CNS Cre-Based Technology.* Cell Metabolism 2013. **18**(1): p. 21-28.
262. Heidenreich, M. and F. Zhang, *Applications of CRISPR-Cas systems in neuroscience.* Nat Rev Neurosci, 2016. **17**(1): p. 36-44.
263. Komor, A.C., A.H. Badran, and D.R. Liu, *CRISPR-Based Technologies for the Manipulation of Eukaryotic Genomes.* Cell, 2017. **168**(1-2): p. 20-36.
264. Robert J. Alpern (Editor), M.J.C.E., Orson W. Moe (Editor), *Seldin and Giebisch's The Kidney, Fifth Edition: Physiology and Pathophysiology* 5th Edition.
265. Yen ST, Z.M., Deng JM, Usman SJ, Smith CN, Parker-Thornburg J, Swinton PG, Martin JF, Behringer RR., *Somatic mosaicism and allele complexity induced by CRISPR/Cas9 RNA injections in mouse zygotes.* Dev Biol.
, 2014. **393**(1): p. 3-9.
266. Yin, W., Kim, H.T., Wang, S.P, et al. , *The potassium channel KCNJ13 is essential for smooth muscle cytoskeletal organization during mouse tracheal tubulogenesis.* Nature Commun., 2018. **9**(2815).
267. Ookata, K., Tojo, A., Suzuki, Y., Nakamura, N., Kimura, K., Wilcox, C. S., et al. , *Localization of inward rectifier potassium channel Kir7.1 in the basolateral membrane of distal nephron and collecting duct.* . J. Am. Soc. Nephrol., 2000. **11**: p. 1987–1994.

268. Suzuki, Y., Yasuoka, Y., Shimohama, T., Nishikitani, M., Nakamura, N., Hirose, S., et al. , *Expression of the K+ channel Kir7.1 in the developing rat kidney: role in K+ excretion.* . Kidney Int., 2003. **63**: p. 969–975.
269. Chen, L., Lee, J. W., Chou, C. L., Nair, A. V., Battistone, M. A., Paunescu, T. G., et al. , *Transcriptomes of major renal collecting duct cell types in mouse identified by single-cell RNA-seq.* Proc. Natl. Acad. Sci. U.S.A. , 2017. **114**: p. E9989–E9998.
270. Phua YL, G.T., Combes A, Wilkinson L, Little MH, *Neonatal vascularization and oxygen tension regulate appropriate perinatal renal medulla/papilla maturation.* J Pathol., 2016. **238**(5): p. 665-76. .
271. Chen, L., Lee, J. W., Chou, C. L., Nair, A. V., Battistone, M. A., Paunescu, T. G., et al. , *Transcriptomes of major renal collecting duct cell types in mouse identified by single-cell RNA-seq.* . Proc. Natl. Acad. Sci. U.S.A., 2017. **114**: p. E9989–E9998.
272. Carpenter, K.J. and J. Mayer, *Physiologic observations on yellow obesity in the mouse.* Am. J. Physiol., 1958. **193**(3): p. 499-504.
273. Hughes BA, S.A., *Modulation of the Kir7.1 potassium channel by extracellular and intracellular pH.* Am J Physiol Cell Physiol. , 2008. **294**(2): p. C423-31.
274. Chen, H.Y.T.F.J.S.L.H.M.C.J.D.V.C., *Hyperphagia in male melanocortin 4 receptor deficient mice promotes growth independently of growth hormone.* The Journal of Physiology Volume, 2016. **594**(24).
275. Vaisse, C., et al., *A frameshift mutation in human MC4R is associated with a dominant form of obesity.* Nat Genet, 1998. **20**(2): p. 113-4.
276. Yeo, G.S., et al., *A frameshift mutation in MC4R associated with dominantly inherited human obesity [letter].* Nat Genet, 1998. **20**(2): p. 111-2.
277. Branson, R., et al., *Binge eating as a major phenotype of melanocortin 4 receptor gene mutations.* N Engl J Med, 2003. **348**(12): p. 1096-103.
278. Butler, A.A. and R.D. Cone, *Knockout models resulting in the development of obesity.* Trends Genet, 2001. **17**(10): p. S50-4.
279. Fan, W., et al., *The central melanocortin system can directly regulate serum insulin levels.* Endocrinology, 2000. **141**(9): p. 3072-9.
280. Huszar, D., et al., *Targeted disruption of the melanocortin-4 receptor results in obesity in mice.* Cell, 1997. **88**(1): p. 131-41.
281. Qi, L., et al., *The common obesity variant near MC4R gene is associated with higher intakes of total energy and dietary fat, weight change and diabetes risk in women.* Hum Mol Genet, 2008. **17**(22): p. 3502-8.
282. Loos, R.J., et al., *Common variants near MC4R are associated with fat mass, weight and risk of obesity.* Nat Genet, 2008. **40**(6): p. 768-75.
283. Chambers, J.C., et al., *Common genetic variation near MC4R is associated with waist circumference and insulin resistance.* Nat Genet, 2008. **40**(6): p. 716-8.
284. Marks, D.L. and R.D. Cone, *The role of the melanocortin-3 receptor in cachexia.* Ann N Y Acad Sci, 2003. **994**: p. 258-66.
285. Marks, D.L., N. Ling, and R.D. Cone, *Role of the central melanocortin system in cachexia.* Cancer Res, 2001. **61**(4): p. 1432-8.

286. Cheung, W.W., et al., *Peripheral administration of the melanocortin-4 receptor antagonist NBI-12i ameliorates uremia-associated cachexia in mice.* J Am Soc Nephrol, 2007. **18**(9): p. 2517-24.
287. Cheung, W.W. and R.H. Mak, *Melanocortin antagonism ameliorates muscle wasting and inflammation in chronic kidney disease.* Am J Physiol Renal Physiol, 2012. **303**(9): p. F1315-24.
288. Zechner, J.F., et al., *Weight-independent effects of roux-en-Y gastric bypass on glucose homeostasis via melanocortin-4 receptors in mice and humans.* Gastroenterology, 2013. **144**(3): p. 580-590 e7.
289. Itoh, M., et al., *Melanocortin 4 receptor-deficient mice as a novel mouse model of nonalcoholic steatohepatitis.* Am J Pathol, 2011. **179**(5): p. 2454-63.
290. Perez-Tilve, D., et al., *Exendin-4 increases blood glucose levels acutely in rats by activation of the sympathetic nervous system.* Am J Physiol Endocrinol Metab, 2010. **298**(5): p. E1088-96.
291. Lim, B.K., et al., *Anhedonia requires MC4R-mediated synaptic adaptations in nucleus accumbens.* Nature, 2012. **487**(7406): p. 183-9.
292. Xu, P., et al., *Double deletion of melanocortin 4 receptors and SAPAP3 corrects compulsive behavior and obesity in mice.* Proc Natl Acad Sci U S A, 2013.
293. Cowley, M.A., et al., *Integration of NPY, AGRP, and melanocortin signals in the hypothalamic paraventricular nucleus: evidence of a cellular basis for the adipostat.* Neuron, 1999. **24**(1): p. 155-63.
294. Kievit, P., et al., *Chronic treatment with a melanocortin-4 receptor agonist causes weight loss, reduces insulin resistance, and improves cardiovascular function in diet-induced obese rhesus macaques.* Diabetes, 2012. **62**(2): p. 490-7.
295. Gilbert W. Kim, J.E.L., Erik S. Blomain, and Scott A. Waldman, *Antiobesity pharmacotherapy: new drugs and emerging targets.* Clin Pharmacol Ther. , 2014. **95**(1): p. 53-66.
296. Chen KY, M.R., Abel BS, Mullins KP, Staker P, Brychta RJ, Zhao X, Ring M, Psota TL, Cone RD, Panaro BL, Gottesdiener KM, Van der Ploeg LH, Reitman ML, Skarulis MC, *RM-493, a melanocortin-4 receptor (MC4R) agonist, increases resting energy expenditure in obese individuals.* J Clin Endocrinol Metab, 2015. **100**(4): p. 1639-45.
297. Lee EC, C.P., *Melanocortin-4 receptor modulators for the treatment of obesity: a patent analysis (2008-2014).* Pharm Pat Anal., 2015. **2**(4): p. 95-107.
298. Sohn, J.W., et al., *Melanocortin 4 receptors reciprocally regulate sympathetic and parasympathetic preganglionic neurons.* Cell, 2013. **152**(3): p. 612-9.
299. Zhong H, C.Y., Li Y, Chen R, Mardon G, *CRISPR-engineered mosaicism rapidly reveals that loss of Kcnj13 function in mice mimics human disease phenotypes.* Sci Rep. , 2015. **10**(5).
300. Ghamari-Langroudi, M., *Electrophysiological Analysis of Circuits Controlling Energy Homeostasis.* Molecular Neurobiology, 2012. **45**(2): p. 258-278.
301. Breit, A., et al., *The natural inverse agonist agouti-related protein induces arrestin-mediated endocytosis of melanocortin-3 and -4 receptors.* J Biol Chem, 2006. **281**(49): p. 37447-56.
302. Gropp, E., et al., *Agouti-related peptide-expressing neurons are mandatory for feeding.* Nat Neurosci, 2005. **8**(10): p. 1289-91.

303. Luquet, S., et al., *NPY/AgRP neurons are essential for feeding in adult mice but can be ablated in neonates.* Science, 2005. **310**(5748): p. 683-5.
304. Wu, Q., et al., *Starvation after AgRP neuron ablation is independent of melanocortin signaling.* Proc Natl Acad Sci U S A, 2008. **105**(7): p. 2687-92.
305. Mountjoy, K.G., et al., *Melanocortin-4 receptor messenger ribonucleic acid expression in rat cardiorespiratory, musculoskeletal, and integumentary systems.* Endocrinology, 2003. **144**(12): p. 5488-96.
306. Arora T, A.R., Pais R, Bergqvist L, Johansson BR, Schwartz TW, Reimann F, Gribble FM, Bäckhed F, *Microbial regulation of the L cell transcriptome.* Sci Rep., 2018. **8**(1): p. 1207.
307. Michael J Krashes, B.B.L., and Alastair S Garfield, *Melanocortin-4 receptor–regulated energy homeostasis.* Nat Neurosci. , 2016 **19**(2): p. 206–219.
308. Srisai, D., et al., *Characterization of the hyperphagic response to dietary fat in the MC4R knockout mouse.* Endocrinology, 2011. **152**(3): p. 890-902.
309. Owen P. McGuinness, J.E.A., Maren R. Laughlin, and David H. Wasserman, *NIH experiment in centralized mouse phenotyping: the Vanderbilt experience and recommendations for evaluating glucose homeostasis in the mouse.* Am J Physiol Endocrinol Metab., 2009. **297**(4): p. E849–E855.
310. Berglund, E.D., et al., *Glucose metabolism in vivo in four commonly used inbred mouse strains.* Diabetes, 2008. **57**(7): p. 1790-9.
311. Xu J, B.C., Low CS, et al. , *Genetic identification of leptin neural circuits in energy and glucose homeostasis.* Nature, 2018. **556**: p. 505 - 509.
312. van de Wall E, L.R., Xu AW, et al. , *Collective and individual functions of leptin receptor modulated neurons controlling metabolism and ingestion.* Endocrinology, 2008. **149**: p. 1773 - 1785.
313. Spanswick, D., et al., *Leptin inhibits hypothalamic neurons by activation of ATP-sensitive potassium channels.* Nature, 1997. **390**: p. 521 - 525.
314. Miki T, N.K., Tashiro F, et al. , *Defective insulin secretion and enhanced insulin action in KATP channel - deficient mice.* . Proc Natl Acad Sci USA, 1998. **95**: p. 10402 - 10406.
315. Seghers V, N.M., DeMayo F, Aguilar - Bryan L, Bryan J. , *Sur1 knockout mice. A model for K(ATP) channel - independent regulation of insulin secretion.* . J Biol Chem, 2000. **275**: p. 9270 - 9277.
316. Katherine E.Wortley, K.D.A., Jason Yasenchak, Andrew Murphy, David Valenzuela, Sabrina Diano, George D.Yancopoulos, Stanley J.Wiegand, Mark W.Sleeman, *Agouti-related protein-deficient mice display an age-related lean phenotype.* Cell Metab, 2005. **2**(6): p. 421-427.
317. Sternson, S.M. and D. Atasoy, *Agouti-related protein neuron circuits that regulate appetite.* Neuroendocrinology, 2014. **100**(2-3): p. 95-102.
318. Mutulis, J.E.S.W.F., *Targeting melanocortin receptors: an approach to treat weight disorders and sexual dysfunction*
the Melanocortin-4 Receptor: Physiology, Pharmacology, and Pathophysiology. Nature Reviews Drug Discovery 2008. **7**: p. 307–323.
319. Julio E. Ayala, V.T.S., Gregory J. Morton, Silvana Obici, Colleen M. Croniger, Gerald I. Shulman, David H. Wasserman, Owen P. McGuinness, *Standard*

operating procedures for describing and performing metabolic tests of glucose homeostasis in mice. Disease Models & Mechanisms, 2010. **3**: p. 525-534.